NUI MAYNOOTH

Ollscoil na hÉireann Má Nuad

Integrating Cell-level Kinetic Modeling into the Optimization of Cancer Therapeutics

A dissertation
submitted for the degree of
Doctor of Philosophy

by

Ben-Fillippo Krippendorff

Head of Department: Prof. Douglas Leith
Supervisor: Dr. Wilhelm Huisinga

Hamilton Institute
National University of Ireland, Maynooth

December 2009

Für meine wundervolle Frau Stefanie

Abstract

Cancer therapy benefits today from the availability of new promising classes of drugs such as therapeutic proteins. Due to their ability to specifically bind targets in the body they allow to modulate specific chemical reactions and ultimately to modify the functional response of the cell, such as cell growth or cell division. Targeting receptor systems by competitive inhibition is the objective of various protein drugs in development and on the market. Many targeted receptor systems also constitute a degradation mechanism for the drug via endocytosis and a thorough understanding of the complex interplay between the drug's pharmacokinetics and its effect, is largely missing.

For complex diseases such as cancer, systems biology models of therapeutically relevant cellular processes have proven valuable for identifying potent drug targets. So far, such information about the dynamics of the targeted system is neglected in later stages of the drug development process when pharmacokinetic modeling is used to guide dose finding and analyze preclinical or clinical *in vivo* data. This is especially critical for therapeutic proteins where, due to the degradation mediated by the targeted receptor, drug effect and pharmacokinetics are inherently interdependent.

This thesis combines the points of view of systems biology and pharmacokinetics. We present a detailed mechanistic model of the targeted cellular system that explicitly takes into account receptor binding and trafficking inside the cell and that is used to derive reduced models of drug degradation which retain a mechanistic interpretation. By integrating cell-level models with established pharmacokinetic models, we translate biophysical properties of protein drugs into a transient drug effect *in vivo*. We illustrate the approach for antibodies against the epidermal growth factor receptor used in cancer therapy. The cell-level pharmacokinetic/pharmacodynamic model identifies options and limits for future therapeutic antibodies and links their inhibitory effect with genomic alteration of tumor cells.

Acknowledgments

This work was carried out at the Hamilton Institute and the Freie Universität Berlin. I want to express warm thanks to everybody I have learned from and supported me during the last years. This was first and foremost Wilhelm. He introduced me to pharmacokinetics back in my bachelor studies and I have to express my sincere gratitude for his scientific support and guidance in the following years.

I very much enjoyed the time working in Ireland, especially because of my past and present colleagues at the Hamilton institute. Also, I felt the strong support by the International Max-Planck Research School, Berlin and especially Dr. Hannes Luz. I gratefully acknowledge discussions and advises from Prof. Charlotte Kloft, Dr. Andreas Reichel, Dr. Philip Lienau, Diego Oyarzun and also Dr. Franz Schulte. Special thanks to Max von Kleist, who visited the most interesting conferences with me and also Benjamin Nietsche, Martin Wetzel, and Marcel Schulz for being such close friends. And, of course, I want to thank my family for their warm support and that they listened to success stories and stories about failures with the same attention.

But the last and most important acknowledgement goes to my wife Stefanie. Her love and support in the last ten years are in this thesis. Stefanie, with you I feel everything to be possible.

Publications

Parts of this thesis subsume the content of publications conducted during my PhD studies. Chapter 2 was published in the Journal of Pharmacokinetics and Pharmacodynamics [74] together with Katharina Kuester, Charlotte Kloft, and Wilhelm Huisinga. Parts of Chapter 3 were published as proceedings to the FOSBE conference 2009 [72], together with Diego Oyarzun and Wilhelm Huisinga. A manuscript covering Chapter 4 with the title *Integrating cell-level kinetics into systemic pharmacokinetics models for optimizing therapeutic antibodies in cancer therapy* has been submitted for publication.

Besides the articles covered in this thesis I published during my PhD studies an article regarding mathematical models for the detection of drug-drug interactions in the Journal of Biomolecular Screening with the title *Mechanism-Based Inhibition: Deriving KI and kinact Directly from Time-Dependent IC50 Values*[71] together with Philip Lienau, Andreas Reichel, Roland Neuhaus, and Wilhelm Huisinga.

Contents

Abstract iii

Acknowledgments iii

Publications iii

1 Introduction 1

1.1 Cancer drug development today 1
1.2 Objective of the thesis 5
1.3 Thesis organization 7

2 The influence of cell level dynamics on pharmacokinetics 9

2.1 *The pharmacokinetics of therapeutic proteins* 9
2.2 *Pharmacokinetic compartment models* 10
2.3 *Target-mediated drug disposition* 11
2.4 Our approach to pharmacokinetic modelling of therapeutic proteins 12
2.5 A detailed cell level model of receptor mediated endocytosis 13
2.6 Model reduction 16
2.7 Integration of RME into compartmental PK models 19
2.8 Protein distribution and elimination by RME 21
2.9 Nonlinear PK caused by RME 22
2.10 Case study: modelling zalutumumab (2F8) disposition 23
2.11 RME in the monoclonal antibody/EGFR system 28
2.12 Summary of this chapter 29

3 The *in vitro* inhibitory effect of therapeutic antibodies 31

3.1 *Mathematical models for receptor kinetics* 31
3.2 Our mathematical model for the inhibitory effect of therapeutic antibodies . 35
3.3 Translating biophysical properties into an inhibitory effect 38
3.4 Impact of affinity and dose on inhibitory effect 39
3.5 Impact of receptor downregulation 40
3.6 Derivation of an exact formula for the inhibitory effect 42
3.7 Impact on cells with increased receptor levels 42

3.8 Inhibition of receptor activation in the microenvironment of tumor cells . . . 45
3.9 Summary of this chapter . . . 49

4 The *in vivo* effect of therapeutic antibodies 51
4.1 Our model of the inhibitory effect of therapeutic proteins . . . 51
4.2 Integrating in vitro determined cell-level receptor dynamics into whole-body pharmacokinetic models . . . 55
4.3 Optimizing drug characteristics . . . 57
4.4 Tumor cell specificity . . . 60
4.5 Summary and Conclusions of this chapter . . . 62

5 Conclusions and Extensions 64

6 Appendix 69
6.1 Derivation of an exact formula for the inhibitory effect . . . 69
6.2 Quantification of the integral of effect *in vivo* . . . 71
6.3 Effect of receptor overexpression on the drug specificity . . . 73

Bibliography 76

1 Introduction

1.1 Cancer drug development today

Cancer medicine is rapidly changing. Recent advances in many different disciplines like chemotherapy, hormone therapy, radiotherapy and diagnostic imaging have improved our understanding of cancer and the clinical practice. The current view on cancer development envisions cells undergoing a series of genetic alterations which results in the six hallmarks of cancer: (i) self-sufficiency in growth signals, (ii) insensitivity to antigrowth signals, (iii) evasion of programmed cell death, (iv) limitless replicative potential, (v) sustained angiogenesis, and (vi) tissue invasion and metastasis [50]. Since each of these alterations confers a growth advantage, the progressive conversion of normal human cells into cancer cells is thought of resembling Darwinian evolution [104]. Cancer therapy today is particularly influenced by the ability of molecular cell biology to elucidate the detailed cellular processes involved in each of these steps of cancer development. This is nicely illustrated by the development of the drug *Imatinib* (Gleevec/Glivec) against a form of cancer called *chronic myelogenous leukemia* (CML). CML is characterized by the alteration of a single gene, termed *Bcr-Abl* whose expressed protein shows enhanced tyrosine kinase activity [116, 33]. This molecular understanding of CML secondary allowed the development of Imatinib as an inhibitor to the enzyme Bcr-Abl. Imatinib, in the majority of patients, leads to a normalization of the blood cells within 3 weeks of initiation of therapy[33]. The high efficacy of Imatinib can be attributed to the identification of Bcr-Abl as a fragile node in the cancer mediating signalling cascade which only exists in target cells [65]. Imatinib and the underlying understanding of the genetic and biochemical processes therefore "converted a fatal cancer into a manageable chronic condition"[1].

Such a success stimulated the development of many therapies guided by validated effects on a defined molecular target [44, 27, 120, 37, 100, 103, 61]. Although different target therapies have made it to the clinical practice, the development of good rational drugs remains extremely difficult and the overall rate of new drug approvals has failed to keep pace with ever-increasing spending on pharmaceutical research [29, 32, 59, 75, 70]. The story of Imatinib was probably more an exception than a role model for the development of potent cancer drugs, or as Fishman and Porter called it, it was "a low-hanging fruit" [38]. In other situations, instead of focusing on a single hyperactive/underactive protein, this protein has to targeted in the context of

[1] The Lasker DeBakey Clinical Medical Research Award 2009

its cellular network. These signalling pathways are triggered by external stimulus, sensed by the cell through cell-surface receptors [63]. The activation of such receptors is translated by signalling pathways into a specific change in gene expression. Gene activation or suppression ultimately leads then to a change in the cell's behavior. Examples for such functional responses of the cell to the external stimulus are changes in its ability to grow or differentiate, and to undergo division or self-destruction. As examples, Fig. 1.1 depicts the core components of five signaling pathways where a misregulation of several of these components is directly associated with cancer development. The dynamics occurring in such signalling networks, including

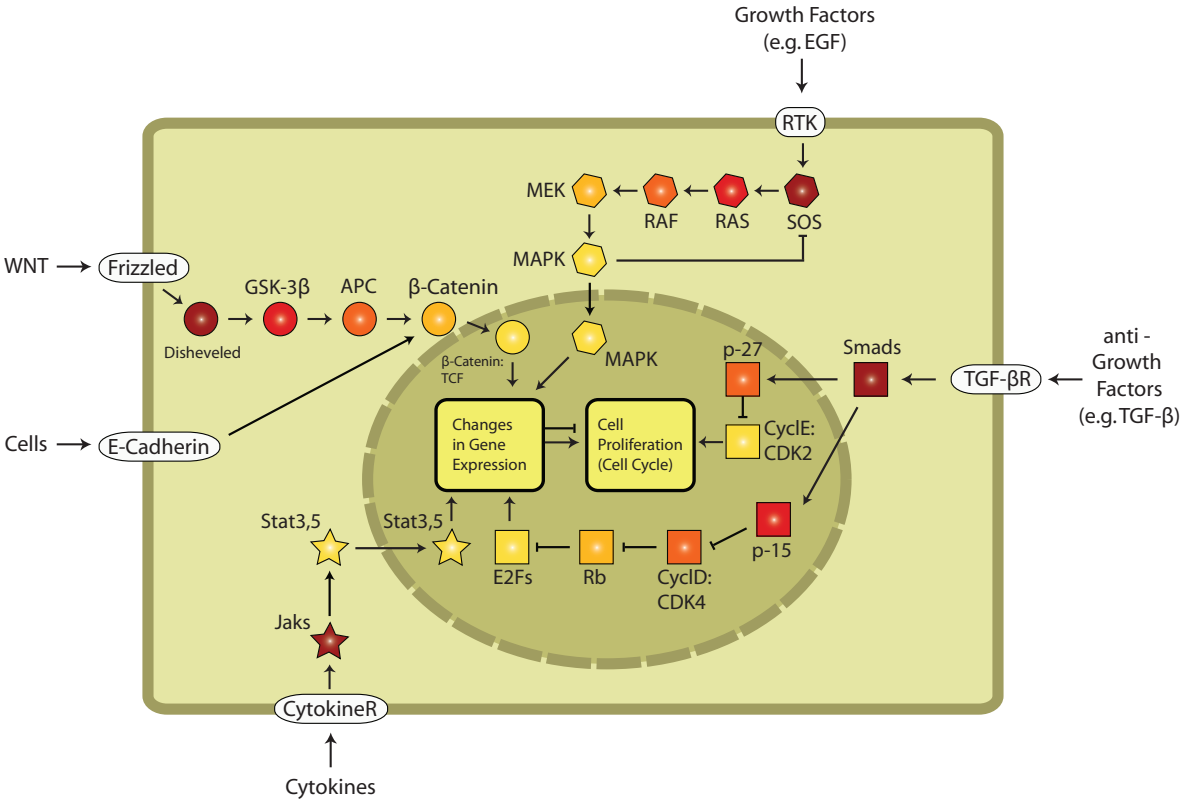

Figure 1.1: *Receptor tyrosine kinase (RTK) receptor, E-Caherin, Frizzled, transforming growth factor-β receptor (TGF-βR) and cytokine receptor receptor are examples for receptors which stimulate signalling pathways modulating gene expression and cell proliferation. The arrows and T-bars describe an activation and inhibition, respectively. For simplicity, only the core elements of the pathways are depicted here. The elements of the different pathways follow descriptions of signalling cascades in Hanahan and Weinberg [50], Klipp and Liebermeister [66], and Kumar et al. [78].*

circular dependencies (such as the negative feedback from *MAPK* to *SOS* in Fig. 1.1), differ substantially from the current view on drug development which " at its core, [...] seeks to define a linear pathway, or causal chain, leading to disease, and then to interfere at one of these steps – by inhibiting a crucial enzyme or blocking an important receptor, for example" [126].

Hence, understanding signalling pathways is crucial in cancer research. Due to their com-

plexity it becomes evident that for a successful development of cancer drugs reliable predictions of the impact of perturbations of the network are vital. When analyzing complex systems in engineering, the use of mathematical modelling has been proven useful. Mathematical models allow to connect knowledge about individual parts and formulate hypotheses about the behavior of the sum of these parts. To overcome the limitations of current drug development strategies and to increase the success rate when developing new drugs the integration of mathematic modelling into the development process has been advocated [17, 65, 148, 18, 26, 39, 58, 92]. Indeed, mathematical analysis can demonstrate that living systems may exhibit an intrinsic robustness against various perturbations and hence many potential drugs that specifically target a particular protein (which is considered to underlie a given disease) have been found to be less effective than hoped [65].

Cell-level kinetic models are a language to analyse the robustness of a response to a drug and therefore can identify and rank potential targets in cellular networks [65]. Hence, computational models are of increasing relevance for target identification in drug discovery [58]. A recent prominent example is the use of a kinetic model to identify critical components in the ErbB receptor family mediated signaling pathways [20], an important pathway for cancer development. As a result, a therapeutic antibody was developed which targets the ErbB3 receptor and is currently in early clinical trials [130].

In the patient, the time trajectory of the drug concentration is a critical component of drug efficacy [111]. Therefore, in addition to the increasing level of detail of systems biology models, there exists a great need to place cell-level models in the context of the condition *in vivo* [111, 109, 1]. Hence, the shift from a "target-centric" to a "biochemical network-centric" view of drug development alone is unlikely to be sufficient to predict the *in vivo* effect in the complex human system.

Another aspect is that after the target was identified, in the later stages of the drug development process prior knowledge about the targeted system is invariably ignored when analyzing preclinical or clinical data [80]. As a result, knowledge about the dynamics of the target *in vitro* cannot be used in later stages of the drug development, where knowledge about drug disposition *in vivo* has been obtained. Such knowledge is usually in the drug development process described by pharmacokinetic/ pharmacodynamic models.

This thesis advocates to integrate the pharmacokinetics and pharmacodynamics of the studied drug into the systems view on its effect. Second, we propose to use more mechanistic information about cellular processes when analyzing clinical data in the later stages of drug development.

Current pharmacokinetics describes absorption, distribution, metabolism, and excretion of a drug in the body using empirical or semi-empirical models of the processes involved. In contrast to systems biology, current pharmacokinetic modelling (with the exception of physiologically based pharmacokinetic models discussed in section 5.1) is mostly a top down

approach, which relates observations to models, selected based on, e.g., established statistical criteria (such as maximum likelihood), the precision of estimates of model parameters, and in few cases on model evaluation techniques [35, 137, 135, 136]. However, being empirical in nature, these models do not provide a mechanistic understanding of, for example, how the different processes of receptor trafficking contribute to the overall pharmacokinetic profile.

We think, combining systems biology and pharmacokinetic models is particularly useful for the optimization and development of a relatively new class of drugs, *therapeutic proteins*. The therapeutic potential of proteins results from their ability to bind—with high affinity—to specific targets such as cell-surface receptors.

In recent years, therapeutic proteins have been a major focus of research and development activities in the pharmaceutical industry [93]. Currently, approximately 100 therapeutic proteins have been approved for human use, most of them being biotechnology-derived drug products and many more are under development [93]. Important classes of therapeutic proteins are monoclonal antibodies, growth factors, and cytokines. Generally, therapeutic proteins provide highly attractive but sometimes exceptional behavior in the body [76]. The largest class of therapeutic proteins developed today are therapeutic monoclonal antibodies (mAbs). Antibodies can interfere with specific cellular targets and signaling pathways and have demonstrated their potential in therapies for cancer and other complex diseases [94].

Therapeutic antibodies are produced by immunization of a mouse with a specific antigen. The subsequent immune reaction of the mouse leads to the production of antibody producing B lymphocytes which accumulate in the spleen [94]. These cells are capable of producing the corresponding antibody to the administered antigen, but for the production of larger quantities of the antibody those B lymphocytes have to be fused with malignant myeloma cells to form immortal cells, called *hybridomas*. This technique was developed by Koehler and Milstein [69] and for this discovery they were awarded the 1984 Nobel prize for medicine. Because the produced antibodies by those hybridoma cells are cloned from only one original B lymphocyte, and hence are identical, they are also called *monoclonal Antibodies* (mAbs).

The use of rodent systems to produce mAbs however prevented their use in indications in humans where prolonged dosing was required due to their high immunogenicity [82]. To overcome this limitation chimeric, humanized, and fully human mAbs have recently been developed.

Chimeric mAbs are developed by exchanging the regions of the human antibody genes for those derived from the mouse which generates chimeric genes. These genes are then introduced into eukaryotic cells which can produce chimeric antibodies that are about 70% human [150]. For fully human antibodies the mouse from which the B lymphocyte is derived is genetically engineered. First, the antibody gene clusters are inactivated which prevents those mouse from producing antibodies and mature B lymphocytes. Subsequently, DNA segments containing large parts of the human gene clusters are introduced into the mice which, after

being immunized with any target, enables them to produce high affinity antibodies [150]. Since the antibodies are produced from the human antibody genes after fusing the B lymphocyte with myeloma cells the resulting hybridomas cells produce fully human monoclonal antibodies.

Trastuzumab (Herceptin) was the first antibody for the treatment of cancer approved by the Food and Drug Administration (FDA) in 1998. It created great interest in the scientific community as well as outside [2]. Trastuzumab is an anti-Her2 antibody used in the treatment of breast cancer against tumors overexpressing the Her2 receptor. The development followed the identification of the oncogene Her2/neu in 1984 [127] and its cloning [131, 22]. In 1986 Drebin, Link, Weinberg, and Greene demonstrated that an anti-HER-2 monoclonal antibody is able to inhibit Her2/neu transformed cells [31] and the following clinical studies found that this antibody, trastuzumab, halves the risk of tumor recurrence which corresponds to an absolute increase in 4-year disease free survival (DFS) of 17% [110].

Other antibodies against receptors of the ErbB family on the market are Cetuximab (Erbitux) and Panitumumab, which inhibit the epidermal growth factor receptor (EGFR). Cetuximab is currently approved for the treatment of colorectal cancer and squamous cell carcinoma of the head and neck, Panitumumab for colorectal cancer. Additionally, three anti-ErbB antibodies are in late clinical phases (Nimotuzumab, Zalutumumab, IMC-11F8) [107].

Due to their similarity to endogenous proteins, after binding to their cell surface target, many protein drugs and especially antibodies are internalized into the cell by Receptor Mediated Endocytosis (RME)[90, 141, 138]. Within the cell, the complex may be recycled to the cell surface or intracellularly be cleaved [121, 139]. RME therefore mutually links the effect of a therapeutic protein with its pharmacokinetics. As a consequence, the design and the biophysical optimization of therapeutic proteins based on cell-based assays and preclinical pharmacology, becomes a considerable challenge [111].

One example of a biophysical property of a therapeutic protein affecting both, the cellular therapeutic effect and the PK, is the affinity of therapeutic antibodies to their target. Currently, mAbs on the market have a high receptor affinity in the sub-nM range, but the traditional design criterion that "the best binder makes the best drug" has been questioned[111, 24, 19]. To date, no model exists which predicts both, the pharmacokinetics and the inhibitory effect of therapeutic proteins [109] and can guide the optimization of biophysical properties of therapeutic proteins.

1.2 Objective of the thesis

This thesis systematically investigates the dependencies between systemic pharmacokinetic models and cell-level kinetic models. First, we examine how pharmacokinetic models can be improved when incorporating cell-level dynamics. This extends current pharmacokinetic

[2] the discovery of Trastuzumab by Dr. Dennis Slamon and others at UCLA was made into the film *Living Proof*, directed by Dan Ireland.

models and gives a rationale in which situations this extended model or already available pharmacokinetic models should be used. Second, we analyze cell-level kinetic models of antibody action under the conditions of a typical *in vitro* experiment. We investigate how drug properties influence the potential of the antibody to inhibit the activation of the epidermal growth factor receptor which mediates a variety of malicious cellular responses of cancer cells such as proliferation, differentiation, survival, and angiogenesis [96]. As the final step, we combine the *in vivo* and *in vitro* models into a cell-level pharmacokinetic/pharmacodynamic model. This model allows to integrate preclinical pharmacokinetic data and to investigate the biochemical properties of antibodies currently used in cancer therapy under *in vivo* conditions. Using this model, we identify options and limits for the optimization of efficacy and tumor selectivity of future therapeutic antibodies.

1.3 Thesis organization

In a more detailed summary, we will perform three steps to mechanistically model the pharmacokinetics and the inhibitory effect of antibodies used in cancer therapy.

In Chapter 2 we develop a detailed mechanistic models of the binding of therapeutic proteins to targets on a cells surface as well as subsequent intracellular processes of antibody degradation. We then reduce this mechanistic model to resemble empirical models currently used in the analysis of clinical pharmacokinetic data. The mechanistic derivation of the empirical models allows us to give a rationale in which situations to use the different models. Further, the reduction of the detailed model connects the processes on a cell-level with the effective dynamics on a whole body level usually determined in pharmacokinetic studies.

Chapter 3 investigates the inhibitory effect of therapeutic antibodies on the epidermal growth factor receptor under the conditions of a typical *in vitro* experiment. The action of the drug is studied in the presence of the natural ligand by extending an established model of receptor activation. The model is used to translate biophysical properties of the antibody, like the affinity, into a transient inhibitory effect and to predict tumor cell selectivity. Further, under the *in vitro* conditions an analytical study of the receptor system allows to derive an exact formula for the cumulative antagonistic effect of therapeutic antibodies and identifies the synthesis rate of the receptor as the critical parameter of the cellular system regarding the inhibitory effect of the drug. Also, we investigate drug action in a closed microenvironment of a tumor cell where the exchange of molecules with the surrounding is limited. This identifies ligand accumulation as a potential counter response to the drug action in such a closed system.

In Chapter 4, we develop a strategy to include a cell-level model into a whole body model of drug disposition. We use the relations between the cell-level processes and the effective dynamics on the whole body level determined in Chapter 2. This allows us to estimate the number of target expressing cells which come in contact with the drug. This number facilitates the integration of cell-level kinetics into a systemic pharmacokinetic model because the impact of a single cell can be scaled up to an impact on the whole body level. As in Chapter 3 we investigate the properties of therapeutic antibodies regarding their antagonistic effect on the epidermal growth factor receptor, but here under conditions which reflect the conditions *in vivo* more closely than the *in vitro* setting. This allows us, for the first time, to study the optimization of biophysical properties of therapeutic proteins by coupling cellular dynamics of the target with the drugs disposition in the body.

A final comment to the models the reader will find in the different chapters. The systemic pharmacokinetic model will be the same in the different parts of the thesis. The rationale of this is that the used two-compartment model has been found useful by many authors for analyzing preclinical/clinical pharmacokinetic data of protein drug trials [30, 77, 101, 67, 147]. In contrast, we use different cell-level models in the different chapters.

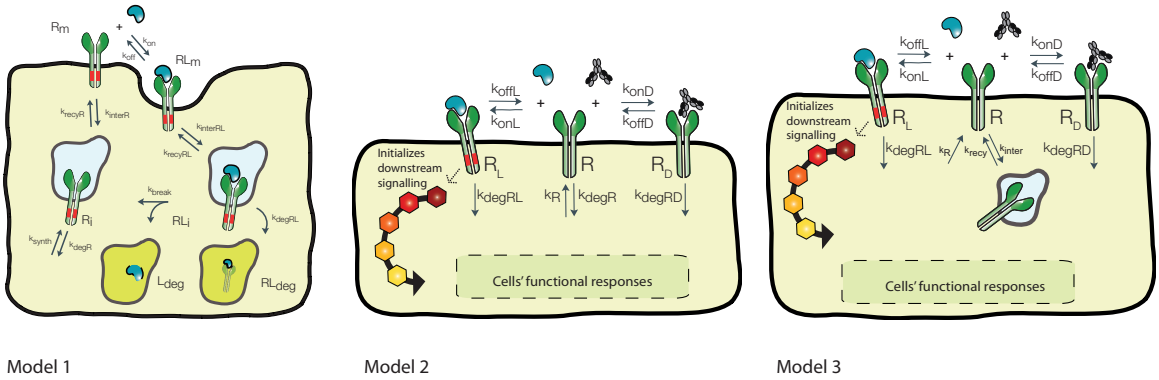

Figure 1.2: *Illustration of the different cell-level models used in the thesis.*

Fig. 1.2 illustrates the different cell-level models of receptor activation, inhibition and trafficking used in this thesis. Model 1 is used to structurally characterize the impact of the cell surface/intracellular processes on the pharmacokinetics. Model 2 and 3 lump different processes of receptor trafficking. These descriptions of receptor activation and trafficking are in correspondence with established models in the literature [158, 156, 161, 159, 133] and provide experimentally determined parameter values [68, 53, 55, 54, 140] which allows us to make quantitative predictions. A more detailed justification of the different cell-level models is given in the different chapters (see section 2.5, 3.2, and 4.1) and their ability to act as an interface to detailed models of signalling cascades is discussed in Chapter 5.

2 The influence of cell level dynamics on pharmacokinetics

In the Introduction we discussed the interdependence of the pharmacokinetics and the inhibitory effect of therapeutic proteins because of RME. In this Chapter, we develop a detailed model of RME to study the impact of antibody binding and receptor dynamics on the pharmacokinetics of the drug. In the following Sections 2.1–2.3 some basic concepts of current pharmacokinetic modelling techniques for therapeutic proteins are presented. These concepts and techniques will subsequently be used to derive reduced models of RME which still allow for a mechanistic interpretation of the parameters and can be used to analyse clinical pharmacokinetic data.

2.1 *The pharmacokinetics of therapeutic proteins*

Frequently, it is said that pharmacokinetics (PK) is what the body does to the drug, and pharmacodynamic (PD) is what the drug does to the body. Pharmacokinetic is subdivided into the absorption of the drug, its distribution in the body, metabolic processes, and the elimination of the drug.

Therapeutic proteins are usually administered intravenously, subcutaneously, or intramuscularly due to gastrointestinal enzymatic degradation and poor permeability of the gastrointestinal mucosa [94]. Studying absorption is therefore usually not necessary in pharmacokinetic studies of therapeutic proteins [90]. The distribution of therapeutic proteins is determined by their biophysical properties. Due to their large size (> 1000 Da) the distribution through membranes into peripheral tissues is limited. Protein drugs with a size above the glomerular filtration limit (> 60 kDa) are not significantly excreted by the kidney [94], which contributes to the large halflife of many therapeutic proteins in the body. Also their distribution in the body is typically limited to the extracellular space [114]. As discussed above, one feature of protein drugs is their highly specific binding to epitopes expressed on certain cells in the body. Besides the proteolysis by proteases and peptidases in the blood, liver, kidneys and gastrointestinal tissue, uptake subsequent to the binding to target receptors plays a major role in the elimination of protein drugs from the body [90]. Because the number of available target receptors and therefore the capacity of the cells to clear the drug from the body is limited, receptor binding and RME is suspected to be a major source for the nonlinear

pharmacokinetic behavior that is observed in clinical data for numerous protein drugs [141].

In conclusion, the pharmacokinetic of therapeutic proteins is distinct and can simply be summarized as long halflife with nonlinear elimination kinetics. While the long halflife of several weeks is seen as an advantage because it minimizes the occasions the drug has to be injected into the patient, the nonlinearity is traditionally seen as complicating the dose finding process.

2.2 Pharmacokinetic compartment models

When aiming at analyzing preclinical/clinical pharmacokinetic data of protein drug trials, typically *empirical* 1-, 2- or 3-compartmental models including linear and/or nonlinear disposition processes have been developed. These models have been selected based on, e.g., established statistical criteria (such as maximum likelihood), the precision of estimates of model parameters, and in few cases on model evaluation techniques [35, 137, 135, 136].

Compartment systems consist of a number of homogeneous, well-mixed, lumped subsystems, called compartments, which exchange with each other the modelled drug. Depending on the type of model the compartments represent specific physiological organs (like in physiologically based pharmacokinetic models) or organs lumped due to e.g. their diffusibility for the specific drug (like in empirical pharmacokinetic models) [46]. The amount of a drug in a compartment, A_i, for a linear system with p compartments can be described by the following equation [46]:

$$\frac{d\ A_i}{dt} = \sum_{j=1, j\neq i}^{p} k_{ij} A_j - \sum_{j=1, j\neq i}^{p} k_{ji} A_i - k_{0i} A_i + u_i(t)\ , i = 1, 2, ..., p \tag{2.1}$$

where A_i is the the amount of drug in the compartment i, k_{ij} is the rate constant describing the transport to compartment i from compartment j, and k_{0i} denotes the rate constant of elimination of drug from the compartment i. Also the drug is administered to the compartment, which is described with the flow $u_i(t)$.

Often instead of the amount, concentrations are determined and the systems has to incorporate the volumes of the p compartments V_p. Therefore the system changes to

$$\frac{d\ C_i}{dt} = \sum_{j=1, j\neq i}^{p} Q_{ij} C_j - \sum_{j=1, j\neq i}^{p} Q_{ji} C_i - \mathrm{CL_i} C_i + u_i(t)\ , i = 1, 2, ..., p \tag{2.2}$$

with $Q_{ij} = k_{ij} \cdot V_j$, $C_j = A_j / V_j$, $\mathrm{CL_i} = k_{0i} \cdot V_i$, and $C_i = A_i / V_i$. An illustration for the case of linear elimination from the central compartment ($p = 1$) and an additional distribution into a peripheral compartment ($p = 2$) is depicted in Fig. 2.1, a and b, respectively. The excretion from the central compartment is proportional to the drug concentration in this compartment

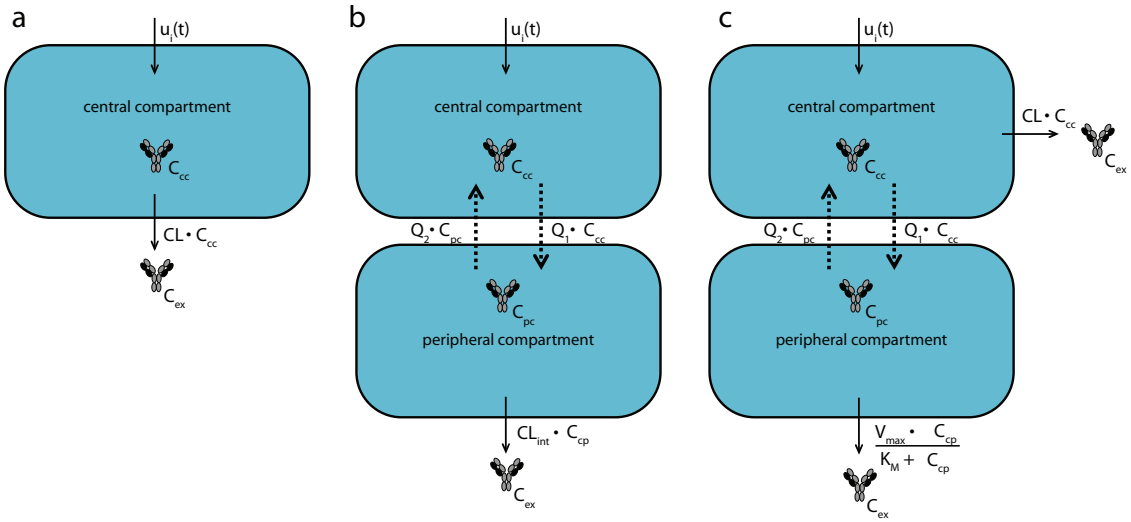

Figure 2.1: *Pharmacokinetic compartment models.* ***(a)*** *One-compartment model with linear elimination.* ***(b)*** *Two-compartment model with distribution into a second compartment and metabolisation of the drug.* ***(c)*** *Two-compartment model with linear elimination from the first compartment, distribution into a second compartment with saturable elimination. The drug is administered into the compartment with rate $u_i(t)$. In case of a bolus dose $u_i(t)$ is a delta distribution at t=0.*

with the factor of proportionality CL called the *clearance* of the drug.

For therapeutic proteins the elimation capacity is often found to be nonlinear and Michaelis–Menten terms have often been used to analyze experimental data in order to account for the observed nonlinearity [30, 77, 102, 67, 147] (see Fig. 2.1, c).

2.3 *Target-mediated drug disposition*

As discussed above, protein drugs are developed to bind with high specificity to targets in the body like enzymes, receptors, or transporters. In case that the amount of drug bound to the target is significant compared to the given dose, the pharmacokinetics of the drug will be influenced by the binding.

In PK/PD modeling, target mediated drug disposition (TMDD) has been proposed as a general semi-mechanistic model for drugs that bind with high affinity to a pharmacologic target [88]. Although originally developed to describe effects of extensive drug target binding in tissues, TMDD has more recently gained interest as a model for saturable elimination mechanisms for specific peptide and protein drugs, including RME [141, 87, 84, 155]. Recently, TMDD was extended to the situation where the binding to the target happens much faster than the other processes and therefore a quasi steady state assumption for the complex can be assumed [89].

Although TMDD considers pharmacological target binding as the key process controlling the complex nonlinear processes, particular features of receptor trafficking inside the cell are

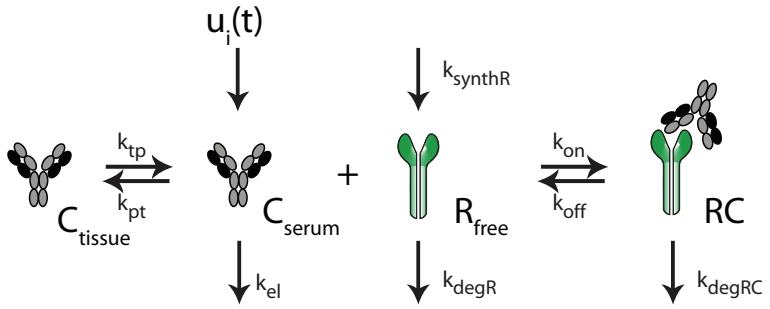

Figure 2.2: *Pharmacokinetic model of target-mediated drug disposition.*

not taken into account i.e., the process by which receptors and ligands are either targeted for intracellular degradation or recycled to the surface for successive rounds of trafficking [55]. Second, whenever a drug molecule is degraded in the TMDD setting, both, a drug and a receptor molecule are degraded. However, for many ligands, including TNF-α, degradation of the drug does not necessarily imply degradation of the receptor, since the receptor can be recycled [139].

2.4 Our approach to pharmacokinetic modelling of therapeutic proteins

The presented compartment models are empirical in nature. Hence, these models do not provide a mechanistic understanding of how the different processes of receptor trafficking contribute to the overall pharmacokinetic profile, which is expected to guide, e.g., lead optimization or the design of more efficient dosing regiments. TMDD models are semi-empirical in the way that they include the binding of the drug but pool the different cell-level processes in a process which happens at a whole body level. Therefore they do not provide a mechanistic understanding of the processes as well. Equally important, there is no theoretical background as to when to use the different existing empirical or semi-empirical models for describing the nonlinear pharmacokinetic of therapeutic proteins.

In this Chapter, the objective is to develop a framework for RME that is specifically tailored to the needs in PK analysis of clinical trials by bridging the points of view in pharmacokinetics and systems biology.

The aims are (i) to develop a detailed model that takes into account the most relevant processes in relation to receptor trafficking; (ii) to derive reduced models of RME which retain a mechanistic interpretation and are defined in terms of a few parameters only, (iii) to offer guidance as to when use them, and (iv) to analyze the impact of the different processes on the extent of nonlinearity. While our approach applies to many receptor systems in general, we will use the epidermal growth factor receptor (EGFR) signalling pathway to illustrate the approach. The EGFR system has been intensively studied over the past 20 years and is one

of the most important pathways for cell growth and proliferation as well as angiogenesis and metastasis [85]. The EGFR system comprises a tyrosine kinase receptor, which is activated by a variety of ligands such as the epidermal growth factor (EGF) or the transforming growth factor-α (TGF-α) [152, 153, 51]. Mathematical modelling of the EGFR system has proven to be useful for both, measurement of rate constants [158] as well as to elucidate the effects of receptor trafficking as an input to downstream signalling cascades [161, 133]. From a therapeutic point of view, the EGFR system has shown to be a promising target in cancer therapy [6, 7]. Several agents, including therapeutic proteins such as monoclonal antibodies (mAbs), have been developed to specifically target the EGFR with some already approved for drug treatment [5, 47, 112].

2.5 A detailed cell level model of receptor mediated endocytosis

There is a considerable amount of literature about detailed mechanistic descriptions of receptor trafficking systems in the systems biology literature (see, e.g., [139, 161] and references therein). Based on these receptor trafficking systems, our approach is to build a general detailed mechanistic model of RME that takes into account the most relevant kinetic processes of drug binding and receptor trafficking inside the cell. Detailed models derived from the underlying biochemical reaction network have the advantage of a mechanistic interpretation of the kinetic processes and estimated parameters. In [125], a cell-level model of the cytokine granulocyte colony-stimulating factor (G-CSF) and its receptor was incorporated into a pharmacokinetic/pharmacodynamic model to allow for analyzing the life span and potency of the ligand *in vivo*. However, often these advantages come along with the disadvantage of containing more parameters which, e.g., in population PK analysis of clinical trials may result in poorer performance in the model selection process, since models containing more parameters are usually penalized by the corresponding model selection criteria. In this Section, we present a detailed mechanistic model of RME that explicitly takes into account receptor binding and trafficking inside the cell. This model is in the subsequent Sections used to derive reduced models of RME which are suitable for PK analysis and at the same time retain a mechanistic interpretation.

In the following description the term 'ligand' refers to both, a physiological ligand as well as an exogenous drug ligand, since the described processes are identical for both. We propose the following detailed model of RME of a ligand as schematically represented in Fig. 2.3.

The ligand L_{ex} is present in the extracellular space and reversibly binds to free receptor R_{m} at the cell membrane with association rate constant k_{on} to form the ligand-receptor complex RL_{m} that dissociates with rate constant k_{off}. The complex is internalized with the rate constant k_{interRL} forming an endosome. The internalized ligand-receptor complex RL_{i} is either recycled to the membrane with the rate constant k_{recyRL}, degraded with the rate constant

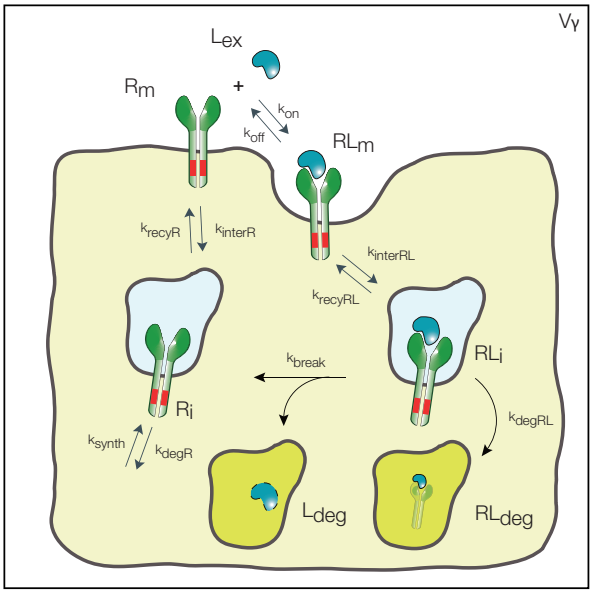

Figure 2.3: *Schematic representation of the detailed model of receptor mediated endocytosis. See text for description.*

k_{degRL} to $\mathrm{RL}_{\mathrm{deg}}$, or dissociates with the rate constant k_{break}. The dissociation results in the subsequent degradation of the ligand L_{deg} and the availability of the free receptor R_{i} inside the cell. Free intracellular receptor R_{i} is recycled to the membrane with the rate constant k_{recyR} and free membrane receptor R_{m} is internalized with the rate constant constant k_{interR}. Inside the cell, the receptor R_{i} is produced with the rate k_{synth} and degraded with the rate constant k_{degR}.

Based on the law of mass action, the rates of change for the various molecular species are given by the following system of ordinary differential equations (ODEs):

$$\begin{aligned}
\mathrm{d}L_{\mathrm{ex}}/\mathrm{d}t &= k_{\mathrm{off}} \cdot RL_{\mathrm{m}} - k_{\mathrm{on}}/(V_\gamma N_A) \cdot R_{\mathrm{m}} \cdot L_{\mathrm{ex}} && (2.3)\\
\mathrm{d}R_{\mathrm{m}}/\mathrm{d}t &= k_{\mathrm{off}} \cdot RL_{\mathrm{m}} - k_{\mathrm{on}}/(V_\gamma N_A) \cdot R_{\mathrm{m}} \cdot L_{\mathrm{ex}} + k_{\mathrm{recyR}} \cdot R_{\mathrm{i}} \\
&\quad -k_{\mathrm{interR}} \cdot R_{\mathrm{m}} && (2.4)\\
\mathrm{d}RL_{\mathrm{m}}/\mathrm{d}t &= k_{\mathrm{on}}/(V_\gamma N_A) \cdot R_{\mathrm{m}} \cdot L_{\mathrm{ex}} - k_{\mathrm{off}} \cdot RL_{\mathrm{m}} - k_{\mathrm{interRL}} \cdot RL_{\mathrm{m}} \\
&\quad +k_{\mathrm{recyRL}} \cdot RL_{\mathrm{i}} && (2.5)\\
\mathrm{d}RL_{\mathrm{i}}/\mathrm{d}t &= k_{\mathrm{interRL}} \cdot RL_{\mathrm{m}} - k_{\mathrm{break}} \cdot RL_{\mathrm{i}} - k_{\mathrm{recyRL}} \cdot RL_{\mathrm{i}} \\
&\quad -k_{\mathrm{degRL}} \cdot RL_{\mathrm{i}} && (2.6)\\
\mathrm{d}R_{\mathrm{i}}/\mathrm{d}t &= k_{\mathrm{interR}} \cdot R_{\mathrm{m}} - k_{\mathrm{recyR}} \cdot R_{\mathrm{i}} + k_{\mathrm{break}} \cdot RL_{\mathrm{i}} - k_{\mathrm{degR}} \cdot R_{\mathrm{i}} \\
&\quad +k_{\mathrm{synth}} && (2.7)
\end{aligned}$$

where N_A is Avogadro´s number and V_γ is the volume of extracellular space per cell. In the above equations, all variables are expressed in number of molecules. All parameters

are first-order rate constants in units [1/time] except for k_{synth}, which is a zero-order rate constant in units [molecules/time], and k_{on} which is a second-order rate constant in units [1/(concentration·time)]. The factor $1/(V_\gamma N_A)$ ensures conversion of units from molar concentration to number of molecules. With respect to the receptor, the above equations comprise the following three overall processes (cf. Fig. 2.3): (1) synthesis and degradation; (2) distribution of the different receptor species within and between the cytoplasm and the cell membrane, and (3) ligand-receptor interaction. With respect to the ligand, its disposition processes consist of the three overall processes: (i) binding to the receptor; (ii) internalization of the ligand-receptor complex; and (iii) intracellular degradation.

Table 2.1: *Parameter values for the EGF/EGFR system. All parameter values have been extracted from Hendriks et al. [55, 53] and Shankaran et al. [133]. See also Section "RME for the EGF/EGFR system".*

	Parameter	**Unit**	**Value**
1	k_{on}	$nM^{-1} \cdot h^{-1}$	5.82
2	k_{off}	h^{-1}	14.4
3	$R_{\text{m}}^{(SS)}$	molecules	$2 \cdot 10^5$
4	k_{recyR}	h^{-1}	3.84
5	k_{interR}	h^{-1}	4.2
6	k_{degR}	h^{-1}	0.96
7	k_{recyRL}	h^{-1}	1.2
8	k_{interRL}	h^{-1}	15
9	k_{degRL}	h^{-1}	1.2
10	V_γ	$l \cdot cell^{-1}$	$4 \cdot 10^{-10}$

The detailed model and its subsequent derived reduced versions will be analyzed using experimentally measured parameters for the degradation of the epidermal growth factor, binding to the epidermal growth factor receptor and subsequent internalization [55, 53]. The rate constants of the corresponding reactions are listed in Table 2.1.

Hendriks et al. [55, 53] explored EGF as ligand to measure rate constants of the EGFR system. However, not all rate constants of the herein proposed detailed model of RME were *explicitly* measured in [55, 53]. Since EGF is predominantly degraded from the EGF-receptor complex [139] rather than from the free form, we set $k_{\text{break}} = 0$ resulting in $k_{\text{lyso}} = k_{\text{degRL}} \neq 0$. Since the parameter k_{synth} was not available in literature, we used the steady state assumption for the receptor system prior to any ligand administration and the experimentally measured steady state number of membrane receptor $R_{\text{m}}^{(SS)}$ [133] to determine k_{synth} using the relation

$k_{\text{synth}} = k_{\text{degR}} \cdot R_{\text{i}}^{(SS)}$ with $R_{\text{i}}^{(SS)} = R_{\text{m}}^{(SS)} \cdot k_{\text{interR}}/k_{\text{recyR}}$. The initial number of receptors are $R_{\text{m}}(0) = R_{\text{m}}^{(SS)}$, $R_{\text{i}}(0) = R_{\text{i}}^{(SS)}$, and $RL_{\text{m}}(0) = RL_{\text{i}}(0) = 0$; the initial concentration of extracellular ligand is $L_{\text{ex}}(0) = 40$ nM.

2.6 Model reduction

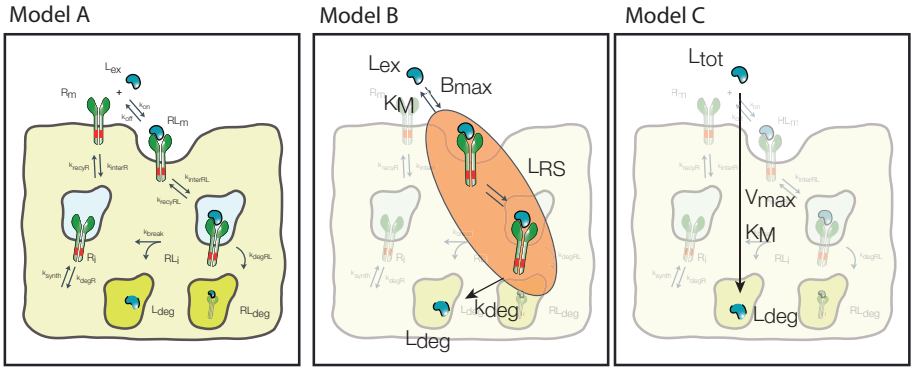

Figure 2.4: *Models of receptor mediated endocytosis of different resolution: Detailed model (Model A), reduced model of saturable distribution into the receptor system with linear degradation (Model B), and reduced model of saturable degradation (Model C). See text for details.*

One objective of this study is to derive and analyze reduced models of RME that capture the impact of receptor dynamics on the distribution and elimination of a ligand and that still allow for a *mechanistic* interpretation. While during short time intervals the transient redistribution processes between the different receptor species R_{m}, RL_{m}, RL_{i} and R_{i} may be of interest, these are usually assumed to be negligible on time scales of interest in pharmacokinetics. Therefore, our approach to reduce the detailed RME model will be based on the assumption that the receptor species R_{m}, RL_{m}, RL_{i} and R_{i} are in quasi-steady state. In order to finally derive reduced models of RME, it is necessary to make an additional assumption on the time-scale of receptor synthesis and degradation. We distinguish the following two scenarios: (1) the time scale of receptor synthesis and degradation is *slow* in comparison to the time scale of ligand disposition. In this case, we formally set $k_{\text{synth}} = k_{\text{degR}} = k_{\text{degRL}} = 0$. As a consequence, the total number of receptors in the system remains constant. Or, (2) the time scale of receptor synthesis and degradation is *fast*, i.e., comparable to the redistribution processes of the different receptor species. The reduced models are derived under the quasi-steady state assumption that the receptor redistribution processes are much faster than the ligand pharmacokinetics. This assumption is of the same type as the assumption underlying the Michaelis- Menten model of enzyme reactions, where it is assumed that the complex formation, dissociation and catalytic transformation are much faster than the transformation of substrate into product. In order to finally derive reduced models, we have to make an additional assumption on the time-scale of receptor synthesis and degradation. There are three different

scenarios: receptor synthesis and degradation is (i) as fast as receptor redistribution (or faster); (ii) slower than the time scale of ligand pharmacokinetics; or (iii) at an intermediate time scale, i.e., comparable or faster than ligand PK but slower than receptor redistribution. The first two scenarios correspond to our *fast* and *slow* scenario. Under these assumptions it is possible to either treat receptor synthesis and degradation the same way as the redistribution processes (in the *fast* scenario) or neglect it and treat the total amount of receptor as a constant (in the *slow* scenario), since in the latter it would not impact the total number of receptors on the time scale of interest.

Both scenarios will be used in the following to establish a link between the reduced and the detailed model.

In the third scenario, however, receptor synthesis and degradation would need to be taken into account in terms of an additional ODE. Unless further assumptions are made, this would require to consider the full system of eqs. (2.3)-(2.7)—which is not suitable for PK parameter estimation in clinical trials.

Reduced model of saturable distribution into the receptor system and linear degradation (Model B)

The idea in deriving a reduced model of RME is to use the quasi-steady state assumption for the receptor system (RS). This transforms the differential equations (2.4)-(2.7) into algebraic equations for $R_{\mathrm{m}}, RL_{\mathrm{m}}, RL_{\mathrm{i}}, R_{\mathrm{i}}$. For a given number of extracellular ligand molecules L_{ex}, these algebraic equations can be solved explicitly. This allows us to compute the total number of ligand molecules in the receptor system $L_{\mathrm{RS}} = RL_{\mathrm{m}} + RL_{\mathrm{i}}$ as a function of the extracellular number of ligands L_{ex}. Based on L_{RS}, the quasi-steady state number of intracellular ligand-receptor complexes RL_{i} can be computed, which determines the extent of elimination.

Model B describes the evolution of the total number of ligands $L_{\mathrm{tot}} = L_{\mathrm{ex}} + L_{\mathrm{RS}}$ in form of the following ODE:

$$\begin{aligned} \mathrm{d}L_{\mathrm{tot}}/\mathrm{d}t &= -k_{\mathrm{deg}} L_{\mathrm{RS}} \quad \text{with} && (2.8)\\ L_{\mathrm{RS}} &= \frac{B_{\max} L_{\mathrm{ex}}}{K_M + L_{\mathrm{ex}}} && (2.9)\\ L_{\mathrm{ex}} &= \frac{1}{2}\Big(L_{\mathrm{tot}} - B_{\max} - K_M + \\ &\qquad \sqrt{(L_{\mathrm{tot}} - B_{\max} - K_M)^2 + 4K_M L_{\mathrm{tot}}}\Big). && (2.10) \end{aligned}$$

The equations comprise three parameters: the maximal ligand binding capacity $B_{\max}$ of the receptor system (in units molecules), the number of extracellular ligand molecules corresponding to a half-maximal binding capacity K_M (in units molecules), and the degradation rate k_{deg} (in units 1/time). In this reduced model the combination of saturable distribution and linear degradation results in the overall saturable elimination of the ligand.

For the two scenarios of *slow* or *fast* receptor synthesis and degradation, the functional relation between the parameters $B_{\max}$, K_M and $k_{\deg}$ and the parameters of the detailed model of RME can be established. In the case of *slow* receptor synthesis and degradation, it is

$$B_{\max} = R_0 \cdot \frac{k_{\text{break}} + k_{\text{recyRL}} + k_{\text{interRL}}}{k_{\text{break}} + k_{\text{interRL}} + k_{\text{recyRL}} + k_{\text{interRL}} \cdot k_{\text{break}}/k_{\text{recyR}}} \tag{2.11}$$

$$K_M = K_D \cdot \frac{V_\gamma N_A \cdot k_{\text{break}} \left(1 + \frac{k_{\text{interRL}}}{k_{\text{off}}} + \frac{k_{\text{recyRL}}}{k_{\text{break}}}\right)}{k_{\text{break}} + k_{\text{interRL}} + k_{\text{recyRL}} + k_{\text{interRL}} \cdot k_{\text{break}}/k_{\text{recyR}}} \tag{2.12}$$

$$k_{\deg} = \frac{k_{\text{break}} \cdot k_{\text{interRL}}}{k_{\text{interRL}} + k_{\text{break}} + k_{\text{recyRL}}}, \tag{2.13}$$

where R_0 is the total number of receptors and $K_D = k_{\text{off}}/k_{\text{on}}$ denotes the dissociation constant of the ligand-receptor complex. In the case of *fast* receptor synthesis and degradation, the relation between the parameters is

$$B_{\max} = \frac{k_{\text{synth}}}{k_{\text{degR}}} \cdot \frac{k_{\text{recyR}} \cdot (k_{\text{recyRL}} + k_{\text{lyso}} + k_{\text{interRL}})}{k_{\text{interRL}} \cdot (k_{\text{lyso}} + k_{\text{recyR}} \cdot k_{\text{degRL}}/k_{\text{degR}})} \tag{2.14}$$

$$K_M = K_D \cdot \frac{V_\gamma N_A \cdot k_{\text{interR}} \cdot (k_{\text{recyRL}} + k_{\text{lyso}} + k_{\text{interRL}} \cdot k_{\text{lyso}}/k_{\text{off}})}{k_{\text{interRL}} \cdot (k_{\text{lyso}} + k_{\text{recyR}} \cdot k_{\text{degRL}}/k_{\text{degR}})} \tag{2.15}$$

$$k_{\deg} = \frac{k_{\text{lyso}} \cdot k_{\text{interRL}}}{k_{\text{interRL}} + k_{\text{lyso}} + k_{\text{recyRL}}}, \tag{2.16}$$

with $k_{\text{lyso}} = k_{\text{break}} + k_{\text{degRL}}$.

Reduced model of saturable degradation (Model C)

The proposed Model C (see Fig. 2.4C) is a further reduction of Model B. It is based on the additional assumption that the amount of ligand distributed into the receptor system is negligible in comparison to the total amount of ligand molecules, i.e., $L_{\text{tot}} = L_{\text{ex}} + L_{\text{RS}} \approx L_{\text{ex}}$. More formally, Model C can be derived from Model B under the assumption

$$\frac{B_{\max}}{K_M + L_{\text{ex}}} \ll 1, \tag{2.17}$$

which implies $L_{\text{RS}} \ll 1$ and thus $L_{\text{tot}} \approx L_{\text{ex}}$ from eq. (2.9). Substituting L_{ex} by L_{tot} in eq. (2.9) and L_{RS} into eq. (2.8) yields the ODE for the total number of ligand molecules:

$$\mathrm{d}L_{\text{tot}}/\mathrm{d}t = -\frac{V_{\max} L_{\text{tot}}}{K_M + L_{\text{tot}}}. \tag{2.18}$$

The model comprises two parameters: the maximal elimination rate of ligand molecules $V_{\max}$ (in units molecules/time) and the number of ligand molecules K_M, at which the elimination

rate is half-maximal. Exploiting the relation

$$V_{\max} = k_{\text{deg}} \cdot B_{\max}, \tag{2.19}$$

we obtain the functional relations between $V_{\max}$ and the parameters of the detailed model of RME (Model A). In the case of *slow* receptor synthesis and degradation, the functional relationship is given by

$$V_{\max} \quad = \quad R_0 \cdot \frac{k_{\text{break}} \cdot k_{\text{interRL}}}{k_{\text{break}} + k_{\text{interRL}} + k_{\text{recyRL}} + k_{\text{interRL}} \cdot k_{\text{break}}/k_{\text{recyR}}} \tag{2.20}$$

and K_M is defined as in eq. (2.12). In the case of *fast* receptor synthesis and degradation, it is

$$V_{\max} \quad = \quad \frac{k_{\text{synth}}}{k_{\text{degR}}} \cdot \frac{k_{\text{lyso}} \cdot k_{\text{recyR}}}{k_{\text{lyso}} + k_{\text{recyR}} \cdot k_{\text{degRL}}/k_{\text{degR}}} \tag{2.21}$$

and K_M is defined as in eq. (2.15).

2.7 Integration of RME into compartmental PK models

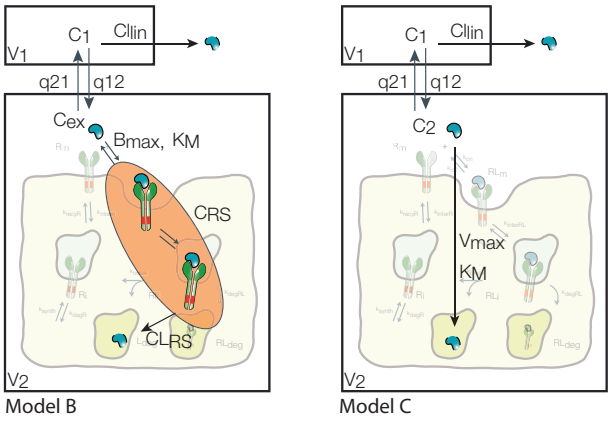

Figure 2.5: *Two two-compartment models with linear clearance from the central compartment and RME based on Model B (left) and Model C (right) in the peripheral compartment.*

In order to facilitate the transfer of reduced models of RME into compartmental PK models underlying PK data analysis and for use in the example of therapeutic protein receptor interaction, we explicitly state the system of ODEs for a two-compartment PK model. The model comprises a central compartment (volume V_1 (in units volume) and ligand concentration C_1 (in units mass/volume)) from which linear elimination CL_{lin} (in units volume/time) takes place and a peripheral compartment (volume V_2 and total ligand concentration C_2), where saturable elimination via receptor mediated endocytosis CL_{RS} takes place (see Figure 2.5). In

the peripheral compartment, we further distinguish between the concentration C_{RS} within the receptor system and the extracellular concentration C_{ex}. The inter-compartmental transfer flows are denoted by q_{12} and q_{21} (in units volume/time).

As in this Chapter we are interested in how to represent RME in PK models, the below mentioned system of ODEs based on the reduced Models B and C represent the proposed structural PK model that can be used for parameter estimation in PK data analysis of non-clinical and clinical trials. The parameter values are determined by performing a fit of the model to the specific *in vivo* data. Alternatively, the model might be used to scale-up *in vitro* derived RME parameter values to the *in vivo* situation.

If Model B is used to describe the elimination by RME, the system of ODEs is

$$
\begin{aligned}
V_1 \cdot \mathrm{d}C_1/\mathrm{d}t &= q_{21} \cdot C_{\mathrm{ex}} - q_{12} \cdot C_1 - \mathrm{CL}_{\mathrm{lin}} \cdot C_1 + \mathrm{dosing} && (2.22)\\
V_2 \cdot \mathrm{d}C_2/\mathrm{d}t &= q_{12} \cdot C_1 - q_{21} \cdot C_{\mathrm{ex}} - \mathrm{CL}_{\mathrm{RS}} \cdot C_{\mathrm{RS}}, \quad \text{with} && (2.23)\\
C_{\mathrm{RS}} &= \frac{B_{\max} \cdot C_{\mathrm{ex}}}{K_M + C_{\mathrm{ex}}} && (2.24)\\
C_{\mathrm{ex}} &= \frac{1}{2}\Big(C_2 - B_{\max} - K_M + \sqrt{(C_2 - B_{\max} - K_M)^2 + 4K_M C_2}\Big), && (2.25)
\end{aligned}
$$

where dosing denotes a mass inflow (in units mass/time) of, e.g., an i.v. infusion over a given time. The parameter $B_{\max}$ denotes the total maximal ligand binding capacity in mass per volume or mol per volume, K_M denotes the concentration at which the binding capacity is half-maximal, $\mathrm{CL}_{\mathrm{lin}}$ and $\mathrm{CL}_{\mathrm{RS}}$ denote the total elimination capacities (in units volume/time). In terms of parameter estimation, the PK model contains eight parameters: V_1, V_2, q_{12}, q_{21}, $\mathrm{CL}_{\mathrm{lin}}$, $\mathrm{CL}_{\mathrm{RS}}$, $B_{\max}$ and K_M, plus additional variables relating to dosing.

If Model C is used to describe the elimination by RME, the system of ODEs is

$$
\begin{aligned}
V_1 \cdot \mathrm{d}C_1/\mathrm{d}t &= q_{21} \cdot C_2 - q_{12} \cdot C_1 - \mathrm{CL}_{\mathrm{lin}} C_1 + \mathrm{dosing} && (2.26)\\
V_2 \cdot \mathrm{d}C_2/\mathrm{d}t &= q_{12} \cdot C_1 - q_{21} \cdot C_2 - \frac{V_{\max} \cdot C_2}{K_M + C_2}, && (2.27)
\end{aligned}
$$

where $V_{\max}$ denotes the total maximal elimination (in units mass/ time), and all remaining parameters are defined as above. In terms of parameter estimation, the PK model contains seven parameters: V_1, V_2, q_{12}, q_{21}, $\mathrm{CL}_{\mathrm{lin}}$, $V_{\max}$ and K_M, in addition to the parameters relating to dosing.

If the reduced models of RME are used as part of structural PK models to estimate parameters in the course of clinical data analysis, the question arises whether or not the identified RME parameters $B_{\max}$, K_M, k_{deg} and $V_{\max}$ allow for a mechanistic interpretation, e.g., whether $B_{\max}$ can be interpreted as the maximal RME ligand binding capacity. This question is tightly linked to the question of identifiability of model parameters, sometimes referred to

as the inverse problem. Identifiability has been studied in detail in the context of compartmental models (see, e.g., [46, Chap. 5-9]). In general, the identifiability of model parameters depends on the structural model (number of compartments, compartment to which the RME process is linked, existence of additional routes of elimination etc.), prior knowledge of model parameters and the quality of the experimental design [46, Chap. 5].

2.8 Protein distribution and elimination by RME

With respect to the pharmacokinetics of therapeutic proteins, two aspects of RME are of particular importance:

1. distribution as a consequence of the drug binding to the receptor and subsequent internalization of the complex; and
2. elimination as a consequence of endocytosis.

Unfortunately both processes typically cannot be differentiated experimentally in pharmacokinetics. Model B explicitly takes into account the amount of drug L_{RS} distributed in the receptor system and the elimination by intracellular degradation, e.g., lysosomes. While the elimination is a linear process in terms of L_{RS}, the distribution into the receptor system itself is a saturable process, specified in terms of $B_{\max}$ and K_M. Model C is derived from model B by assuming in addition that L_{RS} is negligible in comparison to the extracellular amount L_{ex}. In view of the above two sub-processes, this is equivalent to the assumption that the distributional aspect of RME can be neglected. Notably, even if the distributional aspect is negligible, the receptor system could still very efficiently transport ligand molecules into the cell, where they are subsequently degraded. This can be explained from eq. (2.19). It states that the maximal elimination rate $V_{\max}$ is the product of the maximal ligand binding capacity $B_{\max}$ and the degradation rate constant k_{deg}. The maximal elimination rate $V_{\max}$ may still be large due to a large k_{deg}, even if $B_{\max}$ is small. The latter implies a negligible amount of ligand L_{RS} within the receptor system. The receptor system acts as a mechanism that transports ligand molecules into the cell to eventually degrade them. Whether or not the receptor system also serves as a distribution phase is independent from the elimination aspect. This yields the following guidance for the usage of the two reduced models:

Model B: Elimination *and* distribution of ligand into the receptor system are important processes to be considered.

Model C: The distribution of ligand into the receptor system can be neglected, only the elimination process is important, which in this case is non-linear.

Based on Model B and the computable criterion (2.17) it can easily be checked whether the condition for the applicability of Model C are fulfilled. This will be demonstrated for the EGF/EGFR system in Section 2.10 (see Figures. 2.6 and 2.7).

The elimination process of RME is specified in terms of the parameters $V_{\max}$ and K_M. Noteworthy, the maximal elimination rate $V_{\max}$ is *independent* of the processes of complex formation (k_{on}) and dissociation (k_{off}) of the receptor-ligand complex. However, the parameters k_{on} and k_{off} influence the amount of extracellular ligand molecules K_M, at which the elimination rate is half-maximal.

2.9 Nonlinear PK caused by RME

In this Section, we investigate the extent of nonlinearity in the context of the Michaelis-Menten model defined in eqs. (2.26)-(2.27). We aim to examine the effect of drug and cell properties on the nonlinearity of the pharmacokinetics, e.g., different drug affinities to the receptor (different k_{on} and k_{off} values) or different rates of internalization and recycling of the drug in different cells.

In the chosen setting of the two-compartment PK model (cf. eqs. (2.26)-(2.27)), the total clearance CL_{tot} is given by

$$\text{CL}_{\text{tot}} \;=\; \text{CL}_{\text{lin}} + \text{CL}_{\text{RS}} \;=\; \text{CL}_{\text{lin}} + \frac{V_{\max}}{K_M + C}, \tag{2.28}$$

where C denotes the relevant ligand concentration in the RME compartment (e.g., C_2 in eq. (2.27)). While the linear clearance is constant, the clearance attributed to RME varies between $V_{\max}/K_M$ for small ligand concentrations and 0 for high ligand concentrations. Therefore, we consider the quotient $V_{\max}/K_M$ as a measure of the extent of nonlinearity, i.e., the increase in total clearance for small ligand concentrations.

In order to jointly analyze the *slow* and the *fast* receptor synthesis and degradation scenario, we set

$$R_0 \;=\; R_{\text{m}} + R_{\text{i}} \;=\; \frac{k_{\text{synth}}}{k_{\text{degR}}} \cdot \left(1 + \frac{k_{\text{interR}}}{k_{\text{recyR}}}\right) \tag{2.29}$$

and replace the quotient $k_{\text{synth}}/k_{\text{degR}}$ in eq. (2.21) by $R_0/(1 + k_{\text{interR}}/k_{\text{recyR}})$ according to eq. (2.29). Moreover, we extend the definition of k_{lyso} to the *slow* scenario by setting $k_{\text{lyso}} = k_{\text{break}}$ in this case (note: for the *fast* scenario $k_{\text{lyso}} = k_{\text{break}} + k_{\text{degRL}}$). Then, the extent of nonlinearity for both, the *fast* and the *slow* scenario, is given by

$$\frac{V_{\max}}{K_M} = \frac{R_0}{V_\gamma N_A} \cdot \frac{k_{\text{on}}}{\frac{k_{\text{off}}}{k_{\text{interRL}}}\left(1 + \frac{k_{\text{recyRL}}}{k_{\text{lyso}}}\right) + 1} \cdot \left(\frac{1}{\left(1 + \frac{k_{\text{interR}}}{k_{\text{recyR}}}\right)\left(\frac{k_{\text{interR}}}{k_{\text{recyR}}}\right)}\right)^p, \tag{2.30}$$

where $p = 0$ for the *slow* scenario and $p = 1$ for the *fast* scenario. The above equation allows us to study in detail the influence of the various parameters on the extent of nonlinearity.

It can be inferred from Table 2.2 that ligand-specific, receptor system-specific as well as

mixed parameters influence the extent of nonlinearity of the PK: nonlinearity increases for higher affinity drugs (k_{on}) and cell types, which have a higher receptor concentration at the surface of the cell membrane (R_0, k_{recyR}) and faster degradation processes (k_{lyso} etc). In contrast, higher values of k_{off}, k_{recyRL} and higher k_{interR}, k_{degR} will decrease the extent of nonlinearity by resulting in a lower number of intracellular ligand receptor complexes, free receptor molecules, or a smaller number of receptor molecules at the cell surface membrane.

Table 2.2: *Contribution of the different parameters to the extent of nonlinearity. With increasing value of the corresponding parameter the extent of nonlinearity will increase (▲) or decrease (▼). For each parameter, it is indicated by RS or L whether it is related to the receptor system or the ligand, respectively.*

	Parameter	Nonlinearity	RS or L
1	R_0	▲	RS
2	k_{recyR}	▲	RS
3	k_{on}	▲	L
4	k_{lyso}	▲	RS & L
5	k_{interRL}	▲	RS & L
6	k_{off}	▼	L
7	k_{interR}	▼	RS
8	k_{recyRL}	▼	RS & L

In order to more clearly highlight the contribution of the dissociation constant K_D, we also give the following alternative representation of eq. (2.30):

$$\frac{V_{\max}}{K_M} = \frac{R_0}{V_\gamma N_A} \cdot \frac{1}{K_D} \cdot \frac{1}{\frac{1}{k_{\text{interRL}}}\left(1 + \frac{k_{\text{recyRL}}}{k_{\text{lyso}}}\right) + \frac{1}{k_{\text{off}}}} \cdot \left(\frac{1}{\left(1 + \frac{k_{\text{interR}}}{k_{\text{recyR}}}\right)\left(\frac{k_{\text{interR}}}{k_{\text{recyR}}}\right)}\right)^p . \tag{2.31}$$

As can be inferred from the above relation, the extent of nonlinearity can be very different for ligands with the same dissociation constant K_D, but different absolute values of k_{off}. The difference depends on the relative magnitude of the two terms in the first denominator in eq. (2.31), i.e., $1/k_{\text{off}}$ to $1/k_{\text{interRL}} \cdot (1 + k_{\text{recyRL}}/k_{\text{lyso}})$.

2.10 Case study: modelling zalutumumab (2F8) disposition

The analysis of drug-EGFR interaction are performed using data from the monoclonal antibody zalutumumab (2F8), as published by Lammerts van Bueren et al. [147]. Zalutumumab is a human IgG1 EGFR antibody that potently inhibits tumor growth in xenograft mod-

els and has shown encouraging antitumor results in a phase I/II clinical trial [13, 8]. We transformed the originally published system of difference equations [147, Supplement] into the corresponding continuous system of ordinary differential equations[1] (ODEs):

$$\frac{\mathrm{d}}{\mathrm{d}t}A_{\mathrm{pl}} = k_{\mathrm{ip}}A_{\mathrm{int}} - k_{\mathrm{pi}}A_{\mathrm{pl}} - k_{\mathrm{el}}A_{\mathrm{pl}} \tag{2.32}$$

$$\frac{\mathrm{d}}{\mathrm{d}t}A_{\mathrm{int}} = k_{\mathrm{pi}}A_{\mathrm{pl}} - k_{\mathrm{ip}}A_{\mathrm{int}} - k_{\mathrm{b}}\left(\frac{\widehat{B}_{\max}(A_{\mathrm{int}}/V_{\mathrm{int}})^h}{(A_{\mathrm{int}}/V_{\mathrm{int}})^h + K_{\mathrm{M}}^h} - A_b\right) \tag{2.33}$$

$$\frac{\mathrm{d}}{\mathrm{d}t}A_{\mathrm{b}} = k_{\mathrm{b}}\left(\frac{\widehat{B}_{\max}(A_{\mathrm{int}}/V_{\mathrm{int}})^h}{(A_{\mathrm{int}}/V_{\mathrm{int}})^h + K_{\mathrm{M}}^h} - A_b\right) - \widehat{k}_{\mathrm{deg}}A_{\mathrm{b}}, \tag{2.34}$$

where A_{pl}, A_{int} and A_{b} represent the amount of therapeutic protein in the plasma, interstitial and binding compartment, respectively; V_{int} the interstitial volume, k_{pi} and k_{ip} the rate constants for transfer between the plasma and interstitial compartment, k_{b} the rate constant for binding to and dissociation from EGFR, and k_{el} the elimination rate constant. Furthermore, $\widehat{k}_{\mathrm{deg}}$ denotes the rate constant for elimination by EGFR internalization and degradation, $\widehat{B}_{\max}$ the maximal binding capacity of the therapeutic protein to EGFR, K_{M} the concentration corresponding to $\widehat{B}_{\max}/2$, and h the Hill factor. The initial amount of drug $A_{\mathrm{pl}}(0)$ and the parameters are listed in Table 2.3. The reported value of $K_{\mathrm{M}} = 0.5\mu$ g/ml did not allow us to reproduce the results in [147, Fig.1A]. Only a value of $K_{\mathrm{M}} = 0.05\mu$ g/ml exactly reproduced the *in silico* data, hence we choose the corrected value for subsequent analyses. Amounts are converted to concentrations by dividing by the corresponding volume.

Transforming the system of ODEs (2.32)-(2.34) from units [mg/kg] to [mg/ml] by dividing by the corresponding volumes yields equations for $C_{pl} = A_{pl}/V_{pl}$, $C_{int} = A_{int}/V_{int}$, $C_b = A_b/V_{int}$, in terms of the following scaled parameters $q_{12} = V_{pl} \cdot k_{pi}$, $q_{21} = V_{int} \cdot k_{ip}$, $\mathrm{CL}_{\mathrm{lin}} = k_{el} \cdot V_{pl}$, $B_{\max} = \widehat{B}_{\max}/V_{int}$, $\mathrm{CL}_{\mathrm{RS}} = \widehat{k}_{deg} \cdot V_{int}$. The model (2.32)-(2.34) scaled to units [mg/ml] can be directly compared to our PK model (2.22)-(2.25) with $C_1 = C_{pl}$, $C_{\mathrm{ex}} = C_{int}$ and $C_{\mathrm{RS}} = C_b$, parameterized with the scaled parameters above. We remark that alternatively, our compartmental PK models could have been stated in units [mg/kg].

Influence of receptor system properties on RME

We illustrate the approximation features of the two reduced models for predicting concentration-time profiles of the ligand in comparison to the detailed model based on the EGF/EGFR system. The initial concentration is $C_{\mathrm{ex}}(0) = 40$ nM. In Fig. 2.6 (left), the predictions of the extracellular EGF concentration C_{ex} is shown for the three Models A, B, & C. All models result in very similar concentration-time profiles: Almost instantaneously, the amount of lig-

[1] The originally published equations in [147, Supplement] are identical to a certain discretization of the system of ODEs (2.32)-(2.34). The advantage of stating the system as continuous ODEs is that subsequently any numerical scheme can be used to solve them, in particular high accuracy ODE solver with adaptive step size control.

Table 2.3: *Parameter values used by Lammerts van Bueren et al. [147]; K_{M} has been corrected, see text for details. V_{pl} represents the plasma volume.*

	Parameter	Unit	Value
1	k_b	h^{-1}	0.069
2	k_{pi}	h^{-1}	0.043
3	k_{ip}	h^{-1}	0.043
4	k_{el}	h^{-1}	0.0055
5	V_{int}	ml	70
6	V_{pl}	ml	35
7	K_M	$\mu g \cdot ml^{-1}$	0.05
8	$\widehat{B}_{max}$	$mg \cdot kg^{-1}$	2
9	$\widehat{k}_{\mathrm{deg}}$	h^{-1}	0.005
10	$A_{\mathrm{pl}}(0)$	$mg \cdot kg^{-1}$	2 and 20
11	h		1.0

and in the RS is in equilibrium. Due to the high concentration of ligand in comparison to the concentration of receptor, the RS is saturated and the ligand is eliminated at a constant rate. Between approximately 40-60 h, the system undergoes a transition from saturated to non-saturated elimination, which is manifested in the linear decline in the final phase (in the semi-logarithmic representation). For the EGF/EGFR system, the detailed model of RME is well approximated by Model B and also by Model C, the latter taking into account only the apparent saturable elimination. Based on the predictions of Model B, we computed the amount of ligand L_{RS} in the receptor system. In accordance with eq. (2.17), L_{RS} is negligible in comparison to the extracellular EGF concentration (cf. Fig 2.7, solid line).

In order to study the impact of L_{RS} on the approximation quality of Model C, we artificially decrease k_{degRL} by a factor of 10. All other parameters of the detailed Model A, including the initial EGF concentration, are identical. Parameters of Model B and C have been recalculated according to eqs. (2.14)-(2.16) and (2.21)+(2.15), respectively, resulting in particular in an increased maximal binding capacity B_{max}. The predictions of the concentration-time profile of the extracellular EGF concentration C_{ex} based on the three Models A, B & C are shown in Fig. 2.6 (right). While Models A and B give almost identical results, the prediction based on Model C differs significantly. Model C over-predicts the extent of elimination by RME. As shown in Figure 2.7 the over-prediction corresponds to periods in time where the assumption (2.17) is violated: While $B_{\mathrm{max}}/(K_M + C_{\mathrm{ex}})$ is small for both settings up to time 60 h, it starts to increase thereafter, in particular for the setting corresponding to Fig. 2.6 (right).

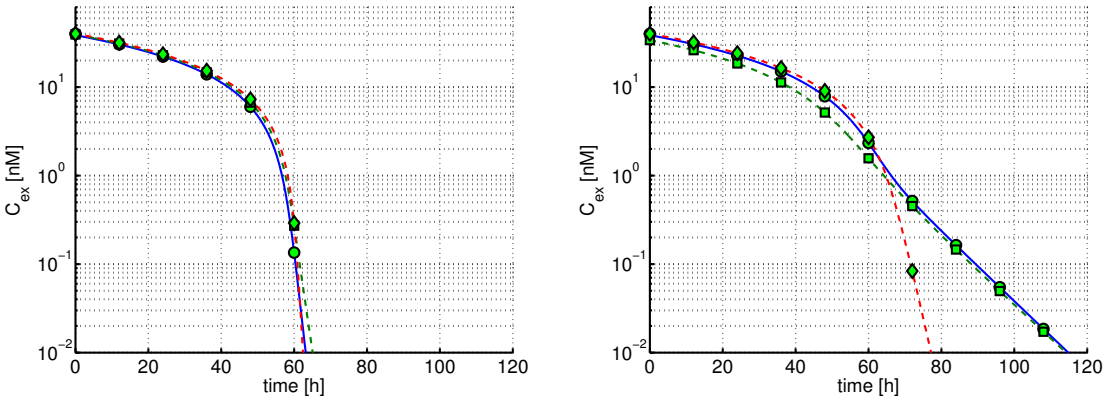

Figure 2.6: *Concentration-time profile of the extracellular ligand concentration for the Model A (), Model B () and Model C (). Left: Parameter values used according to Table 2.1. Right: As in left Figure, but decreasing k_{degRL} 10 fold.*

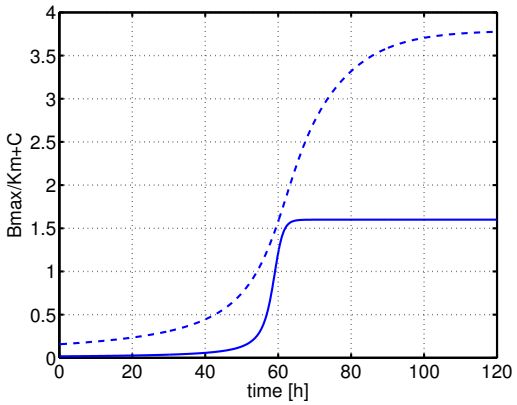

Figure 2.7: *Evolution of the ratio $B_{\max}/(K_M + C_{ex})$ for the two scenarios shown in Fig. 2.6 left () and right ().*

Influence of different cell types on RME

The detailed model A allows us to analyze the influence of processes on the overall disposition of ligand in the extracellular space such as, e.g., the ligand receptor internalization rate constant k_{interRL}. Alterations in k_{interRL} have been observed experimentally [154, 113] and could be the result of a mutation of the EGF receptor. In view of eq. (2.30) we would expect a decrease in the overall elimination capacity with decreasing internalization rate constant k_{interRL}. Figure 2.8 (left) shows the impact of an altered k_{interRL} on the concentration-time course of EGF with $C_{\mathrm{ex}}(0) = 40$ nM. As can be seen, cells with a reduced internalization rate constant $k_{\mathrm{interRL}}/4$ and $k_{\mathrm{interRL}}/16$ show a much lower apparent elimination than the reference cells with the rate constant k_{interRL}. The difference in the apparent elimination does not only depend on the absolute magnitude of change of k_{interRL}, but more precisely on the magnitude of change of $1/k_{\mathrm{interRL}} \cdot (1 + k_{\mathrm{recyRL}}/k_{\mathrm{lyso}})$ in relation to $1/k_{\mathrm{off}}$, as can been

inferred from eq. (2.31). Changes in k_{interRL} will have less impact, if $1/k_{\text{off}}$ is large. This can be seen in Figure 2.8 (right), which shows the same situation as in the left Figure, but with k_{off} decreased by a factor of 100 (we also decreased k_{on} by the same factor in order to keep K_D constant).

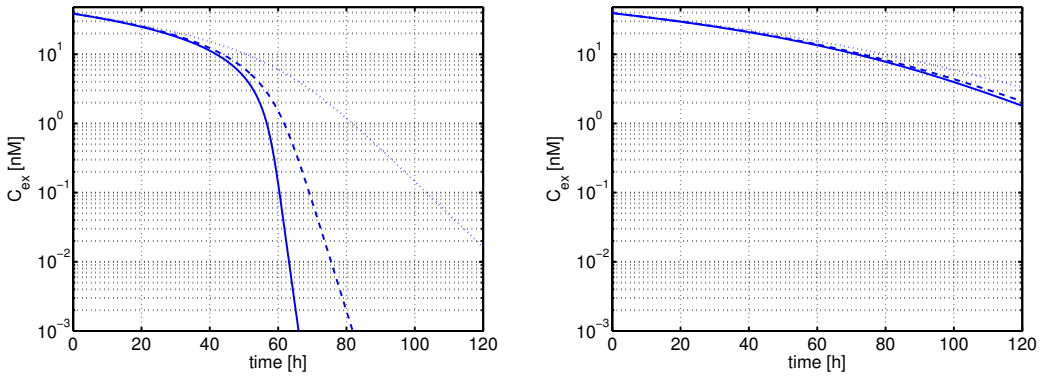

Figure 2.8: *Illustration of the dependence of RME on the rate of internalization using the detailed model of RME (Model A). Parameter values according to Table 2.1. Left: concentration-time profiles of the extracellular ligand EGF (L_{ex}) for three different internalization rate constants of the ligand–receptor complex: k_{interRL} (——), $k_{\text{interRL}}/4$ (– – –), $k_{\text{interRL}}/16$ (- - - -). Right: same as before, but with decreased association and dissociation rate constants: $k_{\text{on}}/100$ and $k_{\text{off}}/100$, respectively. Note that K_D is identical in the left and right graphics.*

In Fig. 2.8, we studied the impact of different internalization rate constants k_{interRL} on RME. An altered k_{interRL} could, e.g., result from a mutation in the EGF receptor, as it has been observed experimentally [154]. Our analysis in Section 2.9 shows that the ligand elimination rate is affected by various processes inside the cell. For example, the elimination rate decreases with decreasing complex internalization rate constant, but the difference is much less pronounced for a ligand with decreased association and dissociation rate constants k_{on} and k_{off}—even though the dissociation constant K_D is the same in both scenarios (see Fig. 2.8, left vs. right). From the detailed Model A, this phenomenon is understandable: given a ligand that forms a complex with rate constant k_{on}, once the ligand-receptor complex is formed at the membrane, its fate is a balance between dissociation (specified in terms of k_{off}) and internalization (specified in terms of k_{interRL}). If, e.g., $k_{\text{off}}/k_{\text{interRL}} \ll 1$ then the complex will predominantely be internalized. Based on K_D alone, this property of receptor systems can not be observed. The ratio $k_{\text{off}}/k_{\text{interRL}}$ has recently been introduced as one of two key parameters to characterize different cell surface receptor systems (termed the consumption parameter) [133]. In general, our analysis shows that reduced ligand elimination from the extracellular space can be due to altered processes inside the cell other than the velocity of internalization of the complex. The influences of the processes can be deduced from eq. (2.30) and is summarized in Table 2.2. The nonlinearity increases with parameters that accelerate' the processes of receptor availability at the surface (R_0, k_{recyR}) or that accelerate' the trans-

port and intracellular degradation of extracellular ligand (k_{on}, k_{interRL}, k_{lyso}). Counteracting processes (related to the parameters k_{off}, k_{interR}, k_{recyRL}) decrease the extent of nonlinearity.

2.11 RME in the monoclonal antibody/EGFR system

In this Section we will illustrate how our unified theoretical approach to RME allows for resolving seemingly contradictory statements about the performance of empirical models of RME. In [147], Lammerts van Bueren et al. reported about a preclinical study involving a mAb against EGFR in monkeys and their subsequent data analysis. They developed the two-compartment pharmacokinetic model comprising a first-order elimination of the mAb from plasma, a binding compartment (representing EGFR-expressing cells) that equilibrates with the interstitial compartment, and a saturable internalization and degradation of bound mAb. Lammerts van Bueren et al. concluded that the observed nonlinear decrease of mAb concentrations in cynomolgus monkeys could not be explained by a saturable elimination in terms of a Michaelis-Menten model and proposed an alternative model, which described the data well. In a different study, the Michaelis- Menten model was reported to successfully describe *in vivo* data for a monoclonal antibody [67].

The model proposed in [147] is comparable to the two-compartment model introduced in the Section 2.7, eqs. (2.22)-(2.25). In order to understand the inferences made by Lammerts van Bueren et al. [147], we simulated their model defined in eqs. (2.32)-(2.34) and compared the results to the correspondingly parameterized Models B and C (see Fig 2.9, left). Since the experimental data presented in [147] were not available and since model simulations and data were reported to be in good agreement, we used the Lammerts van Bueren model as a surrogate for the experimental data. As in [147], we choose a high and low initial mAb input of 2 mg/kg and 20 mg/kg. While the predicted mAb plasma concentrations based on Model B are identical to the prediction based on the Lammerts van Bueren et al. model, predictions based on Model C deviate significantly. A closer inspection reveals that the assumption $B_{\max}/(K_M + C_{\text{ex}}(0)) \ll 1$ is violated for the low dose of 2 mg/kg. Consequently, the amount of mAb inside the RS cannot be neglected and we would expect to see deviations between predictions based on Model B and C. Hence, the use of a Michaelis- Menten based nonlinear elimination in the interstitial compartment, which neglects the drug distributed into the receptor system, leads to an over-prediction of drug elimination by RME (see Figure 2.9, left).

The difference between the predictions based on Model B and C should disappear, if the maximal binding capacity is sufficiently decreased. This is shown in Figure 2.9 (right), where the binding capacity $B_{\max}$ has been decreased to one 20th of its original value.

In summary, the inference made in [147] that a Michaelis- Menten term is not adequate for modeling the nonlinearity present in the data is valid for the specific conditions of their

experimental design. However, this cannot be generalized to a statement about the validity of the Michael- Menten approximation of RME, as can be seen from Fig. 2.9 (right).

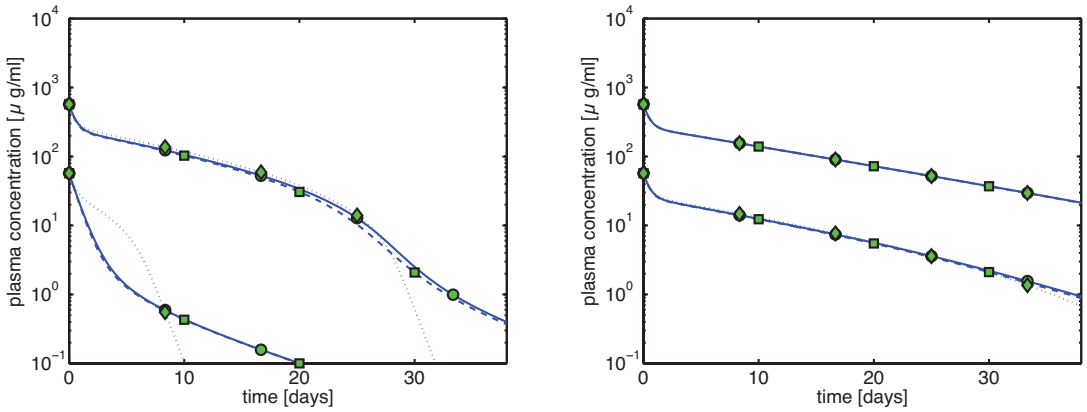

Figure 2.9: *Comparison of model predictions for zalutumumab (2F8) based on the Lammerts van Bueren et al. model (●) and the herein proposed compartment models* (2.22)-(2.25) *(■)and* (2.26)-(2.27) *(◆). Left: parameterization as given in Table 2.3. Right: maximal receptor capacity* $B_{\max}$ *decreased to one 20th of the original capacity.*

2.12 Summary of this chapter

Receptor mediated endocytosis plays a major role in the disposition of therapeutic protein drugs in the body. It is suspected to be a major source of nonlinear pharmacokinetic behavior observed in clinical pharmacokinetic data. So far, mostly empirical or semi-mechanistic approaches have been used to represent RME [30, 77, 102, 67, 147, 35, 137, 135, 136]. A thorough understanding of the impact of the properties of the drug and of the receptor system on the resulting nonlinear disposition was still missing, as is how to best represent RME in pharmacokinetic models. For example, a Michaelis-Menten based RME model as part of a PK model allowed for describing data in one PK data analysis (e.g., [67]), it failed to do so in another (e.g., [147]). Due to lack of a sound theoretical basis to understand the different performances of empirical models, this certainly was an unsatisfactory situation. In this Chapter, we presented a detailed mechanistic model of RME that explicitly takes into account receptor binding and trafficking inside the cell and that is used to derive reduced models of RME which retain a mechanistic interpretation. We find that RME can be described by an extended Michaelis-Menten model that accounts for both the distribution and the elimination aspect of RME. If the amount of drug in the receptor system is negligible a standard Michaelis-Menten model is capable of describing the elimination by RME. The herein presented analysis therefore gives a thorough background of RME and a clear rationale as to when the proposed reduced models are applicable. Notably, a receptor system can efficiently eliminate drug from the extracellular space even if the total number of receptors is small. We

find that drug elimination by RME can result in substantial nonlinear pharmacokinetics. The extent of nonlinearity is higher for drug/receptor systems with higher receptor availability at the membrane, or faster internalization and degradation of extracellular drug.

The analysis of RME in this Chapter elucidates that cell-level target dynamics can have a significant influence on the pharmacokinetics of the drug. By using the here defined functional relations between the parameters of the detailed Model A and the reduced Models B and C we will be able in the following Chapter 3 and 4 to use simpler models of the targeted receptor system and interpret them as reduced models of RME with lumped parameters.

3 The *in vitro* inhibitory effect of therapeutic antibodies

In this Chapter, we will develop a mathematical framework for describing the effect of a promising class of therapeutic proteins, therapeutic antibodies. In more detail, we develop a receptor model which describes the action of the current therapeutic antibodies against the EGFR and describes the time-dependent interactions of the drug, the ligand and the receptor. We aim to develop a mechanistic model of the cell-level processes (as usually done in systems biology) and study a transient drug concentration (as usually done in pharmacokinetic/pharmacodynamic modelling). We are interested in studying *in silico* the result of modifying the antibodies' biophysical properties and predicting the resulting inhibition of the receptor system. In this Chapter we will study the system under conditions of a typical *in vitro* experiment and in the closed microenvironment of a tumor cell *in vivo*. In the following Chapter 4, the here developed cell-level model also will be used as the basis to couple the pharmacokinetics of the drug with therapeutically relevant cellular processes and to study the inhibition under general *in vivo* conditions.

The model focuses on receptor systems where the ligand and the receptor are internalized by RME (which was discussed in chapter 2). RME is important for variety of receptor families [4, 40, 57], including the therapeutically important receptor tyrosine kinase receptors which are activated by growth factors and stimulate tumor growth.

In Chapter 2 we already developed a detailed model of RME (Model A) to derive structures of reduced models. In this Chapter we are interested in making quantitative predictions and therefore have to base our analysis on cell-level models which have been already validated and for which experimentally determined parameter values are available in the literature. In the first part of this Chapter we will present such current kinetic models of receptor activation by ligand binding and receptor trafficking in the literature. Subsequently, we will build our model by including the binding of the antibody to the receptor.

3.1 *Mathematical models for receptor kinetics*

As the basis of the following receptor trafficking models, consider the binding of a ligand L to a receptor R, which forms a complex RL (Fig. 3.1)

Using the principles of mass action kinetics, changes in the number of receptor-ligand

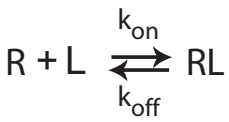

Figure 3.1: *The reversible binding of a ligand to the receptor results in a complex.*

complexes RL can be described by Eq. 3.1.

$$\frac{\mathrm{d}}{\mathrm{d}t}RL = k_{\mathrm{on}} \cdot R \cdot L - k_{\mathrm{off}} \cdot RL. \tag{3.1}$$

The association rate constant k_{on} characterizes the velocity of the second-order interaction between the receptor and the ligand, while the dissociation rate constant k_{off} characterizes the first-order dissociation of the complex.

The early mathematical models describing the activation of receptors on the cells' surface by polypeptide ligands were based on the well developed theory of enzyme kinetics. In this setting, steady-state description of the dynamics of the system were developed [158]. Such models allow to describe cell behavior and to measure parameters under more physiological conditions. A basic model of receptor activation and trafficking based on mass action kinetics was developed by Wiley et al. [158] and Gex-Fabry et al. [45]. The interactions between the considered species are depicted in Fig. 3.2. A free receptor (R) and a free ligand (Ł) can

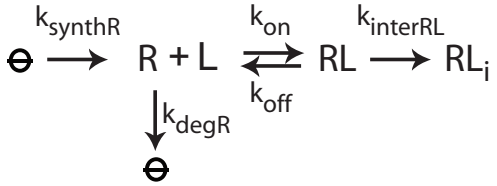

Figure 3.2: *A simple model of receptor activation. The binding of a ligand to the receptor results in a complex which can be internalized by receptor mediated endocytosis. The receptor is subject to a normal turnover described by the synthesis rate and its degradation rate constants.*

reversibly form a complex on the surface of the cell (RL). This complex can be internalized by forming an endosome (RL_{i}). The internalized complex then can degraded by forming a lysosome. The receptor is subject to a normal turnover, described by a synthesis rate (k_{synthR}) and a degradation rate constant (k_{degR}). Interestingly, for many receptor systems the endocytotic rate constant (k_{interRL}), which describes the velocity the complex is getting internalized, is much higher than the normal internalization and degradation rate of the unbound receptor (k_{degR}) [159]. This leads to a decrease in receptors at the cell surface in presence of a ligand, a mechanism referred to as *downregulation* [3, 12, 64, 118, 134].

The developed kinetic and steady-state models of the receptor system were used to measure the rate constants experimentally [159, 68, 86, 160] (a compressive description of the technics can be found in [81]).

An important feature of many receptor systems is the internalization of the receptor. Because receptors and ligands may also be internalized by the process termed endocytosis the model was further extended by considering the internalization and recycling of the free and bound receptor [16, 157] as depicted in Fig. 3.3. There is evidence that this dissociation and

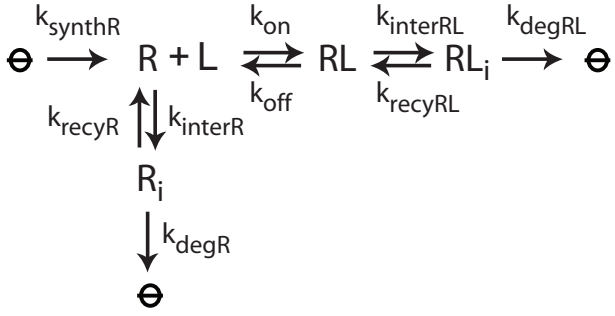

Figure 3.3: *A simple model of receptor activation. The binding of a ligand to the receptor results in a complex which can be internalized by receptor mediated endocytosis. The receptor is subject to a normal turnover described by the synthesis rate and its degradation rate constants.*

the subsequent recycling of the receptor depends on the ligand bound to the receptor. For example the epidermal growth factor (EGF) tends to remain bound to the epidermal growth factor receptor (as described in Fig. 3.3) while transforming growth factor α dissociates from the receptor in the endosome due to a changed pH value and the free receptor may be recycled to the surface [139].

The receptor trafficking model can therefore be extended by the recycling of the free receptor back to the surface (Fig. 3.4). The models discussed above describe the behavior of receptor

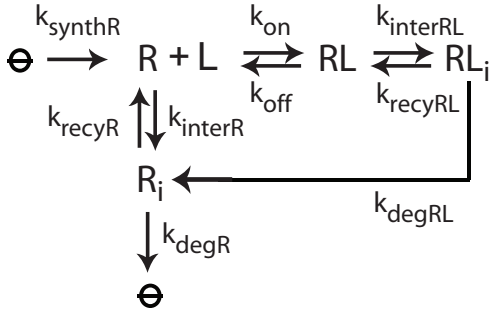

Figure 3.4: *A simple model of receptor activation. The binding of a ligand to the receptor results in a complex which can be internalized by receptor mediated endocytosis. The receptor is subject to a normal turnover described by the synthesis rate and its degradation rate constants.*

systems sharing the common feature of receptor trafficking. They can therefore be used to compare different receptor systems and characterize their behavior by defining specific coefficient of the defined rate constants.

Shankaran et al. recently did this by building such a described generalized kinetic model of receptor-ligand binding and internalization [133]. A given signaling or transport receptor

system then represents a particular implementation of this canonical model with a specific set of kinetic parameters. They identified two parameters, which can characterize the systems as *avidity-controlled*, *consumption-controlled*, or *dual-controlled*. Avidity characterizes how efficiently a receptor system can capture extracellular ligand while the consumption is the partition coefficient quantifying the probability that a captured ligand molecule will be internalized before it dissociates from the receptor. For a receptor system as described in Fig. 3.2 the avidity is defined as

$$\gamma = \frac{k_{\mathrm{onL}}}{k_{\mathrm{offL}}} \frac{R^*}{N_{\mathrm{a}} \cdot V_{cell}}$$

were R^* denotes the steady-state number of molecules of free receptor at the surface at the cell, N_{a} denotes Avagadro's number, and V_{cell} is the volume of extracellular medium per cell. The partition coefficient defining the consumption of the system is defined as

$$\beta = \frac{k_{\mathrm{interRL}}}{k_{\mathrm{offL}}}.$$

The idea presented by Shankaran et al. is that receptors might be sensitive to either one or both coefficients if cellular changes (e.g., due to mutations or genome alterations) leading to a change of the corresponding coefficient also result in a different response of the receptor to the ligand. Changes affecting a coefficient, to which the receptor is not sensitive, will be without consequence for the receptor response.

This sensitivity of the response to changes in the two coefficients can be used to define if the system is

- *avidity-controlled* – changes in the efficiency of capturing extracellular ligands lead to strong changes in the response to a changing ligand concentration
- *consumption-controlled* – changes in the probability that a captured ligand molecule will be internalized before it dissociates from the receptor lead to strong changes in the response to a changing ligand concentration
- *dual-controlled* – changes in both coefficients lead to strong changes in the response to a changing ligand concentration

Interestingly they concluded that changes in the avidity modulates the behavior of the transferrin receptor and low-density lipoprotein receptor systems, whereas the consumption coefficient has a high control over the function of the the vitellogenin receptor. The epidermal growth receptor shows a dual-sensitivity to the coefficients.

3.2 Our mathematical model for the inhibitory effect of therapeutic antibodies

The following analysis of this Chapter is based on a cell-level model which we build by combining the established receptor activation models described in Section 3.1 (Fig. 3.2) with a kinetic model of the mechanism of action of anti-EGFR mAbs. While the drug-ligand interaction together with the experimentally derived parameter values have been inherited from Fig. 3.2, the interaction with the antibody instead of the detailed description of the RME processes used in Chapter 2 has been described by a simpler model. The model corresponds to the mechanism of action of the anti-EGFR mAbs on the market or in clinical development (Zalutumumab, Panitumumab, Cetuximab, IMC-11F8, and Nimotuzumab) [163]. In detail, the reactions included in the model represent the binding of the drug to the receptor and the formation of the drug-receptor complex. All the intracellular distribution processes are lumped into a single net internalization rate of the drug-receptor complex. The extension of the model therefore closely follows the discussed target-mediated drug-disposition models [87]. While the experimentally determined parameter values for receptor activation and trafficking allow to make quantitative prediction, the processes of antibody internalization without experimentally measured rate constants available have been lumped into one downregulation rate. The influence of this downregulation rate on the inhibitory effect will be studied in this Chapter. An important difference between TMDD and the here used submodel is that the receptor dynamics in our model are described on a cell-level instead of the whole body scale. This allows us to study the impact of specific alteration of cells on the inhibitory effect of therapeutic antibodies. The developed model is depicted in Fig. 3.5. In the model, both lig-

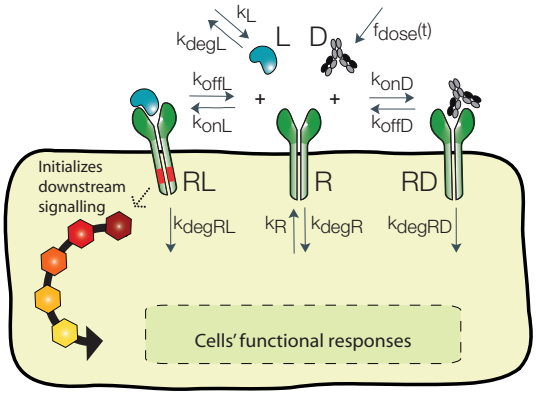

Figure 3.5: *The proposed model of receptor-ligand-drug interaction. The natural ligand and the drug compete for the receptor binding.*

and L and drug D are present in the extracellular space (with volume V). The ligand enters the extracellular space at rate k_L, and is cleared with rate constant k_{degL}. The drug enters the extra-cellular space at rate $f_{dose}(t)$. The free membrane receptor R is produced at rate

k_R and internalized with the rate constant k_{degR}. Both ligand and drug reversibly bind to free receptors R with association rate constant k_{onL} and k_{onD}, respectively, and a dissociation rate constant k_{offL} and k_{offD}, respectively. The resulting ligand-receptor complex RL and drug-receptor complex RD are internalized by forming an endosome with the rate constant k_{degRL} and k_{degRD}, respectively.

Based on the law of mass action, the rates of change for the molecular species are given by the following system of ordinary differential equations (ODEs):

$$\begin{aligned}
\frac{\mathrm{d}\,L}{\mathrm{d}t} &= \frac{k_L}{VN_a} - \frac{k_{onL}}{VN_a} R \cdot L + \frac{k_{offL}}{VN_a} RL - k_{degL} L, \\
\frac{\mathrm{d}\,D}{\mathrm{d}t} &= f_{dose}(t) - \frac{k_{onD}}{VN_a} R \cdot D + \frac{k_{offD}}{VN_a} RD, \\
\frac{\mathrm{d}\,R}{\mathrm{d}t} &= k_R - k_{onL} R \cdot L - k_{onC} R \cdot D + k_{offL} RL \\
&\quad + k_{offD} RD - k_{degR} R, \\
\frac{\mathrm{d}\,RL}{\mathrm{d}t} &= k_{onL} R \cdot L - k_{offL} RL - k_{degRL} RL, \\
\frac{\mathrm{d}\,RL}{\mathrm{d}t} &= k_{onD} R \cdot D - k_{offD} RD - k_{degRD} RD.
\end{aligned} \tag{3.2}$$

The species L and D are expressed in [M]; R, RL and RD are in units [# molecules]. Division by the product of Avogadro's constant N_a and volume V ensures conversion from units [# molecules] to [M]. The non-negative drug dosing rate is given by $f_{dose}(t) = f(t) \cdot \text{dose}$, with

$$\int_0^\infty f(t)\, dt = 1. \tag{3.3}$$

Different dosing regimes can be modeled by choosing $f(t)$ appropriately. Prior to any drug administration, the system is assumed to be in steady state, resulting in some number of active receptor $RL = RL^*$. The effect of the drug results from the inhibition of receptor activation, i.e., from the change in the number of active receptor RL over time.

Parameters

For numerical simulations, we used experimentally determined parameter values [55, 115] for the EGFR system. All receptor system parameters are listed in Tab. 3.1. The association rate constant k_{onD} was set to be similar to the one of EGF while the dissociation rate constant k_{offD} was calculated by $k_{\mathrm{offD}}/k_{\mathrm{onD}} = K_D$ accordingly to $K_{D,drug}$ as stated in Tab. 3.1, which is the affinity of the drug zalutumumab for the EGFR[107]. For the beginning no downregulation was assumed to take place by the antibody (the internalization rate constant of the drug-receptor complex k_{degRD} was set equal to the internalization rate constant of the free receptor k_{degR}). Both, affinity and downregulation will be changed to investigate the optimal biophysical properties of an anti-EGFR antibody.

Table 3.1: *Parameter values for the EGF receptor system. In the absence of ligand the cells were set to have $2 \cdot 10^5$ cell surface receptors (R^*) corresponding to the EGFR level of human mammary epithelial cells [133].*

	Parameter	Unit	Value	
1	k_{degR}	min^{-1}	0.02	[115]
2	R^*		$2 \cdot 10^5$	[133]
3	k_{synthR}	min^{-1}	$k_{\text{degR}} \cdot R^*$	
4	$K_{D,ligand}$	nM	2.47	[55]
5	k_{offL}	min^{-1}	0.24	[55]
6	k_{onL}	$nM^{-1} \cdot min^{-1}$	$k_{\text{offL}}/K_{D,ligand}$	
7	k_{degRL}	min^{-1}	0.15	[115]
8	$K_{D,drug}$	nM	7	[107]
9	k_{offD}	min^{-1}	k_{offL}	
10	k_{onD}	$nM^{-1} \cdot min^{-1}$	$k_{\text{offD}}/K_{D,drug}$	
11	k_{degRD}	min^{-1}	k_{degR}	

For the *in vitro* situation (see Fig. 3.6) the drug is given as a bolus-dose of 10 μg/ml [48] at time $t = 0$ which is represented by choosing f as a delta-distribution at $t = 0$. Also the ligand concentration was 10 ng/ml [48] and assumed to be constant over the time of the experiment by setting k_L and k_{degL} much faster than the other processes. The volume of liquid in the petri dish was set to $4 \cdot 10^{-10}$ l/cell [133].

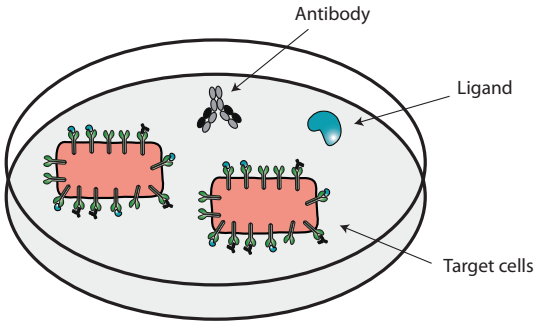

Figure 3.6: In vitro *conditions of cell culture experiments investigating the inhibition of EGFR signalling pathways by antagonistic mAbs*

Inhibitory effect measures

One advantage of the cell-level PK/PD model is its ability to study the interaction of drug and cell properties, like drug-receptor affinity, drug induced receptor internalization. Since we are

investigating a transient inhibitory effect we consider the three following quantitative measures of the response of the number of activated receptors over time (see Fig. 3.7). Following the

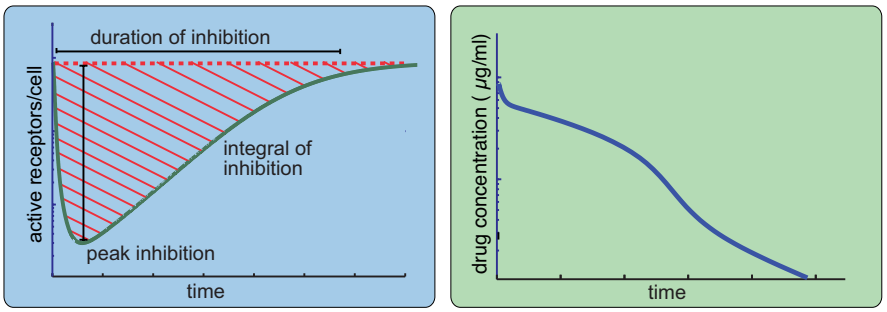

Figure 3.7: *The cellular model of receptor activation and inhibition links an extra-cellular drug concentration (right) to the inhibitory effect on receptor activation (left) and allows for studying three different characteristics of the inhibitory effect: the integral, the peak, and the duration of inhibition.*

administration of the drug the number of active receptors is decreasing because of the drugs inhibitory effect on ligand binding. Subsequently, the drug concentration decreases either because of the internalization of the drug bound to the targeted receptor or target independent metabolization/excretion. Due to the production of receptor we assume that after the drug disappeared, the receptor system goes back to its steady-state activation level from before the treatment. This is the basis of the three transient measures of drug effect presented here and the following mathematical derivation of the effect.

In the following we assume that after the drug The *peak inhibition* is defined as the minimum number of active receptors relative to the steady state, that is,

$$\text{peak} = \frac{RL^* - \min\{RL(t)\}}{RL^*}, \tag{3.4}$$

The *duration of inhibition* is the time it takes for the active receptors to recover back to 99% of the steady-state level. The *integral of inhibition* is the area under the curve of the active receptors with respect to their steady state, i.e.,

$$E = \int_0^\infty (RL^* - RL(t))\, dt. \tag{3.5}$$

3.3 Translating biophysical properties into an inhibitory effect

The cellular model of the mechanism of action of therapeutic antibodies is used in the following to predict the transient response of the receptor system to the presence of the drug in the cells' surrounding. The model generates a trajectory of the receptor species and the drug concentration. This translates the biophysical properties of the drug into a transient change in the number of activated receptors and therefore allows to tune these properties *in silico* for the optimal perturbation of the receptor system of the target cell.

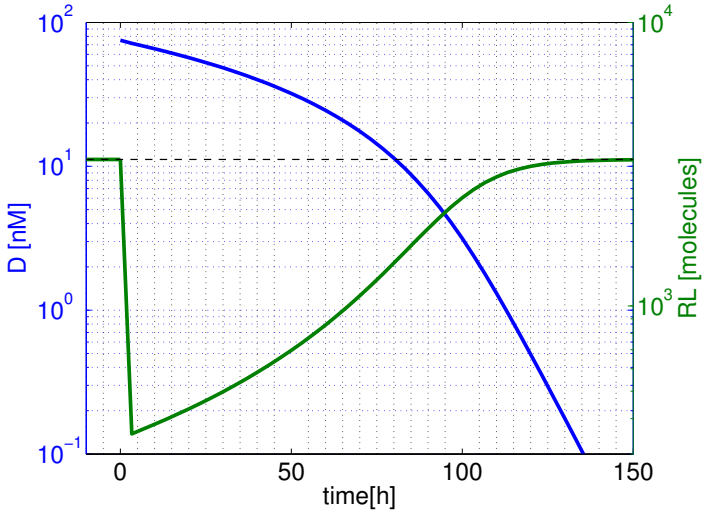

Figure 3.8: *Transient inhibition of receptor activation for the drug cetuximab. The number of active receptors (, right axis) is reduced by the drug (, left axis). Due to the high affinity of the drug, this inhibition happens immediately after administration of the drug. When the drug concentration is reduced by to RME the activation of the receptor system recovers to the original steady-state.*

As the first step we will investigate the transient inhibitory effect resulting from the drug present in the surrounding of the cell. The system is set to be in steady-state when at t=0 the drug is administered. As can be seen from Fig. 3.8 the number of active receptors drops when the drug is competing with the natural ligand for the binding to the receptor. At the same time the drug concentration decreases in the medium due to the binding to the receptor and the subsequent internalization and degradation. This steady decrease of the drug concentration leads to a recovery of the number of active receptors to the same steady-state as prior to drug administration.

3.4 Impact of affinity and dose on inhibitory effect

As the next step, we studied the inhibitory effect of different drug affinities (K_D) and doses on the transient activation of the receptor (see Fig. 3.9). Our study reveals that a higher drug-receptor affinity amplifies the peak inhibition and shortens the duration of inhibition (see Figure 3.9, a). Higher doses of the inhibitor amplify both, the peak and the duration of inhibition (Figure 3.9, b).

As can be seen from Fig. 3.10 (a), *in vitro*, the cumulative inhibitory effect does not dependent on the affinity of the mAb to the receptor. Thus, we found that under the conditions of a typical *in vitro* experiment (i) the cumulative inhibitory effect is the same for mAbs with different affinities; (ii) the peak inhibition is amplified for antibodies with higher affinities and (iii) the duration of inhibition is shorter for high affinity mAbs. In general, we found that there is a trade-off between cumulative inhibition, peak inhibition and duration of inhibition:

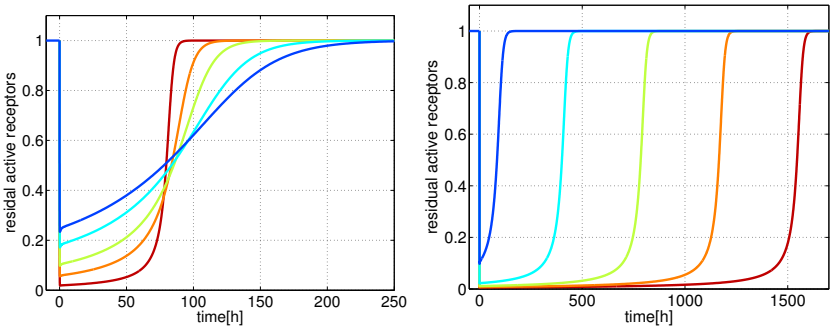

Figure 3.9: *Transient inhibitory effect of a change in the drug properties.* ***(a)*** *Warmer color correspond to higher affinities. The curve marked in (▬) corresponds to the affinity of zalutumumab. The different affinities result in different shapes of the inhibition curves, with a higher peak inhibition and a lower duration of inhibition for antibodies with high affinity.* ***(b)*** *Warmer colors correspond to higher doses of the antibody which increase all three measurements of the inhibitory effect.*

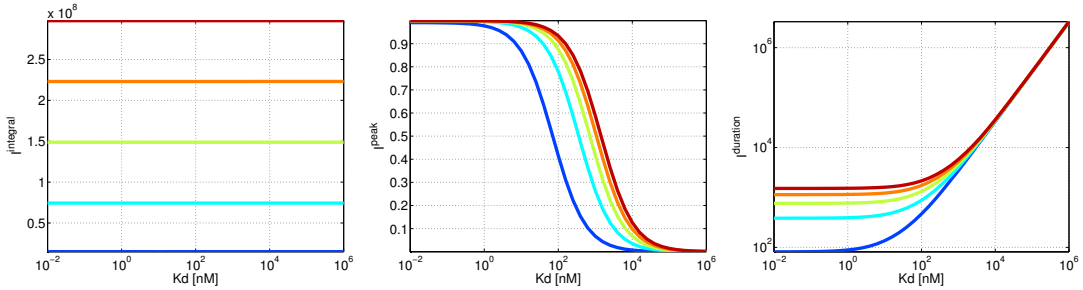

Figure 3.10: *Prediction of in vitro drug efficacy.* ***(a)*** *The cumulative inhibitory effect in vitro does not dependent on the affinity (K_D) but it does increase with the dose.* ***(b)*** *High affinity drugs show a higher peak inhibition and a shorter duration of inhibition* ***(c)***.

mAbs with higher affinity exhibit a higher peak inhibition, but this comes at the cost of a shorter duration of inhibition, resulting in identical cumulative inhibitions. A higher cumulative inhibitory effect can therefore only be achieved by increasing the dose but not by an optimizing of the affinity of the drug.

3.5 Impact of receptor downregulation

Enforcing receptor downregulation by mAbs is argued to be an important part of the drug inhibitory effect [96]. This analysis of the *in vitro* model shows that the cumulative inhibitory effect is independent from the drug-receptor affinity and its downregulation potential. The same dependency is found with respect to the downregulation potential. An increase of the downregulation rate constant lead to a shorter duration of the inhibition and an amplified peak inhibition as denoted in Fig. 3.11. The cumulative inhibitory effect is again invariant for changes of the endocytic downregulation rate.

The downregulation of the receptor by the drug may allow the development of an antibody with lower affinity as the current anti-EGFR antibodies, because a lower affinity together

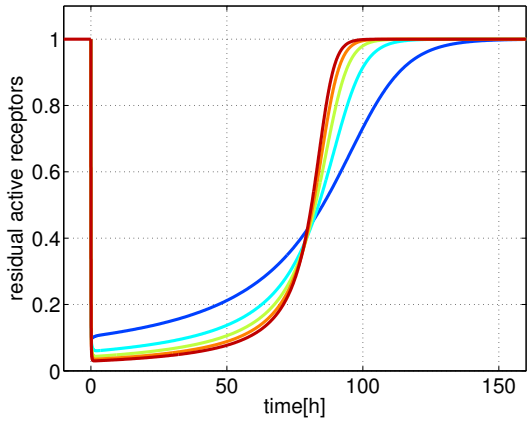

Figure 3.11: *Transient inhibitory effect of different downregulation rate constants. Warmer color correspond to higher downregulation rates. The blue curve represents a downregulation rate constant of the drug-receptor complex which is equal to the rate constant of the free receptor.*

with a higher downregulation results in very similar trajectories of the active receptor (see Fig. 3.12).

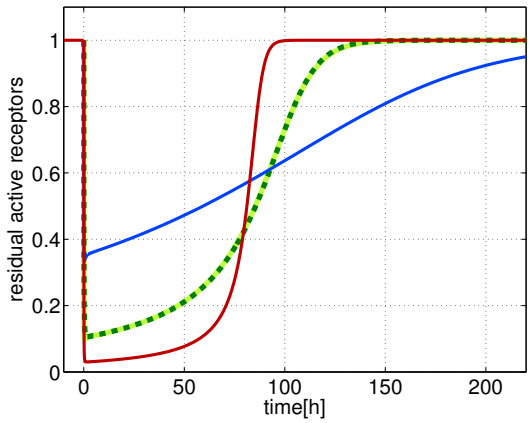

Figure 3.12: *The relationship between downregulation and affinity. The response to zalutumumab is marked in (—). The transient response to an inhibitor with 5-fold lower affinity and higher downregulation than zalutumumab is shown in (—) and (—), respectively. The response to an inhibitor with 5 fold lower affinity and 5 fold higher downregulation rate constant is shown in (- -).*

In conclusion the numerical solutions obtained with the experimentally obtained parameter values for the EGFR system demonstrate that tuning drug parameters can shape the transient inhibitory response, but there is a trade-off between its duration and peak amplitude. The integral of the inhibition can only be increased by increasing the dose and not by tuning the biophysical properties of the antibody. Experimental results suggest that the affinity of the antibody cannot determine their biological activity. Diaz Miqueli et al. [98] examined the biological activities of three monoclonal antibodies (Ior egf/r3, Nimotuzumab, and Cetuximab) *in vitro* and found no difference in their inhibitory effect despite different affinities to the EGFR. Goldstein et al. [48] found also no differences between Cetuximab and a lower

affinity variant anti-EGFR antibodies *in vitro*.

Our analyses suggests that the invariance of the inhibitory effect despite different affinities may either be a consequence of the *in silico* determined invariance of the integral of inhibition to changes in the affinity or the dose of the antibody was to high to see differences in the peak inhibition due to the different antibody affinities.

3.6 Derivation of an exact formula for the inhibitory effect

The invariance of the inhibitory effect integral was demonstrated above by using parameter values experimentally determined for the EGFR system. To prove that this is a inherent feature of all receptor systems with such a structure and does not depend on the specific parameter values we demonstrated that the exact formula for the inhibitory effect integral can be derived. The derivation of the cumulative inhibitory effect is following the draft "Receptor synthesis is the most important process for the cumulative effect of anti-EGFR antibodies" by Krippendorff, Oyarzún & Huisinga [73]. The mathematical derivation of the formula can be found in the Appendix 6.1. The relative inhibitory effect of an antagonistic therapeutic antibody in the system of ODE's denoted by Equations 3.2 is hence given by the simple formula

$$E_r = \frac{dose}{t_{end} k_R}. \tag{3.6}$$

Since *dose* is the number of drug molecules given to the system and $t_{end} \cdot k_R$ corresponds to the number of receptor molecules synthesized in the treatment period (see Appendix 6.1), the ratio of these two numbers defines the percent inhibition of the receptor system during the treatment. Following our theoretical analysis, by measuring only the synthesis rate of the receptor, the dose needed for a desired percent inhibition of the receptor system can be calculated.

3.7 Impact on cells with increased receptor levels

Upregulation of EGFR expression and aberrant activation of EGFR has been shown in many human epithelial cancers, including those of the colon, lung, kidney, head and neck, breast, prostate, brain and ovary [124, 105, 122, 149, 56, 142]. The extent of overexpression also correlates with poorer clinical outcome [106, 95, 49]. Receptor levels as measured by immunohistochemical methods are therefore investigated as a potential predictor of response to receptor inhibitors like mAbs [123, 128, 144]. The cell-level model (Eq. (3.2)) suggests that elevated receptor levels of R^* and RL^* can be a consequence of not only an increased receptor expression (increased k_{synthR}), but also of a reduced internalization of the receptor (decreased k_{degR} and/or k_{degRL}). Alterations in cells influencing those rate constants are

for example gene amplification, increased gene copy numbers, and mutations of the receptor gene which influence receptor internalization. Reddy et al. [113] reports about such an alteration of EFGR where a truncated cytoplasmic domain exhibits a decreased ligand-induced internalization rate constant.

Following the developed kinetic model the steady-state total receptor number on the surface of the cell can be calculated. The steady state of the receptor system is defined by

$$\begin{bmatrix} -(k_{\text{degRL}} + k_{\text{offL}}) & k_{\text{onL}} \\ k_{\text{off}} & -(k_{\text{degR}} + k_{\text{onL}}) \end{bmatrix} \begin{bmatrix} RL \\ R \end{bmatrix} = \begin{bmatrix} 0 \\ -k_{\text{synthR}} \end{bmatrix} \tag{3.7}$$

and hence

$$R^* = k_{\text{synthR}} \cdot \frac{k_{\text{degRL}} + k_{\text{offL}}}{(k_{\text{degRL}} + k_{\text{offL}})(k_{\text{degR}} + k_{\text{onL}} \cdot Ł) - k_{\text{offL}} \cdot k_{\text{onL}} \cdot Ł} \tag{3.8}$$

$$RL^* = k_{\text{synthR}} \cdot \frac{k_{\text{onL}} \cdot Ł}{(k_{\text{degRL}} + k_{\text{offL}})(k_{\text{degR}} + k_{\text{onL}} \cdot Ł) - k_{\text{offL}} \cdot k_{\text{onL}} \cdot Ł}. \tag{3.9}$$

For analysing the inhibitory effect of a alteration of the rate constants k_{synthR}, k_{degR}, and k_{degRL} we developed a cell model representing tumor cells with different alterations (Fig. 3.13). We changed the rate constants of tumor cells to $k_{\text{synthRc}} = k_{\text{synthR}} \cdot \alpha$ or $k_{\text{degRc}} = k_{\text{degR}} \cdot \alpha$

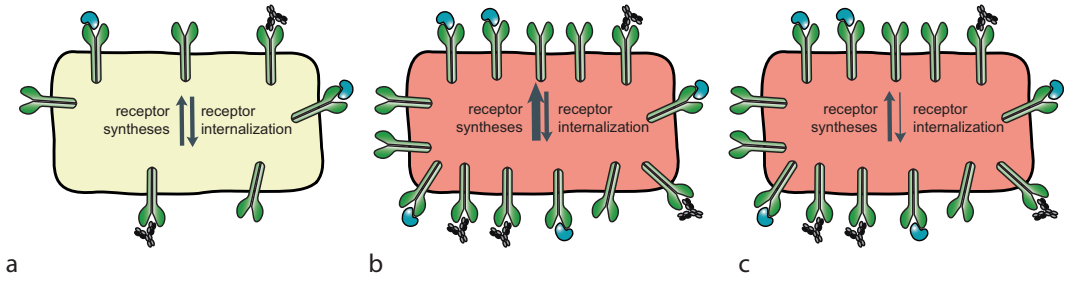

Figure 3.13: *Cells with different alterations of receptor trafficking we analysed for their response to mAbs. In difference of* ***(a)*** *the normal cell the tumor cells have either a higher synthesis of the receptor* ***(b)*** *or a decreased internalization of the receptor* ***(c)****.*

and $k_{\text{degRLc}} = k_{\text{degRL}} \cdot \alpha$, which corresponds to a $\alpha-$fold alteration of receptor synthesis or internalization of the free and bound receptor, respectively.

Using Eq. 3.9 it follows in the case of an alteration of the synthesis rate

$$\frac{RL^{*,\text{c}}}{RL^*} = \frac{k_{\text{synthRc}}}{k_{\text{synthR}}} = \alpha \tag{3.10}$$

and hence the number of bound receptor is changed $\alpha-$fold when the synthesis rate is changed α-fold. In case the internalization rate of both, the free and the bound receptor is changed,

the inhibitory effect on the receptor level is depending on the value of other rate constants:

$$\frac{RL^{*,c}}{RL^{*}} = \frac{1 + \frac{k_{\mathrm{offL}}}{k_{\mathrm{degRL}}} + \frac{k_{\mathrm{onL}} \cdot \mathrm{L}}{k_{\mathrm{degR}}}}{\alpha^2 \left(1 + \frac{k_{\mathrm{offL}}}{k_{\mathrm{degRL}}}\right) + \frac{k_{\mathrm{onL}} \cdot \mathrm{L}}{k_{\mathrm{degR}}}} \tag{3.11}$$

These alterations hence result in changes steady-state activation levels of the receptor system and activate signalling pathways more strongly.

Figure 3.14 shows the transient inhibition time-curve for cells with different levels of the receptor due to the two discussed alterations. In the case of a higher synthesis rate of the

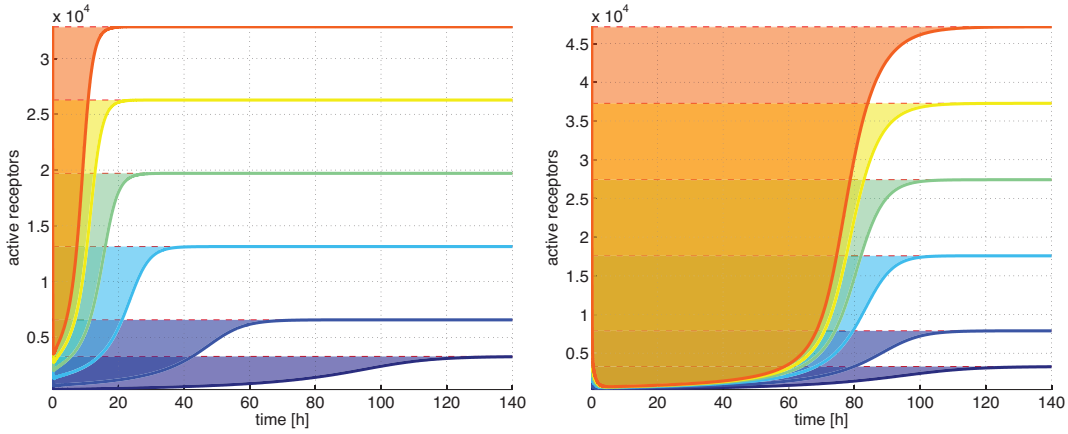

Figure 3.14: *Transient inhibition dynamics for cells with overexpressed receptor proteins.* ***(a)*** *Marked areas denote the cumulative inhibitory effect of the antibody. Warmer colors correspond to higher synthese rates of the receptor,* ***(b)*** *and higher reductions in the internalization rate of the free and activated receptor.*

receptor the absolute cumulative inhibition is the same for all levels of receptor expression (Figure 3.14, a). Since the same number of receptors on the tumor cell is inhibited over time compared to cells with a normal expression, cells with increased expression are not more susceptible to the treatment with mAbs than normal cells.

However, in the case of reduced internalization of the free or the activated receptor, the cumulative inhibitory effect is increased (Fig. 3.14, b), which suggests that such cells are more susceptible to the treatment than normal cells, in terms of the cumulative inhibition.

As shown above, a change in the biophysical properties of the antibody (like the affinity) does not allow to change the cumulative inhibitory effect. Duration and peak inhibition however can be changed. Fig. 3.15 shows the inhibitory effect of a change in the affinity of the antibody on the duration of the inhibition and the peak inhibition. Cells with a higher expression show the same relative peak inhibition as normal cells and a lower affinity reduces this peak for the same amount (Fig. 3.15, a). Cells with a decreased internalization demonstrate a shifted curve. Here an intermediate affinity of the antibody allows to optimize the difference between the peak inhibition in normal and tumor cells. The duration in general

increases for lower affinities (Fig. 3.15, b). Cells with a higher expression show the same change of the duration in case of a modified affinity. An optimization of the affinity in terms of a higher difference between normal and tumor cells is therefore not possible. Cells with decreased inhibition show a longer inhibition than normal cells when a high affinity antibody is used. If the affinity is decreased the duration of inhibition is longer in normal cells.

In conclusion, when aiming to optimize the difference between the inhibitory effect on tumor and normal cells by adjusting the affinity a success depends on the nature of the alteration and not at the number of receptors on the cells surface. This number is just a description of the steady state while the alteration determine the dynamics of the system in the response to a treatment with mAbs.

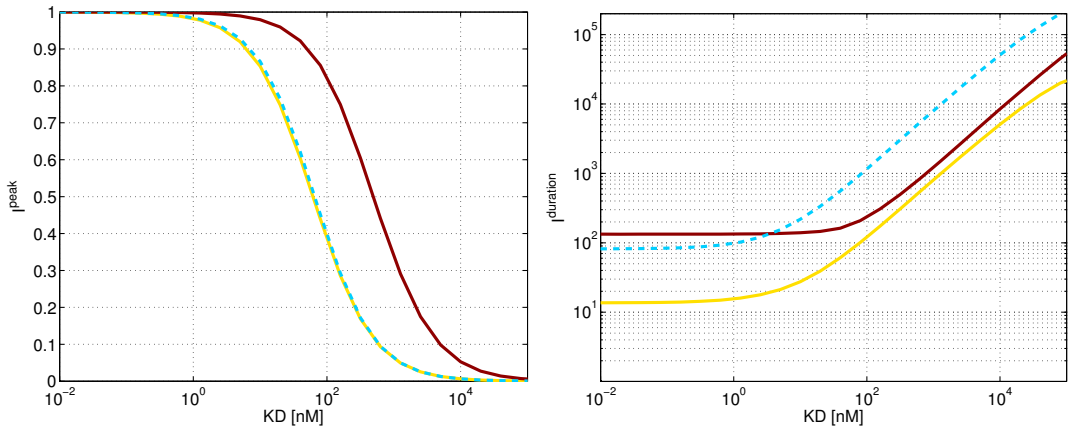

Figure 3.15: *Impact of a change in the affinity for the duration of inhibition and the peak of inhibition.* ***(a)*** *The peak inhibition changes in a normal cell (▬) in the same way as in a cell with higher receptor expression (▬) when changing the affinity of the antibody (K_D). Cells with decreased internalization of receptor (▬) have a shifted curve.* ***(b)*** *This is also the case for the duration of the inhibition. A change of the affinity has the same result on normal cells and cells with a higher expression and no optimization is therefore possible. Cells with decreased internalization show a different reaction to changes in the affinity. For these cells a high affinity antibody maximized the difference between tumor and normal cells.*

3.8 Inhibition of receptor activation in the microenvironment of tumor cells

In this Section we will study the inhibition of receptor activation in a microenvironment of a tumor cell. For this we make the following assumption: In the close proximity of a tumor cell the local ligand concentration is affected by RME. In the last sections we assumed the ligand concentration to be constant and therefore unaffected by the inhibition of the receptor system. Although in general this is a reasonable assumption, (e.g EGF concentration is usually tightly controlled by other mechanisms) there exist situations, where the endocytic machinery acts to regulate growth factors. For example in the development of *Drosophila melanogaster* local

concentrations of growth factor in tissues are controlled by endocytosis [34]. The system of ODE's is described by the equations (3.2) with the ligand concentration changing according to

$$\frac{\mathrm{d}\,L}{\mathrm{d}t} = \frac{k_L}{VN_a} - \frac{k_{onL}}{VN_a} R \cdot L + \frac{k_{offL}}{VN_a} RL - k_{degL} L. \tag{3.12}$$

This is in contrast to the preceding *in vitro* situation, where we set k_L and k_{degL} much faster than the other processes and resulted effectively in a constant ligand concentration. We will see that for the case that RME has an influence on the ligand concentration in the microenvironment, therapeutic inhibition is counteracted by ligand accumulation. This indicates that the processes and concentrations in a microenvironment of tumor cells may not only have a crucial influence on the success of radiotherapy [151], but it also potentially influences antibody based therapies. This Section follows closely [72].

Response to drug administration

Single bolus dose. In the following we consider the response of the receptor system to a single bolus dose of the inhibitor. Figure 3.16 shows the time course of the drug concentration in the microenvironment and the resulting number of active receptors RL for different values of the ligand clearance rate k_{degL}. Following the bolus dose at time $t = 0$, the number of activated receptors drops rapidly to a much lower level. Inhibition of active receptors is due to the competition for free receptors between the natural ligand and the drug. Since binding to receptor implies internalization and degradation, the drug concentration decreases over time such that eventually the number of active receptors recovers to its unperturbed steady-state level (dashed line).

Two phases in Fig. 3.16 can be identified: In a first phase the number of active receptors decays below its steady-state level, resulting in an inhibition of the receptor system; in a second phase, however, the active receptors are above their steady-state, resulting in an induction of the receptor system. The extent of inhibition and induction depends on the clearance k_{degL}. For $k_{degL} = 0.01/\mathrm{min}$, the induction phase is almost absent, whereas for $k_{degL} = 0$ the induction phase is the highest. The inset in Fig. 3.16 shows the increase and decline of the ligand concentration in the microenvironment of the cell. The ligand accumulation is the consequence of the drug binding to the receptor resulting in less ligand bound and degraded. For low values of k_{degL}, the extracellular ligand accumulates considerably, while for high values of k_{degL} it is cleared by the receptor-independent route.

To further understand the relation between inhibition and induction, it is useful to quantify the drugs' inhibitory effect in a precise way. As a measure of the drugs' inhibitory effect we

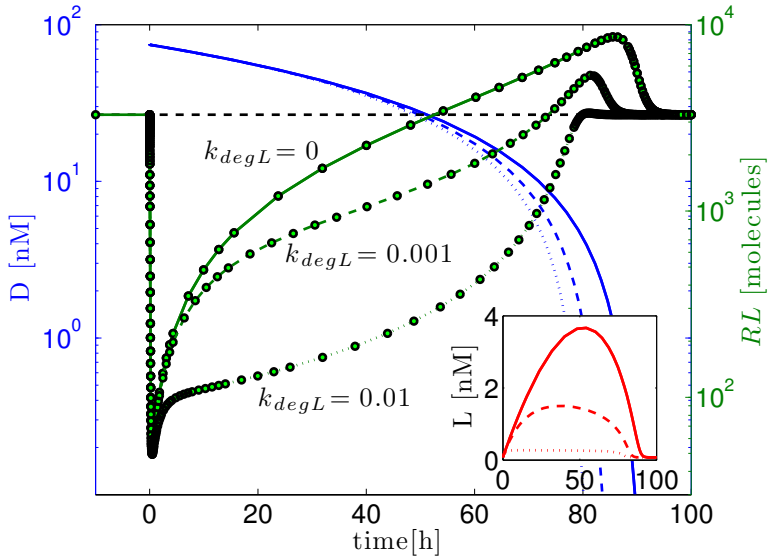

Figure 3.16: *Dynamic response of the number of active receptors (lines with ●) and drug concentration (lines without marker) after bolus dose for different ligand clearance rates k_{degL}. Inset: Ligand accumulation in the microenvironment of the cell over time.*

define:

$$E = \int_0^\infty \big(RL^* - RL(t)\big)dt. \tag{3.13}$$

Thus, E measures the *net inhibition* as the sum of the inhibition and induction. Fig. 3.16 shows that small values of k_{degL} increase the induction phase and decrease the inhibition phase, implying a lower net inhibition according to eq. (3.13). Moreover, in the case of $k_{degL} = 0$ we numerically observe a zero net inhibition ($E = 0$), which suggests that ligand accumulation totally counteracts the drugs' inhibitory effect.

Multiple bolus dose. A dosing strategy to prevent the induction phase, could be to administer a follow-up dose before the induction phase starts. As can be inferred from Fig. 3.17, this first prevents the induction, but comes with the cost of a larger induction phase after the final dose. This is due to a longer ligand accumulation phase (see inset in Fig. 3.17). For $k_{degL} = 0$, numerical computations show a zero net inhibition as in the previous case.

Theoretical analysis of net inhibition

In the following we analytically show that in the limiting case when $k_{degL} = 0$, the net inhibition vanishes and this impact is independent of the parameter values. Therefore, in this scenario the extent of ligand accumulation and the resulting induction phase do not depend on the model parameters, which suggests that it is a structural property of the studied receptor system.

It is convenient to express eqs. (3.2) in terms of the deviations of the species from their

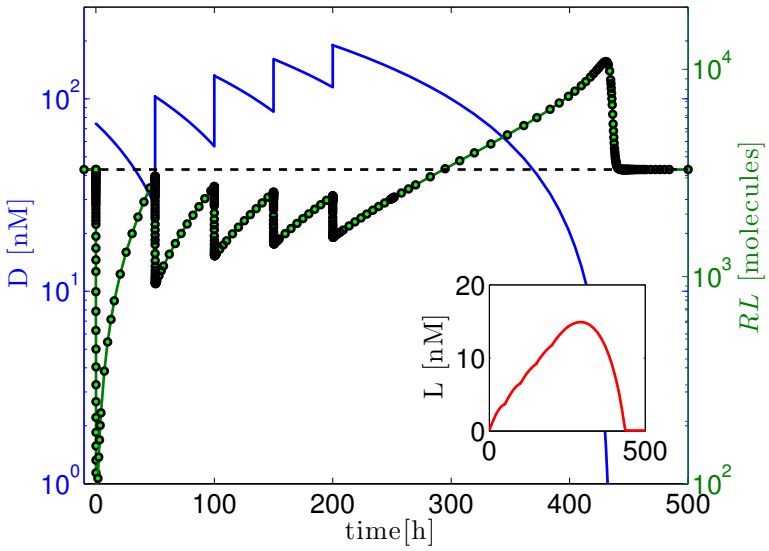

Figure 3.17: *Dynamic response of the number of activated receptors (lines with ●) and drug concentration (lines without marker) after multiple bolus doses for $k_{degL} = 0$. Inset: Ligand accumulation in the microenvironment of the cell over time.*

steady-state values. We define these incremental variables as

$$\bar{L}(t) = L^* - L(t), \qquad \bar{RD} = RD^* - RD(t),$$
$$\bar{R}(t) = R^* - R(t), \qquad \bar{RL} = RL^* - RL(t),$$
$$\bar{D}(t) = D^* - D(t).$$

The resulting system of ODEs in terms of

$$\bar{x}(t) = \begin{bmatrix} \bar{L}(t) & \bar{D}(t) & \bar{R}(t) & \bar{RL}(t) & \bar{RD}(t) \end{bmatrix}^T$$

is then given by

$$\frac{\mathrm{d}\,\bar{x}}{\mathrm{d}t} = \boldsymbol{A}\bar{x}(t) + \boldsymbol{B_{RL}}\bar{R}(t)\bar{L}(t) + \boldsymbol{B_{RD}}\bar{R}(t)\bar{D}(t) - \boldsymbol{B}f(t), \tag{3.14}$$

with $\bar{x}(0) = \begin{bmatrix} 0 & -D(0) & 0 & 0 & 0 \end{bmatrix}^T$, and where $\boldsymbol{A}$ is the Jacobian of the right hand side of (3.2) evaluated at the steady state (given in eq. (3.15)). The vectors $\boldsymbol{B_{RL}}$, $\boldsymbol{B_{RD}}$ and $\boldsymbol{B}$ are given by

$$\boldsymbol{B_{RL}} = \begin{bmatrix} \frac{k_{onL}}{VN_a} & 0 & k_{onL} & -k_{onL} & 0 \end{bmatrix}^T,$$
$$\boldsymbol{B_{RD}} = \begin{bmatrix} 0 & \frac{k_{onD}}{VN_a} & k_{onD} & 0 & -k_{onD} \end{bmatrix}^T,$$
$$\boldsymbol{B} = \begin{bmatrix} 0 & 1 & 0 & 0 & 0 \end{bmatrix}^T.$$

$$\boldsymbol{A} = \begin{bmatrix} -\frac{k_{onL}R^*}{VN_a} & 0 & -\frac{k_{onL}L^*}{VN_a} & \frac{k_{offL}}{VN_a} & 0 \\ 0 & -\frac{k_{onD}R^*}{VN_a} - k_{degD} & 0 & 0 & \frac{k_{offD}}{VN_a} \\ -k_{onL}R^* & -k_{onD}R^* & -k_{onL}L^* - k_{degR} & k_{offL} & k_{offD} \\ k_{onL}R^* & 0 & k_{onL}L^* & -k_{offL} - k_{degRL} & 0 \\ 0 & k_{onD}R^* & 0 & 0 & -k_{offD} - k_{degRD} \end{bmatrix}. \tag{3.15}$$

Integration of (3.14) from $t = 0$ to infinity gives

$$\begin{aligned} \bar{x}(\infty) - \bar{x}(0) = \boldsymbol{A} \int_0^\infty \bar{x}(t)\, dt + \boldsymbol{B_{RL}} \int_0^\infty \bar{R}(t)\bar{L}(t)\, dt \\ + \boldsymbol{B_{RD}} \int_0^\infty \bar{R}(t)\bar{D}(t)\, dt - \boldsymbol{B} \int_0^\infty f(t)\, dt. \end{aligned} \tag{3.16}$$

Under the biologically reasonable assumption that when the drug disappears the receptor system goes back to its old steady-state activation level (described in Section 3.2), the stability of the system implies that $\bar{x}(\infty) = 0$, and using the initial condition yields

$$\begin{aligned} \int_0^\infty \bar{x}(t)\, dt = \boldsymbol{A}^{-1}\boldsymbol{B} \cdot \text{Dose} \\ - \boldsymbol{A}^{-1}\boldsymbol{B_{RL}} \int_0^\infty \bar{R}(t)\bar{L}(t)\, dt \\ - \boldsymbol{A}^{-1}\boldsymbol{B_{RD}} \int_0^\infty \bar{R}(t)\bar{D}(t)\, dt. \end{aligned} \tag{3.17}$$

We notice that $E = \int_0^\infty [\bar{x}(t)]_4\, dt$ and moreover,

$$\left[\boldsymbol{A}^{-1}\boldsymbol{B}\right]_4 = \left[\boldsymbol{A}^{-1}\boldsymbol{B_{RL}}\right]_4 = \left[\boldsymbol{A}^{-1}\boldsymbol{B_{RD}}\right]_4 = 0, \tag{3.18}$$

which finally implies $E = 0$. Hence, in absence of receptor-independent ligand clearance, the inhibition and subsequent induction phase are identical, resulting in a zero net inhibition. Since this phenomenon is independent of any drug- and receptor- specific parameters, it is suggested that it is a structural feature of the considered receptor class.

3.9 Summary of this chapter

In this Chapter, we extended a systems biology model of receptor activation by the mechanism of action of mAbs (section 3.2). This allowed us to study the impact of changed biophysical properties of mAbs on the inhibitory effect (section 3.4 and 3.5).

We numerically studied large perturbation of the system and translated this transient effect of the antibody into three different measures of inhibitory effect. We further derived an exact

formula for the effect of mAbs *in vitro* (Eq. (6.17)), which has two advantages: (i) It describes the exact effect following big perturbations of the network and (ii) needs only a subset of the parameter values. Our theoretical analysis identifies only one parameter value of the cell-level model which is important for the inhibitory effect, the synthesis rate of the receptor.

Another advantage of building a kinetic model of the EGFR is the ability to include cell alteration found in tumor cells (section 3.7). We demonstrated that when tumor cells are characterized by their number of receptor at the cell surface using immunohistochemistry, this only describes a steady state of the system. More interesting for the response to a treatment with mAbs is their dynamic response and this can be remarkably different for different cell alterations, although the cells might present similar numbers of receptors on the surface. A tumor cell with a higher expression of the receptor is harder to inhibit with mAbs due to the change of the before identified most important parameter of the system, k_{synthR}. Tumor cells with decreased internalisation of the receptor show a stronger response to mAbs and, in contrast to cells with a higher expression, may allow to optimize the antibody for a stronger selectivity for tumor cells.

The inhibitory effect of antibody-based therapeutics for targeting tumors is therefore influenced by cell-level kinetic processes. In the last part of this Chapter (section 3.8) we identified another kinetic mechanism with the potential to compromise the inhibitory effect, namely the accumulation of ligands in the microenvironment of tumor cells. Receptor trafficking can have a critical influence on the ligand concentration in the cells' environment as was shown for the EGF-EGFR system in vitro [113]. We therefore analyzed the inhibitory effect of inhibiting such a receptor system, and found that the response of the receptor system to the drug in this case can have two counteracting phases: An initial inhibitory phase and a second inductive phase. The latter is due to extracellular accumulation of the ligand, which is larger for environments where receptor-independent ligand clearance is slow. In such situations the inhibitor only postpones the activation, until the local concentration of the drug has sufficiently declined, acting as a memory of the prevented activation. In the limiting (theoretical) case when there is no receptor-independent ligand clearance, the induction of active receptors totally offsets the inhibitory response and renders a nil total inhibitory effect. The dosing function can be regarded as an external input signal that is applied to the receptor system to control its activation. The phenomenon of counteracting ligand accumulation constitutes a "fundamental limitation" in the inhibition of the receptor system, which is independent of the parameter values and resembles those that typically arise in Control Engineering [132]. The study of fundamental limitations is an extensive field of research [41] that addresses the question how the structure of the system limits certain characteristics of every possible response to a class of inputs. Our analysis suggests that this kind of limitations can also play a role for antibody based cancer treatment.

4 The *in vivo* effect of therapeutic antibodies

As shown in the preceding chapters, the identification of targets for protein drugs against complex diseases benefits today from the availability of systems biology models of therapeutically relevant cellular processes. One practical example is the successful development of MM-121, a previously unidentified anticancer therapeutic designed using a systems approach [130]. So far, such information about the dynamics of the targeted system is neglected in later stages of the drug development process when pharmacokinetic modeling is used to guide dose finding and analyze preclinical or clinical *in vivo* data. As shown in Chapter 2, this is especially critical for therapeutic proteins, where drug effect and pharmacokinetics are inherently interdependent. In this Chapter, by integrating cell-level models with established pharmacokinetic models, we translate biophysical properties of protein drugs into a transient drug effect *in vivo*. As before, we illustrate the approach for anti-EGFR antibodies in cancer therapy. Here we combine *in vitro* determined parameters (as used in Chapter 3) with pharmacokinetic data from cynomolgus monkeys (as used in Chapter 2). The primary objective of this Chapter is to develop a strategy to integrate cell-level kinetic models into systemic pharmacokinetics models and secondary to translate biophysical properties of protein drugs into *in vivo* efficacy. We combine the traditional modeling approaches of systems biology and pharmacokinetics while importantly retaining the single-cell as the fundamental unit of the model.

4.1 Our model of the inhibitory effect of therapeutic proteins

The pharmacokinetic part of the model is represented by a two-compartment model as used in chapter 2 and described in section 2.2. For the cell-level submodel we use a description of RME whose complexity lies between the very detailed description of the model used in Chapter 2 and the reduced model used in Chapter 3 corresponding to the TMDD description of antibody disposition. As before, due to the lack of experimentally determined parameters for the antibody, we lumped the distribution of the antibody inside the cell into one internalization rate (as described in Chapter 3). In contrast to the model in Chapter 3, we explicitly considered the internalization and recycling of the free receptor (which was part of the detailed model). Only this allowed us to accurately describe the measured plasma concentration of zalutumumab in cynomolgus monkeys (see section 4.2). A rationale for this change of the model is given in the discussion in Chapter 5

The developed cell-level PK/PD model is shown in Fig. 4.1(b) and (c). Based on the law of mass action, the rates of change for the molecular species are given by the following system of ordinary differential equations (ODEs):

Compartment model:

$$\begin{aligned} V_c\frac{\mathrm{d}D_c}{\mathrm{d}t} &= -q_{cp}D_c + q_{pc}D_p - \mathrm{CL}_{\mathrm{linD}}\cdot D_c, \\ V_p\frac{\mathrm{d}D_p}{\mathrm{d}t} &= +q_{cp}D_c - q_{pc}D_p \\ &\quad + N_{\mathrm{h}}\cdot k_{\mathrm{offD}}\cdot \mathrm{SF}\cdot RD - N_{\mathrm{h}}\cdot k_{\mathrm{onD}}\cdot \mathrm{SF}\cdot R\cdot D_p \\ &\quad + N_{\mathrm{t}}\cdot k_{\mathrm{offD}}\cdot \mathrm{SF}\cdot RD_{\mathrm{t}} - N_{\mathrm{t}}\cdot k_{\mathrm{onD}}\cdot \mathrm{SF}\cdot R_{\mathrm{t}}\cdot D_p, \end{aligned} \tag{4.1}$$

Normal cells:

$$\begin{aligned} \frac{\mathrm{d}R}{\mathrm{d}t} &= k_{R\mathrm{h}} - k_{\mathrm{onL}}R\cdot L - k_{\mathrm{onD}}R\cdot D_p \\ &\quad + k_{\mathrm{offL}}RL + k_{\mathrm{offD}}RD - k_{\mathrm{degR}}\cdot R + k_{\mathrm{recyR}}\cdot R_{\mathrm{i}}, \\ \frac{\mathrm{d}R_{\mathrm{i}}}{\mathrm{d}t} &= k_{\mathrm{degR}}\cdot R - k_{\mathrm{recyR}}\cdot R_{\mathrm{i}} - k_{\mathrm{exit}}\cdot R_{\mathrm{i}}, \\ \frac{\mathrm{d}RL}{\mathrm{d}t} &= k_{\mathrm{onL}}R\cdot L - k_{\mathrm{offL}}RL - k_{\mathrm{degRL}}RL, \\ \frac{\mathrm{d}RD}{\mathrm{d}t} &= k_{\mathrm{onD}}\cdot R\cdot D_p - k_{\mathrm{offD}}RD - k_{\mathrm{degRD}}\cdot RD, \end{aligned} \tag{4.2}$$

Tumor cells:

$$\begin{aligned} \frac{\mathrm{d}R_{\mathrm{t}}}{\mathrm{d}t} &= k_{R\mathrm{t}} - k_{\mathrm{onL}}R_{\mathrm{t}}\cdot L - k_{\mathrm{onD}}R_{\mathrm{t}}\cdot D_p \\ &\quad + k_{\mathrm{offL}}RL_{\mathrm{t}} + k_{\mathrm{offD}}RD_{\mathrm{t}} - k_{\mathrm{degR}}\cdot R_{\mathrm{t}} + k_{\mathrm{recyR}}\cdot Ri_{\mathrm{t}}, \\ \frac{\mathrm{d}Ri_{\mathrm{t}}}{\mathrm{d}t} &= k_{\mathrm{degR}}\cdot R_{\mathrm{t}} - k_{\mathrm{recyR}}\cdot Ri_{\mathrm{t}} - k_{\mathrm{exit}}\cdot Ri_{\mathrm{t}}, \\ \frac{\mathrm{d}RL_{\mathrm{t}}}{\mathrm{d}t} &= k_{\mathrm{onL}}R_{\mathrm{t}}\cdot L - k_{\mathrm{offL}}RL_{\mathrm{t}} - k_{\mathrm{degRL}}RL_{\mathrm{t}}, \\ \frac{\mathrm{d}RD_{\mathrm{t}}}{\mathrm{d}t} &= k_{\mathrm{onD}}\cdot R_{\mathrm{t}}\cdot D_p - k_{\mathrm{offD}}RD_{\mathrm{t}} - k_{\mathrm{degRD}}\cdot RD_{\mathrm{t}}. \end{aligned} \tag{4.3}$$

The model describes two compartments with volumes of V_c and V_p. The drug is present in concentrations D_c and D_p, respectively. The parameters q_{cp} and q_{pc} denote the transport rate constants from the central compartment to the peripheral, and vice versa. The drug is cleared from the central compartment with rate constant $\mathrm{CL}_{\mathrm{linD}}$. The drug in the peripheral compartment interacts with the receptors of normal cells (Fig. 4.1 a), or normal and tumor cells simultaneously (Fig. 4.1 b), expressed by equations (4.2) and (4.3). R, R_{i}, RL, and

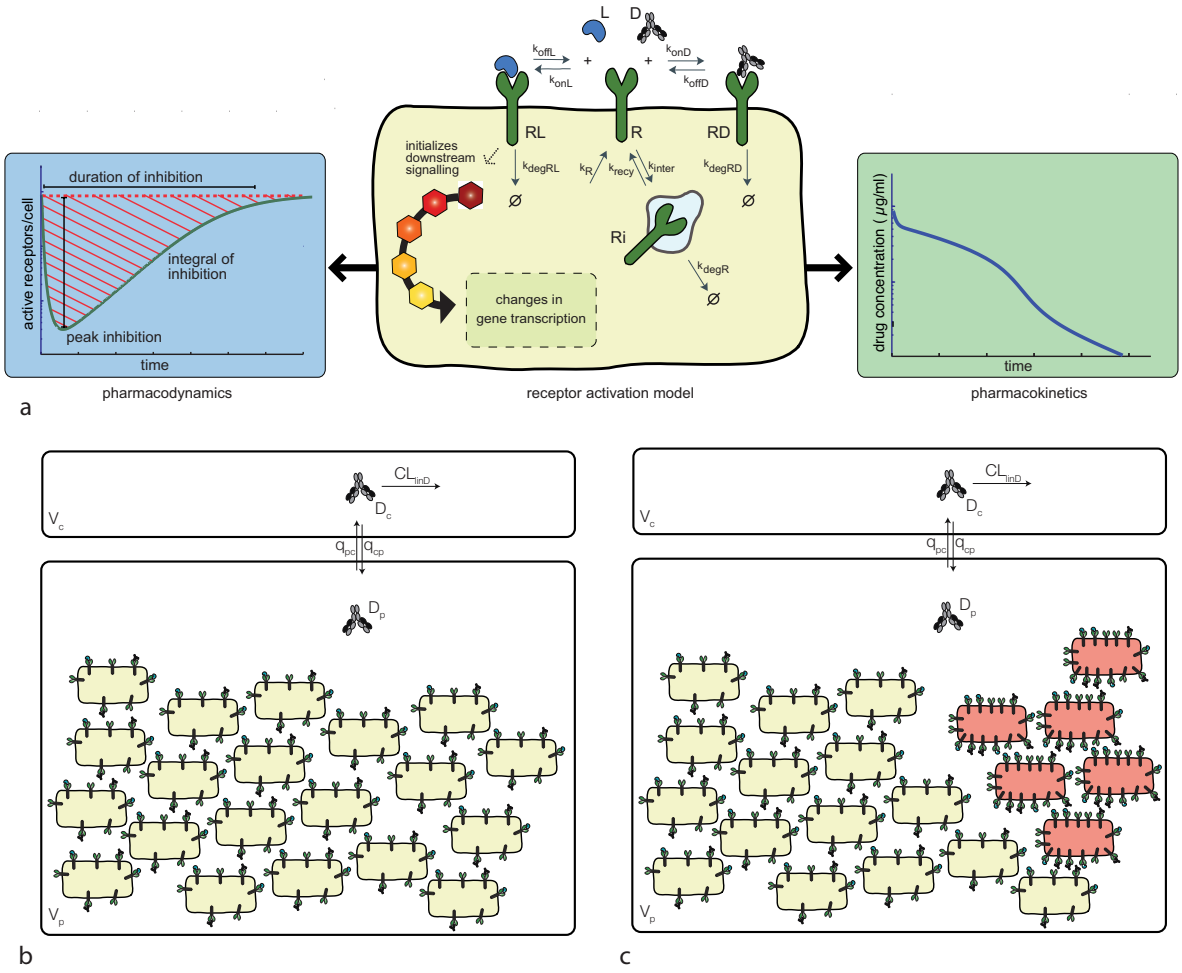

Figure 4.1: *Schematic illustration of the cell-level pharmacokinetic/pharmacodynamic model for analyzing the inhibitory effect on receptor activation of anti-EGFR antibodies.* ***(a)*** *Cell-level receptor model of receptor activation and inhibition. The cellular model describes the transient inhibitory effect of a therapeutic antibody (D) on the formation of active ligand(L)-receptor complexes (RL) through the binding to the free receptor (R) and the formation of a antibody-receptor complex (RD). Left: We studied three different transient measures of the reduction in the number of active receptors: the integral, the peak, and the duration of inhibition. Right: The receptor dynamics, at the same time, effect the antibody concentration in the body, since the binding of the drug constitutes a target-mediated clearance mechanism.* ***(b)*** *Cell-level pharmacokinetic/pharmacodynamic model. The model describes the observed pharmacokinetics of therapeutic antibodies and includes a target independent linear clearance mechanism (CL_{linD}) from the central compartment and an exchange of drug described by the flux (q_{pc} and q_{cp}). The central and the peripheral compartments have a volume of V_c and V_p, respectively. The cell-level model depicted in (a) is integrated in the peripheral compartment. This cell-level pharmacokinetic model is used to study the trajectory of the drug concentration and the optimal biophysical properties of anti-EGFR antibodies.* ***(c)*** *Extended cell-level pharmacokinetic/pharmacodynamic model including tumor cells with elevated EGFR levels due to different alteration of receptor dynamics. The extended cell-level pharmacokinetic model is used to compare the inhibitory effect of therapeutic antibodies on tumor cells and normal cells to optimize tumor specificity.*

RD are the numbers of free receptors, free internalized receptors, ligand–receptor complexes, and drug–receptor complexes per normal cell, respectively. Similarly, R_{t}, Ri_{t}, RL_{t}, and RD_{t} denote the respective numbers in the tumor cells.

Both ligand (L) and drug (D_p) reversibly bind to the free receptors with association rate constants k_{onL} and k_{onD}, and dissociate with rate constants k_{offL} and k_{offD}. The free membrane receptors are internalized with rate constant k_{degR} and recycled with rate constant k_{recyR} or degraded with rate constant k_{exit}. The drug–receptor complex and ligand–receptor complex are internalized with rate constant k_{degRD} and k_{degRL}, respectively. All molecular species are in number of molecules per cell, except L, D_c and D_p which are in mg/ml. In equation (4.1), the factor $\mathrm{SF} = \frac{MW \cdot 10^3}{N_a}$ ensures conversion from units number of molecules to mg.

For numerical simulations, we used the parameter values given in Table 4.1 and 4.2. The comparison of the different therapeutic antibodies against the EGFR are based on the affinity values stated in Table 4.3.

Table 4.1: *Parameter values for the EGF receptor system.* ▲*Calculated in Section 4.2*

	Parameter	**Unit**	**Value**	
1	k_{onL}	$M^{-1} \cdot s^{-1}$	$2.9 \cdot 10^6$	[68]
2	k_{offL}	h^{-1}	0.24	[68]
3	k_{degR}	h^{-1}	0.0172	[68]
4	k_{degRL}	h^{-1}	0.8460	[68]
5	$k_{R\mathrm{h}}$	$cell^{-1} \cdot h^{-1}$	$1.3824 \cdot 10^4$	[68]
6	k_{recyR}	h^{-1}	3.4800	[140]
7	k_{exit}	h^{-1}	0.1320	[140]
8	k_{onD}	$M^{-1} \cdot s^{-1}$	k_{onL}	
9	k_{degRD}	h^{-1}	0.005	[147]
10	N_{h}		$2.9434 \cdot 10^{10}$	▲
11	MW_{mAbs}	dalton	148000	

The parameter k_{onD} in units $\frac{1}{\frac{mg}{ml} \cdot h}$ is converted from the traditionally used k_{onD} in units $\frac{1}{nM \cdot h}$ by multiplying with $\frac{1}{10^{-9} \cdot MW_{mAbs}}$. It was assumed that concentration of all EGFR ligands is five times the concentration of EGF, $L = 5 \cdot 0.35$ ng/ml [15].

Table 4.2: *Pharmacokinetic parameters determined* in vivo *by [147].*

	Parameter	Unit	Value	
1	k_b	h^{-1}	0.067	[147]
2	k_{pi}	h^{-1}	0.043	[147]
3	k_{ip}	h^{-1}	0.043	[147]
4	k_{el}	h^{-1}	0.0055	[147]
5	V_i	ml	70	[147]
6	V_p	ml	35	[147]
7	K_M	$mg \cdot ml^{-1}$	$0.5 \cdot 10^{-3}$	[147]
8	B_{max}	$mg \cdot h^{-1}$	2	[147]
9	$\mathrm{CL}_{\mathrm{linD}}$	$ml \cdot h^{-1}$	$k_{el} \cdot V_p$	

Table 4.3: *Affinities and Isotypes of the considered therapeutic antibodies against the EGFR. Values taken from [107].*

	Antibody	Affinity (M)	Isotype
1	Panitumumab	$5 \cdot 10^{-11}$	IgG2
2	Cetuximab	$4 \cdot 10^{-10}$	IgG1
3	IMC-11F8	$3 \cdot 10^{-10}$	IgG1
4	Nimotuzumab	$1 \cdot 10^{-9}$	IgG1
5	Zalutumumab	$7 \cdot 10^{-9}$	IgG1

4.2 Integrating in vitro determined cell-level receptor dynamics into whole-body pharmacokinetic models

To analyze preclinical or clinical pharmacokinetic data of protein drugs, empirical compartmental models (see Chapter 2 and described in section 2.2) have been typically used[30, 77, 102, 67, 147].

In these models, the interaction of the drug with its target is represented by an empirical or semi-mechanistic term, accounting for the saturable degradation capacity of the target system.

Our approach of integrating cell-level kinetics into systemic pharmacokinetic models is a two step process: Starting with the compartment model, we first replace the empirical or

semi-mechanistic term with a kinetic model at the single cell level, and then secondly scale the effect of this cellular level on the pharmacokinetics with the number of relevant cells. We define relevant cells as those cells expressing the target and coming in contact with the drug. Below, we illustrate the construction of such a cell-level pharmacokinetic model for the *in vivo* effect of the antibody zalutumumab.

Zalutumumab (2F8) is an IgG1 antibody against EGFR that potently inhibits tumor growth in xenograft models and has shown promising results in phase I/II clinical trials[13, 8]. Lammerts van Bueren et al.[147] have developed an empirical pharmacokinetic model of zalutumumab in cynomolgus monkeys which accurately describes experimental plasma data for high and low doses (Chapter 2). The model does however not allow the *in vivo* inhibitory effect of zalutumumab to be predicted. Hence, the impact of the biophysical properties of the drug on its effect can not be addressed using such a model.

In the empirical model, the interaction of zalutumumab with its target is represented by an Michaelis-Menten term representing the saturable drug-receptor binding and subsequent degradation. This term is the key to link pharmacokinetics and target dynamics, since (as demonstrated in Chapter 2) it represents the degradation capacity of the relevant cells. To describe the cell-level kinetics we use a canonical model of ligand-receptor activation and trafficking[133, 68, 140] which is parameterized using rate constants that have been experimentally determined in human fibroblast cells[68, 140] (Fig. 4.1, a). The number of relevant cells was then estimated by comparing the degradation capacities of all relevant cells to the degradation capacity of the single-cell model, which was determined by model reduction:

In quasi-steady state the number of drug-receptor complexes is given by:

$$RD^* = \frac{\frac{k_{R\mathrm{h}}}{k_{\mathrm{degRD}}} \cdot D_p}{\frac{k_{\mathrm{degRD}}+k_{\mathrm{offD}}}{k_{\mathrm{degRD}} \cdot k_{\mathrm{onD}}} \cdot \left(\frac{k_{\mathrm{exit}} k_{\mathrm{degR}}}{k_{\mathrm{exit}}+k_{\mathrm{recyR}}} + L \cdot \frac{k_{\mathrm{onL}} \cdot k_{\mathrm{degRL}}}{k_{\mathrm{offL}}+k_{\mathrm{degRL}}}\right) + D_p}. \tag{4.4}$$

The maximal binding capacity of the cell level model is therefore described by

$$B_{max,cell} = \frac{k_{R\mathrm{h}}}{k_{\mathrm{degRD}}}. \tag{4.5}$$

The number of relevant cells can be estimated by comparing the maximal *in vivo* binding capacity to the *in vitro* binding capacity of a single cell

$$N_{\mathrm{h}} = \frac{B_{max}}{\mathrm{SF} \cdot B_{max,cell}} = \frac{B_{max} \cdot k_{\mathrm{degRD}}}{\mathrm{SF} \cdot k_{R\mathrm{h}}}, \tag{4.6}$$

where SF ensures scaling of units.

This finally allowed us to replace the empirical term in the compartment model by the scaled kinetic model of a single target cell (see Fig. 4.1, b and Section 4.1).

Importantly, our approach does not involve the refitting of parameters; all parameter values

are either inherited from the original compartment model or have been determined *in vitro*. The proposed approach to build cell-level pharmacokinetic models is applicable to various therapeutic proteins where the target dynamic has an definable impact on the pharmacokinetics.

To assess the integration of the single cell kinetic model and how it feeds back on the pharmacokinetics, we compared our model with the original empirical compartment model. The predicted time-courses of the drug concentration showed good agreement for both, a high 20 mg and low 2 mg dose (Fig. 4.2(a)). At the same time, the cell-level pharmacokinetic model was used to predict the dynamics of the receptor system upon drug administration (Fig. 4.2(b)). Our model correctly predicted that the saturation in monkey tissue which expresses normal receptor levels was established at doses between 2 and 20 mg/kg[147] (see Fig. 4.2(b), inset).

The cell-level pharmacokinetic/pharmacodynamic model then was used to predict the number of activated receptors over the duration of the treatment, which is *in vivo* difficult to examine. Our model predicted that the low dose (2 mg) of antibody reduces the number of active receptors by about 35%. It is then followed by a recovery period secondary to a slow reduction of drug concentration (Fig. 4.2(b)). On the other hand, the higher dose (20 mg) almost completely inhibited receptor activation for a period of around 20 days. The start of the recovery period coincided with the transition from saturated to linear pharmacokinetics between days 20 and 25. Thus, the model suggests that changes in pharmacokinetics might act as a biomarker for changes in the inhibitory response. Further, we have compared receptor drug saturation with the inhibition of receptor activation. Both only corresponded initially, while at later points in time the receptor saturation underestimated the inhibitory effect of the antibody. This highlights the importance of adopting an integrated kinetic model to translate the binding of the drug into its actual inhibitory effect on receptor activation.

The model only allowed to reproduce the zalutumumab time-curve when an internalized free receptor was included in the model which can be recycled to the surface. For models which lack such a pool of receptor, there was a poor agreement between our model and the zalutumumab time-curve.

4.3 Optimizing drug characteristics

One important advantage of the cell-level pharmacokinetic/ pharmacodynamic model is its ability to study the impact of drug properties such as the dose, drug-receptor affinity, and drug induced receptor internalization on the inhibitory response under *in vivo* conditions. Since we investigated a transient inhibitory effect we again consider the three quantitative measures of the response defined in section 3.2(see also Fig. 4.1(a)):

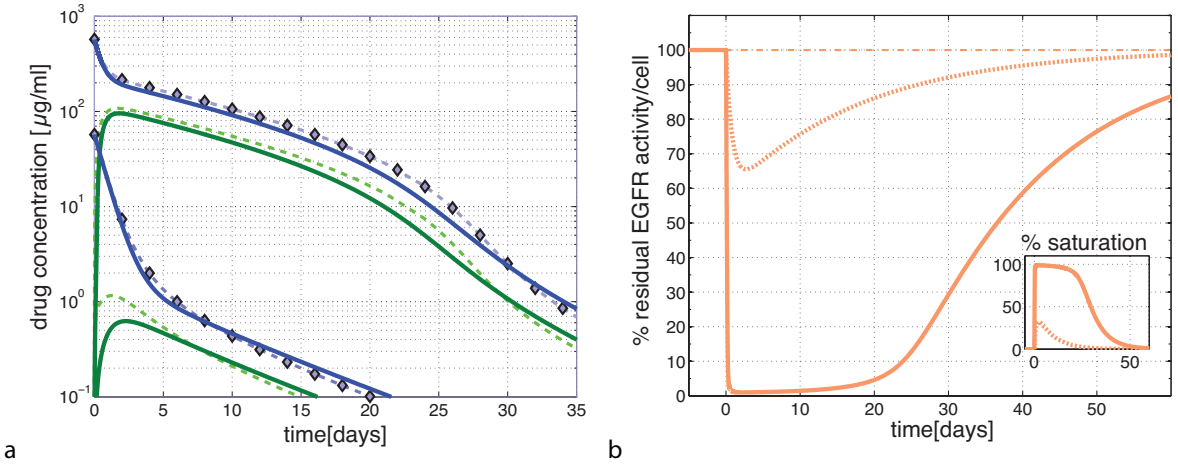

Figure 4.2: *Pharmacokinetics of zalutumumab in cynomolgus monkeys and prediction of the inhibitory effect on a cellular level using the model depicted in Fig.4.1(b).* ***(a)*** *Predictions of zalutumumab in the central compartment (▬) and the peripheral compartment (▬) for a high dose of 20 mg and a low dose of 2 mg by the cell-level pharmacokinetic model. The model predictions are in good agreement with the empirical pharmacokinetic model of Lammerts van Bueren[147] (▬ and ▬). The experimentally validated profiles from Lammerts van Bueren are marked with a ◆.* ***(b)*** *Predictions of the residual EGFR activation per cell based on the cell-level pharmacokinetic model (Fig. 4.1 (b)) for the high dose (▬) and the low dose (▬). The inset depicts the corresponding relative number of drug-bound receptors at the membrane. This predicted saturation corresponds for both doses with the experimentally measured receptor saturation in Lammerts van Bueren[147].*

Affinity and dose.

We studied the inhibitory effect for a range of affinities, including those of anti-EGFR mAbs on the market or in clinical development: zalutumumab, panitumumab, cetuximab, IMC-11F8, and nimotuzumab. All these antibodies act antagonistically [163]. Our analysis focused on optimizing the direct inhibitory effect, i.e., reducing the number of activated receptors at the cell membrane. Since all the analyzed antibodies are either IgG1 or IgG2, their target-independent clearance was assumed to be identical [99]. The percentage of active receptors over time is shown in Figure 4.3(a). Despite 20-fold differences in target affinities (see Table 4.3 in Supplement), the transient inhibition pattern were similar. As seen in Figure 4.3(b)-(d), this phenomenon is a consequence of an effect plateau in the inhibitory responses. For high affinity drugs located in the plateau range, an increased affinity does not translate into a stronger inhibition. For the integral effect our theoretical analysis (Appendix 6.2) suggests that this a structural feature of the system that does not depend on specific parameter values. Shankaran *et al.* [133] identified the ratio between the dissociation and downregulation rate constants ($k_{\mathrm{degRD}}/k_{\mathrm{offD}}$, termed the "consumption parameter") as a key parameter to characterize cell surface receptor systems. As discussed in section 3.1, it quantifies the likelihood that a drug is internalized rather than dissociated upon binding the receptor. We found that this is also an important parameter for antagonistic mAbs, since those with a high consump-

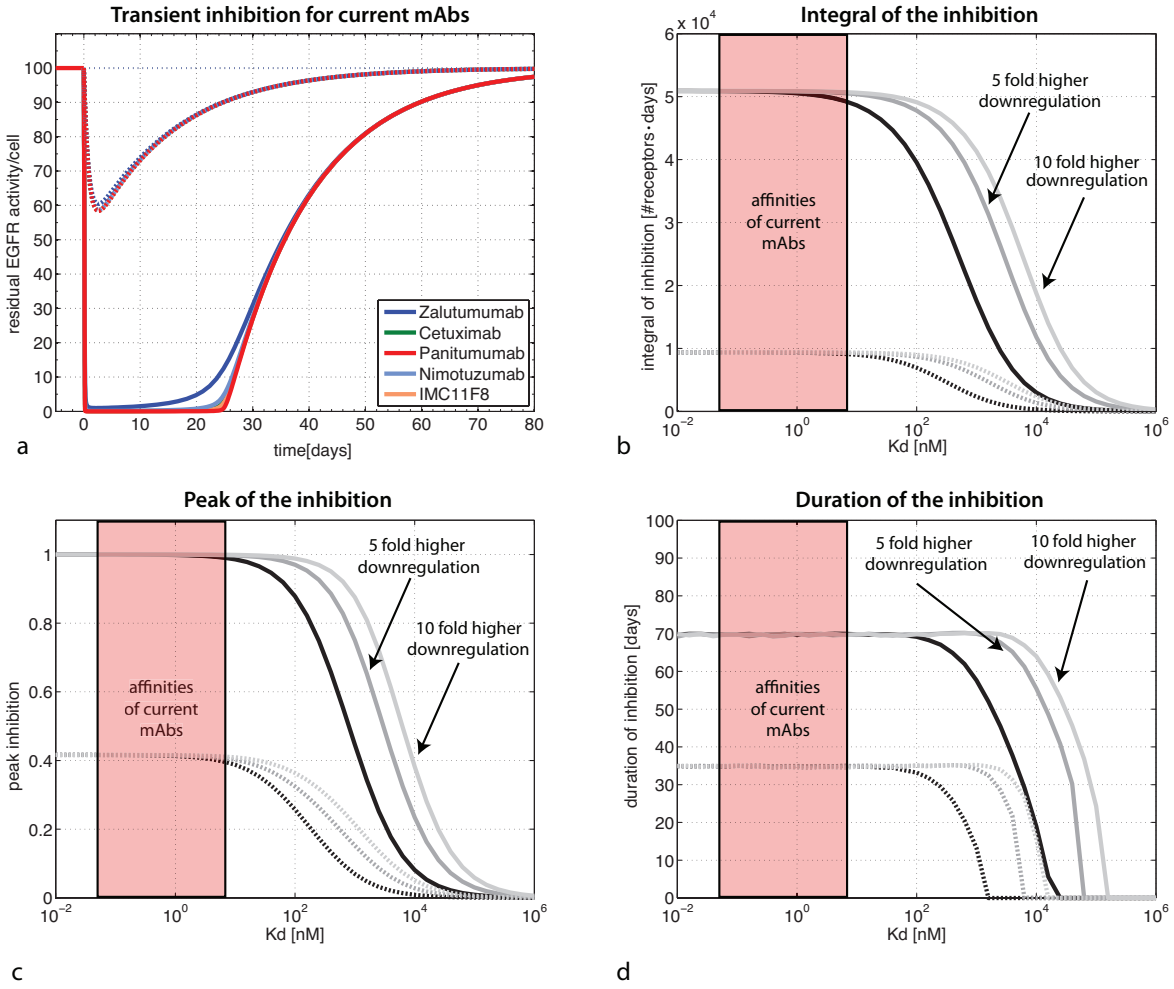

Figure 4.3: *Inhibitory effect of different antibodies using the cell-level pharmacokinetic/pharmacodynamic model shown in Fig.4.1(b).* ***(a)*** *Predicted transient inhibitory effects of five antibodies on the market or in clinical development with different affinities (see Table 4.3) for a 20 mg dose (▬) and a 2 mg dose (▬▬). The different mAbs show a similar transient inhibitory effect despite their affinities vary 20-fold.* ***(b)-(d)*** *Inhibitory effect resulting from different affinities (K_D = 1/affinity = $k_{\mathrm{offD}}/k_{onD}$) and downregulation rates (k_{degRD}). The antibody is quantified by the three different measures defined in Fig.4.1(a):* ***(b)*** *the integral of inhibition,* ***(c)*** *the peak inhibition, and* ***(d)*** *the duration of inhibition, for the 20 mg dose (▬) and 2 mg (▬▬) dose. The shaded area indicate the affinity range of the five considered anti-EGFR antibodies on the market or in late stages of the development. The different affinities were realized in silico by altering the dissociation rate constant k_{offD}, while the association rate constant was kept constant. For low affinity drugs, the inhibitory effects can be increase by increasing the affinity to the target. For high affinity drugs (such as those in the shaded area), the existence of a plateau region does not allow for further optimization of the direct inhibitory effect.*

tion parameter are located on the effect plateau and their direct inhibitory effect could not be further increased (Appendix 6.2). For lower affinity drugs the target independent clearance is more dominant such that RME (and therefore drug effect), decreases for lower affinity.

Receptor downregulation.

Enforcing receptor downregulation by mAbs is argued to be an important part of the drugs' effect[96]. For anti-EGFR antibodies, we found that endocytic downregulation only contributes to a negligible extent to the direct inhibitory effect of high-affinity antibodies (Fig. 4.3(b)-(d)) on the market or in late development. For medium affinity antibodies, however, an increased downregulation could increase the direct inhibitory effect.

4.4 Tumor cell specificity

As a next demonstration of the benefit of the cell-level pharmacokinetic/ pharmacodynamic model we predicted the effect on cells with different alterations to determine how to optimize the specificity of antibodies against tumor cells.

Upregulation of EGFR expression and aberrant activation of EGFR has been shown in many human epithelial cancers, including those of the colon, lung, kidney, head and neck, breast, prostate, brain and ovary[124, 105, 122, 149, 56, 142]. The extent of overexpression also correlates with a poorer clinical outcome[95, 49].

To compare the response of normal and tumor cells to anti-EGFR antibodies, we extended our model by integrating a kinetic cellular model representing tumor cells with elevated EGFR levels (see Fig. 4.1(c)). The cellular model for the tumor cells was chosen to resemble the characteristics of A431 cells, a human squamous carcinoma cell line with high EGFR levels [91, 83, 145]. The overexpression in A431 cell is due to amplification of the EGFR gene[97] and correlates with increased EGF receptor mRNA levels[83]. A431 cells express about $1.8 \cdot 10^6$ EGFR at the cell surface[91]. *In vivo* experiments are typically designed in a way that the A431 tumors do not influence the pharmacokinetics of the mAbs (e.g., Bleeker et al.[13] in mice). We therefore set the number of tumor cells to 1% of the normal cells, which had little impact on the pharmacokinetics. The tumor cell model represents those tumor cells exposed to drug concentrations equivalent to the exposure of cells with normal EGFR levels.

The extended cell-level pharmacokinetic/pharmacodynamic model was also used to study whether cells with higher receptor levels are more susceptible to antibody treatment than normal cells. Figure 4.4 (a) illustrates the predicted inhibitory effect in tumor and normal cells in cynomolgus monkeys. For tumor cells with elevated receptor levels, the inhibitory effect is seen to be stronger than for those cells with normal EGFR levels.

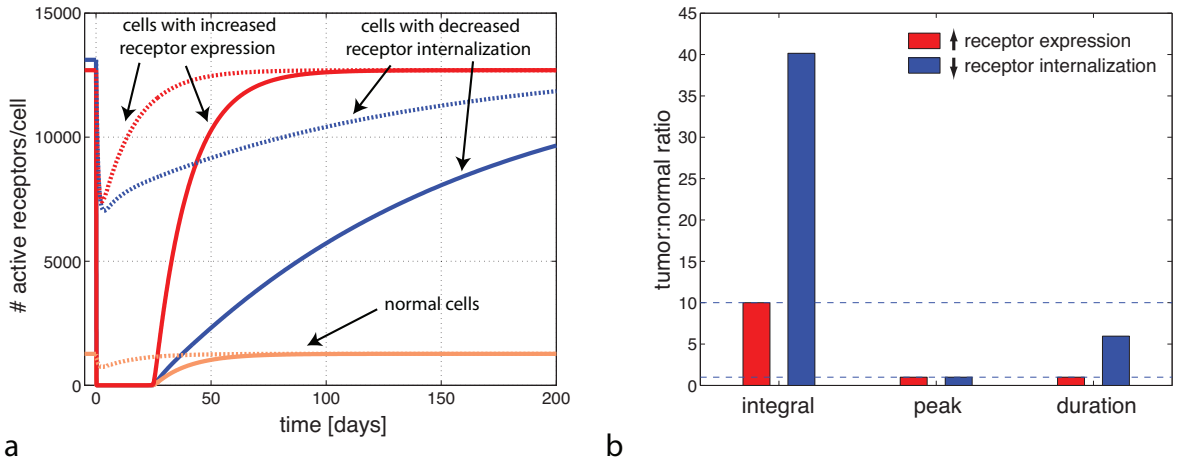

Figure 4.4: *The mechanism underlying increased receptor levels influences tumor specificity of mAbs.* ***(a)*** *Predicted transient inhibition based on the extended cell-level pharmacokinetic model shown in Figure 4.1(c) for normal cells (▬), tumor cells with a 10-fold increased receptor expression (▬), and tumor cells with a 10-fold decreased internalization of the free and bound receptor (▬). Profiles are shown for a high dose of 20 mg (▬) and a low dose of 2 mg (▬). Both scenarios show similar steady-state activation levels of the receptor, but their response to drug treatment is substantially different.* ***(b)*** *Antibody specificity as ratio of effect in tumor cells compared to cells with normal levels of EGFR for the three effect characteristics. Cells with a decreased receptor internalization have a much longer duration of inhibition and therefore a higher integral of inhibition than tumor cells with an increased receptor expression.*

Elevated receptor levels as potential biomarkers

The cell-level model (Fig. 4.1 (a)) suggests that elevated receptor levels can be a consequence of not only an increased receptor expression, but also of a reduced internalization of the receptor. Reddy *et al.*[113] reports about an alteration of EFGR where a truncated cytoplasmic domain exhibits a decreased ligand-induced internalization rate constant. Figure 4.4 (a) compares the predicted transient inhibition for both alterations, increased synthesis rate and reduced internalization. Although both cell alterations resulted in similar steady-state activation levels, their responses to mAbs are remarkably different.

For a quantitative comparison of the inhibitory effect in normal and tumor cells, we defined the tumor specificity S as the ratio of the inhibitory effect on tumor cells relative to normal cells. Thus we have

$$S_{\text{peak}} = \frac{\text{peak}_{\text{t}}}{\text{peak}}, \tag{4.7}$$

$$S_{\text{duration}} = \frac{\text{duration}_{\text{t}}}{\text{duration}}, \tag{4.8}$$

$$S_E = \frac{E_{\text{t}}}{E}. \tag{4.9}$$

We compared the tumor specificity *tumor:normal*, S for both types of alterations for a 20 mg

dose of a high affine mAb (Figure 4.4(b)).

A 10-fold receptor overexpression in tumor cells resulted in the same amplification of the integral of inhibition. Although the initial decrease is stronger in tumor cells overexpressing the receptor, at the same time, due to the increased receptor expression, the recovery was considerably faster and in total leads to the same duration of the inhibition as in normal cells. In the case of overexpression, mAbs are selective only in terms of the integral of inhibition. As supported by a theoretical analysis (Supplementary Material Section 6.3), mAbs specificity holds independently of the model parameterization, mAbs target affinity, downregulation constant and dose. Our findings therefore suggest that when considering the direct inhibitory effect, the specificity of therapeutic antibodies against tumor cells overexpressing the receptor cannot be improved by tuning the drugs properties.

Cells with decreased receptor internalization, in contrast, showed a higher integral and duration of inhibition compared to normal cells. Also, since tumor specificity of mAbs for cells with decreased internalization rates depends on the affinity and dose of the mAbs, further optimization of their tumor specificity can be achieved by lowering affinity and/or dose.

4.5 Summary and Conclusions of this chapter

Mechanism-based pharmacokinetic and pharmacodynamic models constitute a scientific basis for understanding drug efficacy and safety. Such models contribute to improving efficiency in the drug development process and to reduce attrition rates [109]. In cynomolgus monkeys, our cell-level pharmacokinetic/pharmacodynamic model predicts almost identical direct inhibitory effects for a range of antigen-binding affinities. Supporting theoretical analysis of the model suggests that the existence of an effect plateau is a generic feature of this drug-target system and does not depend on specific parameter values. Current anti-EGFR antibodies are located on the effect plateau which relativizes the affinity amongst the properties that can be further tuned to optimize antibody efficacy. In view of our findings, the recent assertions that panitumumab, due to its very high affinity, can compete more effectively with ligands for binding to EGFR compared to high affinity mAbs [61]; and that nimotuzumab, due to its intermediate affinity, relies on the high number of receptors as present on tumor cells for efficient binding [24], should be revisited.

Based on the existence of an effect plateau in the direct inhibitory effect, the clinically observed differences among mAbs are likely to arise from indirect effects, such as the action of immune effector functions (such as antibody dependent cell mediated cytotoxicity or complement dependent cytotoxicity), rather than the direct antagonistic effect. This is consistent with a study of Bleeker et al. showing that effects *in vivo* of zalutumumab and cetuximab differed only by their ability to trigger such indirect effect and not by their direct inhibitory effect [13].

Regarding optimization of tumor specificity, we find that antibody specificity depends on the tumor cell type, i.e., the alterations underlying elevated receptor numbers. Tumor cells with an increased receptor expression seem to recover from the drug treatment faster than those with reduced internalization rates, despite potentially presenting similar receptor numbers. Our analysis suggests that biophysical properties cannot be tuned regarding the specificity of the direct effect on tumor cells overexpressing the receptor (such as A431 cells). In contrast, for tumor cells with a decreased receptor internalization, the specificity is increased for lower affinity and/or dose. This increased specificity, however, comes along with a lower absolute effect.

Using cutaneous toxicities—the most common side effects of anti-EGFR antibodies, affecting 45–100% of patients [79]—as a marker of drug efficacy and clinical outcome was proposed [108]. Clinical experience, however, has shown that EGFR levels, as measured by immunohistochemistry, do not predict clinical benefit [25, 21]. Our finding regarding the dependence of drug efficacy on tumor type suggests that the unsatisfactory correlation between elevated receptor levels and drug efficacy may be improved by a genotypic determination of the underlying cellular alterations.

5 Conclusions and Extensions

Mathematical modelling has become a widely used methodology in preclinical drug discovery, early clinical development, and later stage clinical development [2, 62, 162, 148, 80, 58, 18]. Mechanistic models of cell-level kinetics are of increasing importance for target identification and validation [130]. Mechanistic models can describe the causal path between the drug and the effect and also make an explicit distinction between drug specific and organism specific parameters. A main challenge today is to integrate data and knowledge from different sources such as clinical PK data, *in vitro* data, genomic studies, and bioinformatics to link the exposure of a drug (or combination of drugs) and the modulation of pharmacological targets, physiological pathways and ultimately disease systems [162]. This is the objective of the arising field of systems pharmacology by considering targets in the context of the biological networks in which they exist. In this thesis we developed an approach of combining empirical pharmacokinetic and mechanistic cell-level models to bring the different areas closer together. The model can act as a quantitative framework which allows to accumulate and pool the knowledge over the different stages of the drug development pipeline.

Following the lessons we learned from modelling the nonlinear pharmacokinetics of therapeutic proteins, we want to raise the question if the nonlinear pharmacokinetics of therapeutic proteins is a curse or a gift for analyzing clinical data and adjust dosing of the drug. Traditionally the nonlinearity is seen as a factor which complicates dose finding, and although this might be true, we would argue that the nonlinearity can be well described and predicted using nonlinear pharmacokinetic models, if the physiological reasons and mechanism are understood. Additionally, we are convinced that nonlinear pharmacokinetics occurring because of the interaction of the drug with the target gives precious information about the action of the drug, which can be further enriched by mechanistic modelling of cellular processes.

In a way, therapeutic proteins blur the traditional distinction between pharmacokinetics and pharmacodynamics. Processes, such as the binding of the drug to the receptor, cannot be classified either as only controlling the disposition or the effect of the drug, but influence both at the same time. The development of modelling concepts like TMDD is a first step to include cell-level processes like receptor binding and trafficking into pharmacokinetic models. Nevertheless, we argue that defining the cell as the fundamental unit of the model, as is done in systems biology, is for many applications an advantage over pooling processes on a whole body level. As demonstrated in this thesis, a cellular model allows to mechanistically describe processes, compare alterations in different cell types, and the global optimization

of drug properties. Another aspect is that TMDD describes only processes such as target turnover, drug binding, and the internalization of the drug-target complex. We learned in Chapter 4 these processes alone might not allow to describe the pharmacokinetics of therapeutic antibodies. As we saw for zalutumumab, the existence of an intracellular pool of receptor (dynamically described by the internalization and recycling of the free receptor) can be important. Only this pool in addition to the turnover of the receptor explained the initial decrease of drug concentration right after drug administration as well as the clearance velocity in the terminal phase. This demonstrates how processes according to the knowledge of the cellular level can be added to the pharmacokinetic model and might allow a better explanation of data determined in clinical trials.

In the following, we will discuss possible extensions to the model. A limitation of the proposed cell-level pharmacokinetic/ pharmacodynamic model is that predictions of EGFR inhibition on tumor cells are limited to those malignant cells which are exposed to similar concentration than normal cells, such as avascular metastases embedded in healthy tissue [143]. In solid tumors, due to heterogeneous drug distribution, only malignant cells close to capillaries might be exposed to such concentration. A more physiological description of the pharmacokinetic model may allow to distinguish between the drug concentrations in the different tissues or the tumor. One possible extension we identify, is therefore the use of physiologically based pharmacokinetic models (PBPK).

The difference of PBPK compared to the empirical compartment models described in section 2.2 is that compartments and volumes of PBPK models correspond to discrete tissues, organs and other physiologically identifiable spaces. Further, the distribution of the drug in the body is described by fluxes corresponding to the blood flows connecting the organs or organ groups (see Fig. 5.1). In the different organs the distribution process is modelled in terms of so called partition coefficients which describe the steady-state concentration within the tissue compared to the blood concentration. Additionally to the physiologically based "wiring" of the organs by the bloodstream each organ can be further divided into submodels representing different subcompartments like the interstitial space or the cytosol of cells (see Fig. 5.2). Using this framework, the tumor can be described as a single compartment or be subdivided in different parts which are differentially accessible to the drug.

For describing the disposition of antibody drugs, PBPK models should incorporate the particularities associated with antibody disposition such as convective movement of antibodies into tissues, lymphatic circulation, RME, and catabolism in the different tissues [84, 141]. Several PBPK models for antibodies have been developed [10, 23, 36, 9, 42, 60, 164, 165, 43, 28, 52, 146]. In contrast to PBPK models for small molecules these models should include the lymphatic system and usually also a submodel which describes the flux of macromolecules from the blood capillaries to the interstitial space of the organs [117]. A two-pore model which

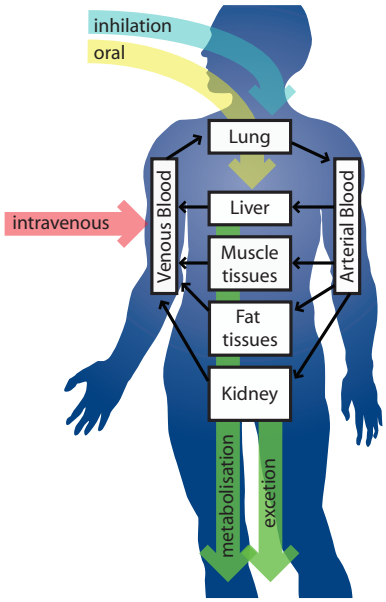

Figure 5.1: *Schematic structure of a physiologically based pharmacokinetic model (PBPK). The modelled organs or organ groups are connected by the blood flow.*

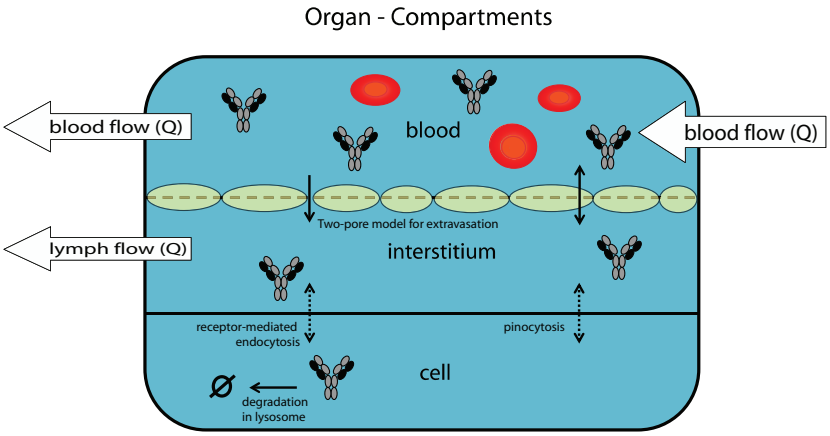

Figure 5.2: *A submodel in a PBPK model which describes the processes involved in the distribution of antibodies inside a tissue.*

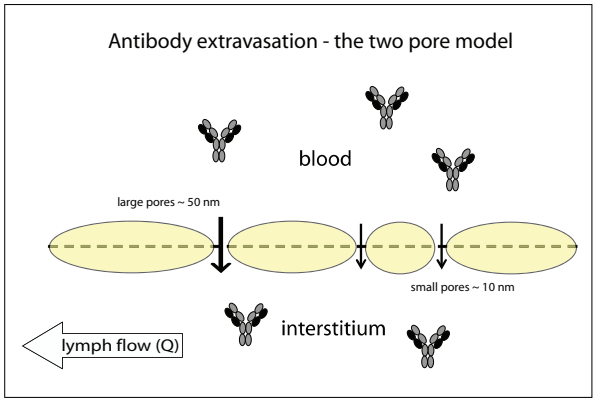

Figure 5.3: *Schematic illustration of the two pore model describing the extravasation of antibodies.*

describes this is depicted in Fig. 5.3. Another exceptional aspect of antibody disposition in the body is binding to the neonatal Fc receptor (FcRn). FcRn contributes to effective humoral immunity by recycling IgG and extending its half-life in the circulation [119]. FcRn binds tightly to the Fc portion of IgG at acidic pH 6.0 in endosomes, but not at physiological pH 7.4 and therefore can recycle IgG back the circulation secondary to internalization by RME. Because of its important role for the pharmacokinetics usually the FcRn is incorporated into PBPK model for mAbs.

Because of their mechanistic nature, PBPK models in the future probably will play a key role when aiming to include mechanistic pharmacodynamic models of mAbs [111]. PBPK models together with mechanistic pharmacodynamic models of cellular processes have the potential to account simultaneously for processes such as systemic distribution, extravasation into tissue, lymphatic drainage, target binding, target dynamics, and metabolisation of mAbs.

The advantage of a more detailed description of the pharmacokinetics comes with the need for many parameters and detailed drug concentration data from different compartments/tissues for a validation of the model. This limits the use of PBPK models in the analysis of sparse clinical data where usually only drug concentrations in plasma are determined. This was the reason why we used empirical compartment models to describe the pharmacokinetics in this thesis. Moreover, it is known that the main space of antibody distribution is the plasma and the interstitial space. Hence, the used two-compartment model seems physiologically and pharmacokinetically motivated. Nevertheless, in the cases where detailed measurements of drug concentrations from different organs are available (like it might be the case for preclinical studies in animal models) PBPK models might be a rational basis for the integration of cellular models such as the ones described in this thesis.

A further limitation of the current cell-level pharmacokinetic/ pharmacodynamic model is that it predicts decrease in receptor activation instead of the actual biological response of the cell. While Knauer et al. [68] reported a linear dependence between the number of activated EGFR at steady-state and the cellular responses of fibroblasts and epithelial cells, other

models describe a more complex relationship between receptor activation and downstream signaling [129]. A possible extension of the cell-level pharmacokinetic/ pharmacodynamic model is therefore the integration of more detailed cell-level models.

Additionally to the receptor activation models discussed in Section 3.1, many very detailed systems biology models of receptor activation, trafficking and downstream signalling have been developed. Schoebel et al. [129] derived and validated a comprehensive model of 94 ordinary differential equations with 95 parameters connecting the activated EGFR to the downstream kinase ERK (Extracellular signal–Regulated Kinase). The model provides insight into the high robustness of the downstream signalling of EGFR, where over a range of 100 fold ligand concentration the activation of ERK seems to be remarkably stable. The important parameter for signal efficacy is the initial velocity of receptor activation and this is mainly determined by the affinity of the ligand.

Studying the input-output behavior of the EGFR signalling network became even more detailed when Birtwistle et al. [11] and Chen et al. [20] included also the activation and signalling of the other cell surface receptors of the ErbB/Her family. Birtwistle found that the overexpression of the receptor ErbB2 leads to change in the activation of ERK over time. The overexpression transformed a transient activation of the cell-surface receptors into a sustained activation of the ERK. Chen et al. eluminated the dependence of the signalling behavior on the conditions (which ligand binds to the cell surface receptors) and the feature (the downstream effector kinase which gets activated). Very recently, the model of the signalling of the ErbB family has been further extended to study the crosstalk between the signalling downstream of the EGFR and the Insulin receptor [14].

Our approach to couple systems biology models with pharmacokinetic models in general allows for integrating such detailed models of downstream signalling into systemic pharmacokinetic models. To couple such detailed downstream signalling models, the cell-level model has to provide the species which act as an interface between the signalling inside the cell and the receptor dynamics on the cell surface. For example, models which describe the activation of the different receptors of the ErbB family[11, 20] would need a more detailed receptor activation and inhibition model than the ones we developed in this thesis. On the other hand, models of EGFR downstream signalling where the free EGF receptor at the cell membrane is already part of model (like, e.g., the comprehensive model of Schoeberl et al. [129]), may allow a direct coupling with our developed cell-level PK/PD model.

In conclusion, we propose that detailed cell-level models combined with pharmacokinetic models will prove valuable in the emerging field of systems pharmacology. Further, the use of more detailed systems biology models describing downstream signaling processes relevant to human diseases [20, 14, 63] may allow to translate a drugs' plasma concentration into receptor activation and ultimately into a biological responses of tumor cells.

6 Appendix

6.1 Derivation of an exact formula for the inhibitory effect

We consider the model defined in Eq. (3.2) and define the steady state as R^*, RL^*, RD^* and $D^* = 0$. The integral of the inhibitory effect is defined as

$$E = \int_0^\infty RL(t) - RL^* \, dt. \tag{6.1}$$

We rewrite model (3.2) in terms of the deviations of the species from their steady state values. We define these deviation variables as

$$\begin{aligned} \bar{R}(t) &= R(t) - R^*, & \bar{D}(t) &= D(t) - D^*, \\ \bar{RD}(t) &= RD(t) - RD^*, & \bar{RL}(t) &= RL(t) - RL^*, \end{aligned}$$

and the state vector as

$$\bar{x}(t) = \begin{bmatrix} \bar{D}(t) & \bar{R}(t) & \bar{RL}(t) & \bar{RD}(t) \end{bmatrix}^T. \tag{6.2}$$

A taylor expansion around the steady state x^* gives

$$\frac{\mathrm{d}\, x(t)}{\mathrm{d}t} = Nv(x,t) \mid_{x=x^*} + N\frac{\mathrm{d}}{\mathrm{d}x} v(x,t) \mid_{x=x^*} \bar{x} + \frac{1}{2}\bar{x}^T N \frac{\mathrm{d}^2}{\mathrm{d}^2 x} v(x,t) \mid_{x=x^*} \bar{x} \tag{6.3}$$

Because

$$\frac{\mathrm{d}\, \bar{x}}{\mathrm{d}t} = \frac{\mathrm{d}\, x(t)}{\mathrm{d}t} - \frac{\mathrm{d}\, \bar{x}}{\mathrm{d}t} = \frac{\mathrm{d}\, x(t)}{\mathrm{d}t} \tag{6.4}$$

and

$$Nv(x,t) \mid_{x=x^*} = 0 \tag{6.5}$$

it follows that the resulting system of ODEs in terms of the new state variable is given by

$$\frac{\mathrm{d}\, \bar{x}}{\mathrm{d}t} = \boldsymbol{A}\bar{x}(t) + \boldsymbol{B}\bar{x}_1\bar{x}_2, \tag{6.6}$$

where the matrix $\boldsymbol{A} = N\frac{\mathrm{d}}{\mathrm{d}x}v(x,t)\mid_{x=x^*} \in R^{4\times 4}$ is the Jacobian of the right hand side of (3.2) evaluated at the steady state

$$\boldsymbol{A} = \begin{bmatrix} -\frac{k_{\mathrm{onD}}R^*}{VN_a} & 0 & 0 & \frac{k_{\mathrm{offD}}}{VN_a} \\ -k_{\mathrm{onD}}R^* & -k_{\mathrm{onL}}L - k_{\mathrm{degR}} & k_{\mathrm{offL}} & k_{\mathrm{offD}} \\ 0 & k_{\mathrm{onL}}L & -k_{\mathrm{offL}} - k_{\mathrm{degRL}} & 0 \\ k_{\mathrm{onD}}R^* & 0 & 0 & -k_{\mathrm{offD}} - k_{\mathrm{degRD}} \end{bmatrix}, \tag{6.7}$$

and

$$\boldsymbol{B} = \begin{bmatrix} \frac{k_{\mathrm{onD}}}{VN_a} & k_{\mathrm{onD}} & 0 & -k_{\mathrm{onD}} \end{bmatrix}^T. \tag{6.8}$$

Integration of (6.6) from $t = 0$ to infinity gives

$$\bar{x}(\infty) - \bar{x}(0) = \boldsymbol{A}\int_0^\infty \bar{x}(t)dt + \boldsymbol{B}\int_0^\infty \bar{x}_1(t)\bar{x}_2(t)dt. \tag{6.9}$$

For a bolus dose C at $t = 0$ the initial condition for (6.6) is

$$\bar{x}(0) = \begin{bmatrix} C & 0 & 0 & 0 \end{bmatrix}^T. \tag{6.10}$$

Under the biologically reasonable assumption that when the drug disappears the receptor system goes back to its old steady-state activation level (described in Section 3.2), the stability of the system implies that $\bar{x}(\infty) = 0$. Substitution in (6.9) yields

$$\int_0^\infty \bar{x}(t)dt = \boldsymbol{A}^{-1}\bar{x}(0) + \boldsymbol{A}^{-1}\boldsymbol{B}\int_0^\infty \bar{x}_1(t)\bar{x}_2(t)dt. \tag{6.11}$$

From (6.1) and (6.2) we notice that $E = \int_0^\infty \bar{x}_3(t)dt$, that is,

$$E = \left[\boldsymbol{A}^{-1}\boldsymbol{B}\right]_3 + \left[\boldsymbol{A}^{-1}\bar{x}(0)\right]_3. \tag{6.12}$$

Computing $\boldsymbol{A}^{-1}$ it can be shown that $\left[\boldsymbol{A}^{-1}\boldsymbol{B}\right]_3 = 0$ and (6.12) leads to

$$E = VN_aC\frac{k_{\mathrm{onL}}L}{Lk_{\mathrm{onL}}k_{\mathrm{degRL}} + k_{\mathrm{degR}}k_{\mathrm{offL}} + k_{\mathrm{degR}}k_{\mathrm{degRL}}}. \tag{6.13}$$

From model (3.2) the steady state concentration RL^* is given by

$$RL^* = \frac{k_{\mathrm{onL}}k_RL}{Lk_{\mathrm{onL}}k_{\mathrm{degRL}} + k_{\mathrm{degR}}k_{\mathrm{offL}} + k_{\mathrm{degR}}k_{\mathrm{degRL}}}. \tag{6.14}$$

Combining (6.14) with (6.13) finally yields a simple formula for the cumulative effect

$$E = \frac{VN_aRL^*}{k_R}C. \tag{6.15}$$

Assume t_{end} to be the length of the treatment period and sufficiently large so that

$$E = \int_0^\infty (RL^* - RL(t))\, dt \approx \int_0^{t_{end}} (RL^* - RL(t))\, dt. \tag{6.16}$$

Then the *relative* inhibitory effect can be expressed as

$$E_r = \frac{\int_0^{t_{end}} (R_L^* - R_L(t))\, dt}{\int_0^{t_{end}} R_L^*\, dt} = \frac{VN_aCR_L^*}{t_{end}k_RR_L^*} = \frac{VN_aC}{t_{end}k_R} = \frac{dose}{t_{end}k_R}. \tag{6.17}$$

6.2 Quantification of the integral of effect *in vivo*

The steady state of model (4.1)-(4.3) is

$$x^* = \begin{bmatrix} D_p^* & D_c^* & R^* & R_{\mathrm{i}}^* & RL^* & RD^* & R_{\mathrm{t}}^* & Ri_{\mathrm{t}}^* & RL_{\mathrm{t}}^* & RD_{\mathrm{t}}^* \end{bmatrix},$$

and we know that $D_p^* = D_c^* = RD^* = RD_{\mathrm{t}}^* = 0$. We assume that the steady state is exponentially stable, which for any realistic scenario is trivially satisfied. This guarantees that the integral of the inhibition

$$E = \int_0^\infty (RL^* - RL(t))\, dt, \tag{6.18}$$

is a finite number. The deviations of the model variables with respect to the steady state are

$$\begin{aligned}
\bar{R} &= R^* - R & \bar{R}_{\mathrm{t}} &= R_{\mathrm{t}}^* - R_{\mathrm{t}} & \bar{D}_p &= -D_p \\
\bar{R}_{\mathrm{i}} &= R_{\mathrm{i}}^* - R_{\mathrm{i}} & \bar{Ri}_{\mathrm{t}} &= Ri_{\mathrm{t}}^* - Ri_{\mathrm{t}} & \bar{D}_c &= -D_c \\
\bar{RL} &= RL^* - RL & \bar{RL}_{\mathrm{t}} &= RL_{\mathrm{t}}^* - RL_{\mathrm{t}} & & \\
\bar{RD} &= -RD & \bar{RD}_{\mathrm{t}} &= -RD_{\mathrm{t}} & &
\end{aligned}$$

We define a state vector as

$$\bar{x} = \begin{bmatrix} \bar{D}_p & \bar{D}_c & \bar{R} & \bar{R}_{\mathrm{i}} & \bar{RL} & \bar{RD} & \bar{R}_{\mathrm{t}} & \bar{Ri}_{\mathrm{t}} & \bar{RL}_{\mathrm{t}} & \bar{RD}_{\mathrm{t}} \end{bmatrix}^T. \tag{6.19}$$

The model is linearized around the steady state. This leads to the following linear system of ODEs

$$\frac{\mathrm{d}\,\bar{x}}{\mathrm{d}t} = \boldsymbol{A}\bar{x}. \tag{6.20}$$

The matrix $\boldsymbol{A} \in \mathbb{R}^{10\times 10}$ is given in (6.7) and corresponds to the Jacobian of the right hand side of (4.1)-(4.3) evaluated at the steady state. Integration of (6.20) from $t = 0$ up to $t = \infty$ gives

$$\bar{x}(\infty) - \bar{x}(0) = \boldsymbol{A} \int_0^\infty \bar{x}(t)dt. \tag{6.21}$$

For a bolus dose C at $t = 0$ the initial condition for (6.20) is

$$\bar{x}(0) = \begin{bmatrix} -C & 0 & 0 & \cdots & 0 \end{bmatrix}^T. \tag{6.22}$$

As before, the return to the old steady-state activation level of the receptor after the drug disappears implies that $\bar{x}(\infty) = 0$, which upon substitution in (6.21) yields

$$\int_0^\infty \bar{x}(t)dt = -\boldsymbol{A}^{-1}\bar{x}(0). \tag{6.23}$$

From (6.19) we notice that the integral of inhibition E is the 5^{th} entry of the vector in (6.23). Hence

$$E = \int_0^\infty \bar{x}_5(t)dt = -\left[\boldsymbol{A}^{-1}\bar{x}(0)\right]_5. \tag{6.24}$$

Computing the inverse $\boldsymbol{A}^{-1}$ we get

$$E = \frac{\alpha R L^*}{\beta + \gamma \frac{1}{k_{\text{onD}}}\left(\frac{1}{\text{CP}} + 1\right)}, \tag{6.25}$$

with the constants:

$$\alpha = V_c R^* q_{\text{cp}} C \frac{k_{\text{degR}}}{k_{\text{onL}} L}\left(\frac{k_{\text{offL}} + k_{\text{degRL}}}{k_{\text{recyR}} + k_{\text{exit}}}\right), \tag{6.26}$$

$$\beta = k_{R\text{h}}\text{SF}(q_{\text{cp}} + \text{CL}_{\text{linD}})(N_{\text{h}} R^* + N_{\text{t}} R_{\text{t}}^*), \tag{6.27}$$

$$\gamma = k_{R\text{h}}\text{CL}_{\text{linD}} q_{\text{pc}}. \tag{6.28}$$

The parameter $K_D = 1/\text{affinity}$ and the "consumption parameter" defined by Shankaran *et al.* [133] are given by

$$K_D = \frac{k_{\text{offD}}}{k_{\text{onD}}} \qquad\qquad \text{CP} = \frac{k_{\text{degRD}}}{k_{\text{offD}}}. \tag{6.29}$$

The effect E is a decreasing function of k_{offD} and shows little variations for the values of K_D for the mAbs in Table 4.3. All these mAbs are located in a plateau region of the effect E. This linear analysis suggests that the effect plateau is a structural feature of the system and does not depend on the parameter values.

6.3 Effect of receptor overexpression on the drug specificity

From the model (4.2)-(4.3), the ODEs for the free and bound receptors in the tumor cells are

$$\begin{aligned}
\frac{\mathrm{d}R_\mathrm{t}}{\mathrm{d}t} &= k_{R\mathrm{t}} - k_\mathrm{onL} R_\mathrm{t} \cdot L - k_\mathrm{onD} R_\mathrm{t} \cdot D_p + k_\mathrm{recyR} Ri_\mathrm{t} \\
&\quad + k_\mathrm{offL} RL_\mathrm{t} + k_\mathrm{offD} RD_\mathrm{t} - k_\mathrm{degR} \cdot R_\mathrm{t}, \\
\frac{\mathrm{d}Ri_\mathrm{t}}{\mathrm{d}t} &= k_\mathrm{degR} \cdot R_\mathrm{t} - k_\mathrm{recyR} \cdot Ri_\mathrm{t} - k_\mathrm{exit} \cdot Ri_\mathrm{t}, \\
\frac{\mathrm{d}RL_\mathrm{t}}{\mathrm{d}t} &= k_\mathrm{onL} R_\mathrm{t} \cdot L - k_\mathrm{offL} RL_\mathrm{t} - k_\mathrm{degRL} RL_\mathrm{t}, \\
\frac{\mathrm{d}RD_\mathrm{t}}{\mathrm{d}t} &= k_\mathrm{onD} \cdot R_\mathrm{t} \cdot D_p - k_\mathrm{offD} RD_\mathrm{t} - k_\mathrm{degRD} \cdot RD_\mathrm{t}.
\end{aligned} \tag{6.33}$$

We assume that the tumor cells have a receptor synthesis rate that is α times higher than in normal cells, i.e., $k_{R\mathrm{t}} = \alpha k_{R\mathrm{h}}$. Since the equilibrium values R_t^*, Ri_t^*, RL_t^* and RD_t^* are proportional to $k_{R\mathrm{t}}$, we have that

$$R_\mathrm{t}^* = \alpha R^*, \qquad Ri_\mathrm{t}^* = \alpha R_\mathrm{i}^*, \tag{6.34}$$

$$RL_\mathrm{t}^* = \alpha RL^*, \qquad RD_\mathrm{t}^* = \alpha RD^*. \tag{6.35}$$

Substituting $k_{R\mathrm{t}} = \alpha k_{R\mathrm{h}}$ in (6.33) and dividing by α yields

$$\begin{aligned}
\frac{\mathrm{d}}{\mathrm{d}t}\left(\frac{R_\mathrm{t}}{\alpha}\right) &= k_{R\mathrm{h}} - k_\mathrm{onL} \frac{R_\mathrm{t}}{\alpha} \cdot L - k_\mathrm{onD} \frac{R_\mathrm{t}}{\alpha} \cdot D_p + k_\mathrm{recyR} \frac{Ri_\mathrm{t}}{\alpha} \\
&\quad + k_\mathrm{offL} \frac{RL_\mathrm{t}}{\alpha} + k_\mathrm{offD} \frac{RD_\mathrm{t}}{\alpha} - k_\mathrm{degR} \cdot \frac{R_\mathrm{t}}{\alpha}, \\
\frac{\mathrm{d}}{\mathrm{d}t}\left(\frac{Ri_\mathrm{t}}{\alpha}\right) &= k_\mathrm{degR} \cdot \frac{R_\mathrm{t}}{\alpha} - k_\mathrm{recyR} \cdot \frac{Ri_\mathrm{t}}{\alpha} - k_\mathrm{exit} \cdot \frac{Ri_\mathrm{t}}{\alpha}, \\
\frac{\mathrm{d}}{\mathrm{d}t}\left(\frac{RL_\mathrm{t}}{\alpha}\right) &= k_\mathrm{onL} \frac{R_\mathrm{t}}{\alpha} L - k_\mathrm{offL} \frac{RL_\mathrm{t}}{\alpha} - k_\mathrm{degRL} \frac{RL_\mathrm{t}}{\alpha}, \\
\frac{\mathrm{d}}{\mathrm{d}t}\left(\frac{RD_\mathrm{t}}{\alpha}\right) &= k_\mathrm{onD} \cdot \frac{R_\mathrm{t}}{\alpha} \cdot D_p - k_\mathrm{offD} \frac{RD_\mathrm{t}}{\alpha} - k_\mathrm{degRD} \cdot \frac{RD_\mathrm{t}}{\alpha}.
\end{aligned} \tag{6.36}$$

By comparing the ODES in (6.36) with those for the normal cells in (4.2), we see that receptor overexpression translates into scaled responses in the tumor cells (note that according to (6.34)-(6.35) the initial conditions are also scaled), i.e.,

$$R_\mathrm{t}(t) = \alpha R(t), \qquad Ri_\mathrm{t}(t) = \alpha R_\mathrm{i}(t),$$

$$RL_\mathrm{t}(t) = \alpha RL(t), \qquad RD_\mathrm{t}(t) = \alpha RD(t).$$

$$\boldsymbol{A} = \begin{bmatrix} a_{11} & \frac{q_{\mathrm{pc}}}{V_c} & 0 & 0 & 0 & 0 & 0 & 0 & 0 & 0 \\ \frac{q_{\mathrm{cp}}}{V_p} & a_{22} & 0 & 0 & 0 & \frac{k_{\mathrm{offD}} N_{\mathrm{h}} \mathrm{SF}}{V_p} & 0 & 0 & 0 & \frac{k_{\mathrm{offD}} N_{\mathrm{t}} \mathrm{SF}}{V_p} \\ 0 & -k_{\mathrm{onD}} R^* & -k_{\mathrm{onL}} L - k_{\mathrm{degR}} & k_{\mathrm{recyR}} & k_{\mathrm{offL}} & k_{\mathrm{offD}} & 0 & 0 & 0 & 0 \\ 0 & 0 & k_{\mathrm{degR}} & -k_{\mathrm{recyR}} - k_{\mathrm{exit}} & 0 & 0 & 0 & 0 & 0 & 0 \\ 0 & 0 & k_{\mathrm{onL}} L & 0 & -k_{\mathrm{offL}} - k_{\mathrm{degRL}} & 0 & 0 & 0 & 0 & 0 \\ 0 & k_{\mathrm{onD}} R^* & 0 & 0 & 0 & -k_{\mathrm{offD}} - k_{\mathrm{degRD}} & 0 & 0 & 0 & 0 \\ 0 & -k_{\mathrm{onD}} R_{\mathrm{t}}^* & 0 & 0 & 0 & 0 & -k_{\mathrm{onL}} L - k_{\mathrm{degR}} & k_{\mathrm{recyR}} & k_{\mathrm{offL}} & k_{\mathrm{offD}} \\ 0 & 0 & 0 & 0 & 0 & 0 & k_{\mathrm{degR}} & -k_{\mathrm{recyR}} - k_{\mathrm{exit}} & 0 & 0 \\ 0 & 0 & 0 & 0 & 0 & 0 & k_{\mathrm{onL}} L & 0 & -k_{\mathrm{offL}} - k_{\mathrm{degRL}} & 0 \\ 0 & k_{\mathrm{onD}} R_{\mathrm{t}}^* & 0 & 0 & 0 & 0 & 0 & 0 & 0 & -k_{\mathrm{offD}} - k_{\mathrm{degRD}} \end{bmatrix}, \tag{6.30}$$

$$a_{11} = \frac{-1}{V_c} \left(q_{\mathrm{cp}} + \mathrm{CL}_{\mathrm{linD}} \right) \tag{6.31}$$

$$a_{22} = \frac{-1}{V_p} \left(k_{\mathrm{onD}} N_{\mathrm{h}} \mathrm{SF} R^* + k_{\mathrm{onD}} N_{\mathrm{t}} \mathrm{SF} R_{\mathrm{t}}^* + q_{\mathrm{pc}} \right) \tag{6.32}$$

The definitions of S_{peak}, S_{duration} and S_E in Section 4.4 lead to

$$S_{\text{peak}} = 1, \tag{6.37}$$

$$S_{\text{duration}} = 1, \tag{6.38}$$

$$S_E = \alpha. \tag{6.39}$$

Bibliography

[1] Agoram, B. Use of pharmacokinetic/pharmacodynamic modelling for starting dose selection in first-in-human trials of high-risk biologics. *Br J Clin Pharmacol 67*, 2 (2009), 153–60.

[2] Agoram, B., Martin, S., and van der Graaf, P. H. The role of mechanism-based pharmacokinetic–pharmacodynamic (PK–PD) modelling in translational research of biologics. *Drug Discov Today 12*, 23-24 (2007), 1018–1024.

[3] Bache, K. G., Slagsvold, T., and Stenmark, H. Defective downregulation of receptor tyrosine kinases in cancer. *EMBO J 23*, 14 (Jul 2004), 2707–12.

[4] Backer, J. M., Shoelson, S. E., Haring, E., and White, M. F. Insulin receptors internalize by a rapid, saturable pathway requiring receptor autophosphorylation and an intact juxtamembrane region. *J Cell Biol 115*, 6 (Dec 1991), 1535–45.

[5] Baselga, J. New therapeutic agents targeting the epidermal growth factor receptor. *J Clin Oncol 18*, 21 Suppl (Oct 2000), 54S–9S.

[6] Baselga, J. The EGFR as a target for anticancer therapy–focus on cetuximab. *Eur J Cancer 37 Suppl 4* (Aug 2001), S16–22.

[7] Baselga, J. Why the epidermal growth factor receptor? the rationale for cancer therapy. *Oncologist 7 Suppl 4* (Dec 2002), 2–8.

[8] Bastholt, L., Specht, L., Jensen, K., Brun, E., Loft, A., Petersen, J., Kastberg, H., and Eriksen, J. G. Phase I/II clinical and pharmacokinetic study evaluating a fully human monoclonal antibody against EGFr (HuMax-EGFr) in patients with advanced squamous cell carcinoma of the head and neck. *Radiother Oncol 85*, 1 (Oct 2007), 24–8.

[9] Baxter, L. T., Zhu, H., Mackensen, D. G., Butler, W. F., and Jain, R. K. Biodistribution of monoclonal antibodies: scale-up from mouse to human using a physiologically based pharmacokinetic model. *Cancer Res 55*, 20 (Oct 1995), 4611–22.

[10] Baxter, L. T., Zhu, H., Mackensen, D. G., and Jain, R. K. Physiologically based pharmacokinetic model for specific and nonspecific monoclonal antibodies and

fragments in normal tissues and human tumor xenografts in nude mice. *Cancer Res 54*, 6 (Mar 1994), 1517–28.

[11] Birtwistle, M., Hatakeyama, M., Yumoto, N., Ogunnaike, B., Hoek, J., and Kholodenko, B. N. Ligand-dependent responses of the ErbB signaling network: experimental and modeling analyses. *Mol Syst Biol 3* (Jan 2007), 144.

[12] Birtwistle, M. R., and Kholodenko, B. N. Endocytosis and signalling: a meeting with mathematics. *Mol Oncol 3*, 4 (Aug 2009), 308–20.

[13] Bleeker, W. K., van Bueren, J. J. L., van Ojik, H. H., Gerritsen, A. F., Pluyter, M., Houtkamp, M., Halk, E., Goldstein, J., Schuurman, J., van Dijk, M. A., van de Winkel, J. G. J., and Parren, P. W. H. I. Dual mode of action of a human anti-epidermal growth factor receptor monoclonal antibody for cancer therapy. *J Immunol 173*, 7 (Oct 2004), 4699–707.

[14] Borisov, N., Aksamitiene, E., Kiyatkin, A., Legewie, S., Berkhout, J., Maiwald, T., Kaimachnikov, N. P., Timmer, J., Hoek, J. B., and Kholodenko, B. N. Systems-level interactions between insulin-EGF networks amplify mitogenic signaling. *Mol Syst Biol 5* (Jan 2009), 256.

[15] Brzeziński, J., and Lewiński, A. Increased plasma concentration of epidermal growth factor in female patients with non-toxic nodular goitre. *Eur J Endocrinol 138*, 4 (Apr 1998), 388–93.

[16] Burke, P., Schooler, K., and Wiley, H. S. Regulation of epidermal growth factor receptor signaling by endocytosis and intracellular trafficking. *Mol Biol Cell 12*, 6 (Jun 2001), 1897–910.

[17] Butcher, E. C. Can cell systems biology rescue drug discovery? *Nat Rev Drug Discov 4*, 6 (Jun 2005), 461–7.

[18] Butcher, E. C., Berg, E. L., and Kunkel, E. J. Systems biology in drug discovery. *Nat Biotechnol 22*, 10 (Oct 2004), 1253–9.

[19] Carter, P. Improving the efficacy of antibody-based cancer therapies. *Nat Rev Cancer 1*, 2 (2001), 118–129.

[20] Chen, W. W., Schoeberl, B., Jasper, P. J., Niepel, M., Nielsen, U. B., Lauffenburger, D. A., and Sorger, P. K. Input-output behavior of ErbB signaling pathways as revealed by a mass action model trained against dynamic data. *Mol Syst Biol 5* (Jan 2009), 239.

[21] Chung, K., Shia, J., Kemeny, N., Shah, M., Schwartz, G., Tse, A., Hamilton, A., Pan, D., Schrag, D., and Schwartz, L. Cetuximab shows activity in colorectal cancer patients with tumors that do not express the epidermal growth factor receptor by immunohistochemistry. *J Clin Oncol 23*, 9 (2005), 1803–1810.

[22] Coussens, L., Yang-Feng, T. L., Liao, Y. C., Chen, E., Gray, A., McGrath, J., Seeburg, P. H., Libermann, T. A., Schlessinger, J., and Francke, U. Tyrosine kinase receptor with extensive homology to EGF receptor shares chromosomal location with neu oncogene. *Science 230*, 4730 (Dec 1985), 1132–9.

[23] Covell, D. G., Barbet, J., Holton, O. D., Black, C. D., Parker, R. J., and Weinstein, J. N. Pharmacokinetics of monoclonal immunoglobulin G1, F(ab')2, and Fab' in mice. *Cancer Res 46*, 8 (Aug 1986), 3969–78.

[24] Crombet, T., Osorio, M., Cruz, T., Roca, C., del Castillo, R., Mon, R., Iznaga-Escobar, N., Figueredo, R., Koropatnick, J., Renginfo, E., Fernández, E., Alvárez, D., Torres, O., Ramos, M., Leonard, I., Pérez, R., and Lage, A. Use of the humanized anti-epidermal growth factor receptor monoclonal antibody h-R3 in combination with radiotherapy in the treatment of locally advanced head and neck cancer patients. *J Clin Oncol 22*, 9 (Apr 2004), 1646–54.

[25] Cunningham, D., Humblet, Y., Siena, S., Khayat, D., Bleiberg, H., Santoro, A., Bets, D., Mueser, M., Harstrick, A., and Verslype, C. Cetuximab monotherapy and cetuximab plus irinotecan in irinotecan-refractory metastatic colorectal cancer. *N Engl J Med 351*, 4 (2004), 337–345.

[26] Dahl, S., Aarons, L., Gundert-Remy, U., Karlsson, M., Schneider, Y., Steimer, J., and Trocóniz, I. Incorporating physiological and biochemical mechanisms into pharmacokinetic-pharmacodynamic models: A conceptual framework. *Basic Clin Pharmacol Toxicol* (Jul 2009).

[27] Dassonville, O., Bozec, A., Fischel, J. L., and Milano, G. EGFR targeting therapies: monoclonal antibodies versus tyrosine kinase inhibitors. Similarities and differences. *Crit Rev Oncol Hematol 62*, 1 (Apr 2007), 53–61.

[28] Davda, J. P., Jain, M., Batra, S. K., Gwilt, P. R., and Robinson, D. H. A physiologically based pharmacokinetic (PBPK) model to characterize and predict the disposition of monoclonal antibody CC49 and its single chain Fv constructs. *Int Immunopharmacol 8*, 3 (Mar 2008), 401–13.

[29] DiMasi, J. A., Hansen, R. W., and Grabowski, H. G. The price of innovation: new estimates of drug development costs. *Journal of health economics 22*, 2 (Mar 2003), 151–85.

[30] Dirks, N. L., Nolting, A., Kovar, A., and Meibohm, B. Population pharmacokinetics of cetuximab in patients with squamous cell carcinoma of the head and neck. *J Clin Pharmacol 48*, 3 (Mar 2008), 267–78.

[31] Drebin, J. A., Link, V. C., Weinberg, R. A., and Greene, M. I. Inhibition of tumor growth by a monoclonal antibody reactive with an oncogene-encoded tumor antigen. *PNAS 83*, 23 (Dec 1986), 9129–33.

[32] Drews, J. Strategic trends in the drug industry. *Drug Discov Today* (Jan 2003), 411–20.

[33] Druker, B., and Lydon, N. Lessons learned from the development of an ab1 tyrosine kinase inhibitor for chronic myelogenous leukemia. *J Clin Invest 105*, 1 (2000), 3–8.

[34] Dubois, L., Lecourtois, M., Alexandre, C., Hirst, E., and Vincent, J. P. Regulated endocytic routing modulates wingless signaling in drosophila embryos. *Cell 105*, 5 (May 2001), 613–24.

[35] Ette, E. I., Williams, P. J., Kim, Y. H., Lane, J. R., Liu, M.-J., and Capparelli, E. V. Model appropriateness and population pharmacokinetic modeling. *J Clin Pharmacol 43*, 6 (Jun 2003), 610–23.

[36] Ferl, G. Z., Wu, A. M., and DiStefano, J. J. A predictive model of therapeutic monoclonal antibody dynamics and regulation by the neonatal Fc receptor (FcRn). *Ann Biomed Eng 33*, 11 (Oct 2005), 1640–52.

[37] Fisher, R. I., Kaminski, M. S., Wahl, R. L., Knox, S. J., Zelenetz, A. D., Vose, J. M., Leonard, J. P., Kroll, S., Goldsmith, S. J., and Coleman, M. Tositumomab and iodine-131 tositumomab produces durable complete remissions in a subset of heavily pretreated patients with low-grade and transformed non-Hodgkin'slymphomas. *J Clin Oncol 23*, 30 (Oct 2005), 7565–73.

[38] Fishman, M. C., and Porter, J. A. Pharmaceuticals: a new grammar for drug discovery. *Nature 437*, 7058 (Sep 2005), 491–3.

[39] Fitzgerald, J. B., Schoeberl, B., Nielsen, U. B., and Sorger, P. K. Systems biology and combination therapy in the quest for clinical efficacy. *Nat Chem Biol 2*, 9 (Sep 2006), 458–66.

[40] Flores-Morales, A., Greenhalgh, C. J., Norstedt, G., and Rico-Bautista, E. Negative regulation of growth hormone receptor signaling. *Mol Endocrinol 20*, 2 (Feb 2006), 241–53.

[41] Franklin, G., Powell, J. D., and Emami-Naeini, A. Feedback control of dynamic systems. *Prentice Hall* (Jan 2002).

[42] Friedrich, S. W., Lin, S. C., Stoll, B. R., Baxter, L. T., Munn, L. L., and Jain, R. K. Antibody-directed effector cell therapy of tumors: analysis and optimization using a physiologically based pharmacokinetic model. *Neoplasia 4*, 5 (Aug 2002), 449–63.

[43] Garg, A., and Balthasar, J. P. Physiologically-based pharmacokinetic (PBPK) model to predict IgG tissue kinetics in wild-type and FcRn-knockout mice. *J Pharmacokinet Pharmacodyn 34*, 5 (2007), 687–709.

[44] Geffen, D. B., and Man, S. New drugs for the treatment of cancer, 1990-2001. *Isr Med Assoc J 4*, 12 (Dec 2002), 1124–31.

[45] Gex-Fabry, M., and Delisi, C. Receptor-mediated endocytosis: a model and its implications for experimental analysis. *Am J Physiol Regul Integr Comp Physiol 247*, 5 (Oct 1984), 768–79.

[46] Godfrey, K. Compartmental models and their application. *Academic Press* (Jan 1983).

[47] Goel, S., Mani, S., and Perez-Soler, R. Tyrosine kinase inhibitors: a clinical perspective. *Curr Oncol Rep 4*, 1 (Dec 2002), 9–19.

[48] Goldstein, N. I., Prewett, M., Zuklys, K., Rockwell, P., and Mendelsohn, J. Biological efficacy of a chimeric antibody to the epidermal growth factor receptor in a human tumor xenograft model. *Clin Cancer Res 1*, 11 (Nov 1995), 1311–8.

[49] Grandis, J. R., Melhem, M. F., Gooding, W. E., Day, R., Holst, V. A., Wagener, M. M., Drenning, S. D., and Tweardy, D. J. Levels of TGF-alpha and EGFR protein in head and neck squamous cell carcinoma and patient survival. *J Natl Cancer Inst 90*, 11 (Jun 1998), 824–32.

[50] Hanahan, D., and Weinberg, R. A. The hallmarks of cancer. *Cell 100*, 1 (Jan 2000), 57–70.

[51] Harari, P. M. Epidermal growth factor receptor inhibition strategies in oncology. *Endocr Relat Cancer 11*, 4 (Nov 2004), 689–708.

[52] Heiskanen, T., Heiskanen, T., and Kairemo, K. Development of a PBPK model for monoclonal antibodies and simulation of human and mice PBPK of a radiolabelled monoclonal antibody. *Curr Pharm Des 15*, 9 (Jan 2009), 988–1007.

[53] Hendriks, B. S., Opresko, L. K., Wiley, H. S., and Lauffenburger, D. A. Coregulation of epidermal growth factor receptor/human epidermal growth factor receptor 2 (HER2) levels and locations: quantitative analysis of HER2 overexpression effects. *Cancer Res 63*, 5 (Feb 2003), 1130–7.

[54] Hendriks, B. S., Opresko, L. K., Wiley, H. S., and Lauffenburger, D. A. Quantitative analysis of HER2-mediated effects on HER2 and epidermal growth factor receptor endocytosis: distribution of homo- and heterodimers depends on relative HER2 levels. *J Biol Chem 278*, 26 (Jun 2003), 23343–51.

[55] Hendriks, B. S., Orr, G., Wells, A., Wiley, H. S., and Lauffenburger, D. A. Parsing ERK activation reveals quantitatively equivalent contributions from epidermal growth factor receptor and HER2 in human mammary epithelial cells. *J Biol Chem 280*, 7 (Feb 2005), 6157–69.

[56] Henzen-Logmans, S. C., van der Burg, M. E., Foekens, J. A., Berns, P. M., Brussée, R., Fieret, J. H., Klijn, J. G., Chadha, S., and Rodenburg, C. J. Occurrence of epidermal growth factor receptors in benign and malignant ovarian tumors and normal ovarian tissues: an immunohistochemical study. *J Cancer Res Clin Oncol 118*, 4 (Jan 1992), 303–7.

[57] Hilton, D. J., and Nicola, N. A. Kinetic analyses of the binding of leukemia inhibitory factor to receptor on cells and membranes and in detergent solution. *J Biol Chem 267*, 15 (May 1992), 10238–47.

[58] Hood, L., and Perlmutter, R. M. The impact of systems approaches on biological problems in drug discovery. *Nat Biotechnol 22*, 10 (Oct 2004), 1215–7.

[59] Horrobin, D. F. Realism in drug discovery-could cassandra be right? *Nat Biotechnol 19*, 12 (Dec 2001), 1099–100.

[60] Ismail, M., Abd-Elsalam, M. A., and Al-Ahaidib, M. S. Pharmacokinetics of 125I-labelled walterinnesia aegyptia venom and its distribution of the venom and its toxin versus slow absorption and distribution of IGG, F(AB')2 and F(AB) of the antivenin. *Toxicon 36*, 1 (Jan 1998), 93–114.

[61] Jakobovits, A., Amado, R., Yang, X., Roskos, L., and Schwab, G. From XenoMouse technology to panitumumab, the first fully human antibody product from transgenic mice. *Nat Biotechnol 25*, 10 (2007), 1134–1143.

[62] Jonker, D., Visser, S., van der Graaf, P. H., Voskuyl, R., and Danhof, M. Towards a mechanism-based analysis of pharmacodynamic drug–drug interactions in vivo. *Pharmacol Ther 106*, 1 (2005), 1–18.

[63] Kholodenko, B. N. Cell-signalling dynamics in time and space. *Nat Rev Mol Cell Biol 7*, 3 (Feb 2006), 165–76.

[64] Kirisits, A., Pils, D., and Krainer, M. Epidermal growth factor receptor degradation: an alternative view of oncogenic pathways. *Int J Biochem Cell Biol 39*, 12 (Jan 2007), 2173–82.

[65] Kitano, H. A robustness-based approach to systems-oriented drug design. *Nat Rev Drug Discov 6*, 3 (Mar 2007), 202–10.

[66] Klipp, E., and Liebermeister, W. Mathematical modeling of intracellular signaling pathways. *BMC Neurosci 7*, Suppl 1 (Oct 2006), S10.

[67] Kloft, C., Graefe, E.-U., Tanswell, P., Scott, A. M., Hofheinz, R., Amelsberg, A., and Karlsson, M. O. Population pharmacokinetics of sibrotuzumab, a novel therapeutic monoclonal antibody, in cancer patients. *Invest New Drugs 22*, 1 (Dec 2004), 39–52.

[68] Knauer, D. J., Wiley, H. S., and Cunningham, D. D. Relationship between epidermal growth factor receptor occupancy and mitogenic response. Quantitative analysis using a steady state model system. *J Biol Chem 259*, 9 (May 1984), 5623–31.

[69] Köhler, G., and Milstein, C. Continuous cultures of fused cells secreting antibody of predefined specificity. *Nature 256*, 5517 (Aug 1975), 495–7.

[70] Kola, I., and Landis, J. Can the pharmaceutical industry reduce attrition rates? *Nat Rev Drug Discov 3*, 8 (Aug 2004), 711–5.

[71] Krippendorff, B., Neuhaus, R., Lienau, P., Reichel, A., and Huisinga, W. Mechanism-based inhibition: Deriving KI and kinact directly from time-dependent IC50 values. *J Biomol Screen 14*, 8 (Aug 2009), 913–23.

[72] Krippendorff, B., Oyarzún, D., and Huisinga, W. Ligand accumulation counteracts therapeutic inhibition of receptor systems. *Proceedings FOSBE 2009, Denver, USA* (2009), pp173–176.

[73] Krippendorff, B., Oyarzún, D., and Huisinga, W. Receptor synthesis is the most important process for the cumulative effect of anti-EGFR antibodies. *Draft* (2009).

[74] Krippendorff, B.-F., Kuester, K., Kloft, C., and Huisinga, W. Nonlinear pharmacokinetics of therapeutic proteins resulting from receptor mediated endocytosis. *J Pharmacokinet Pharmacodyn 36*, 3 (May 2009), 239–60.

[75] Kubinyi, H. Drug research: myths, hype and reality. *Nat Rev Drug Discov 2*, 8 (Aug 2003), 665–8.

[76] Kuester, K., and Kloft, C. Pharmacokinetics of monoclonal antibodies. *in: Pharmacokinetics and Pharmacodynamics of Biotech Drugs Wiley-VCH Verlag GmbH & Co. KGaA* (Jan 2007).

[77] Kuester, K., Kovar, A., Lüpfert, C., Brockhaus, B., and Kloft, C. Population pharmacokinetic data analysis of three phase I studies of matuzumab, a humanised anti-EGFR monoclonal antibody in clinical cancer development. *Br J Cancer 98*, 5 (Mar 2008), 900–6.

[78] Kumar, N., Afeyan, R., Kim, H.-D., and Lauffenburger, D. A. Multipathway model enables prediction of kinase inhibitor cross-talk effects on migration of Her2-overexpressing mammary epithelial cells. *Mol Pharmacol 73*, 6 (Jun 2008), 1668–78.

[79] Lacouture, M. E. Mechanisms of cutaneous toxicities to EGFR inhibitors. *Nat Rev Cancer 6*, 10 (Oct 2006), 803–12.

[80] Lalonde, R. L., Kowalski, K. G., Hutmacher, M. M., Ewy, W., Nichols, D. J., Milligan, P. A., Corrigan, B. W., Lockwood, P. A., Marshall, S. A., Benincosa, L. J., Tensfeldt, T. G., Parivar, K., Amantea, M., Glue, P., Koide, H., and Miller, R. Model-based drug development. *Clin Pharmacol Ther 82*, 1 (Jul 2007), 21–32.

[81] Lauffenburger, D., and Linderman, J. J. Receptors: models for binding, trafficking, and signaling. *Oxford University Press* (Dec 1993).

[82] Li, J., Sai, T., Berger, M., Chao, Q., Davidson, D., Deshmukh, G., Drozdowski, B., Ebel, W., Harley, S., Henry, M., Jacob, S., Kline, B., Lazo, E., Rotella, F., Routhier, E., Rudolph, K., Sage, J., Simon, P., Yao, J., Zhou, Y., Kavuru, M., Bonfield, T., Thomassen, M. J., Sass, P. M., Nicolaides, N. C., and Grasso, L. Human antibodies for immunotherapy development generated via a human B cell hybridoma technology. *PNAS 103*, 10 (Mar 2006), 3557–62.

[83] Lin, C., Chen, W., Kruiger, W., Stolarsky, L., Weber, W., Evans, R., Verma, I., Gill, G., and Rosenfeld, M. Expression cloning of human EGF receptor complementary DNA: gene amplification and three related messenger RNA products in A431 cells. *Science 224*, 4651 (May 1984), 843–8.

[84] Lobo, E. D., Hansen, R. J., and Balthasar, J. P. Antibody pharmacokinetics and pharmacodynamics. *J Pharm Sci 93*, 11 (Oct 2004), 2645–68.

[85] Luca, A. D., Carotenuto, A., Rachiglio, A., Gallo, M., Maiello, M. R., Aldinucci, D., Pinto, A., and Normanno, N. The role of the EGFR signaling in tumor microenvironment. *J Cell Physiol 214*, 3 (Mar 2008), 559–67.

[86] Lund, K. A., Opresko, L. K., Starbuck, C., Walsh, B. J., and Wiley, H. S. Quantitative analysis of the endocytic system involved in hormone-induced receptor internalization. *J Biol Chem 265*, 26 (Sep 1990), 15713–23.

[87] Mager, D. E. Target-mediated drug disposition and dynamics. *Biochem Pharmacol 72*, 1 (Jun 2006), 1–10.

[88] Mager, D. E., and Jusko, W. J. General pharmacokinetic model for drugs exhibiting target-mediated drug disposition. *J Pharmacokinet Pharmacodyn 28*, 6 (Dec 2001), 507–32.

[89] Mager, D. E., and Krzyzanski, W. Quasi-equilibrium pharmacokinetic model for drugs exhibiting target-mediated drug disposition. *Pharm Res 22*, 10 (Oct 2005), 1589–96.

[90] Mahmood, I., and Green, M. D. Pharmacokinetic and pharmacodynamic considerations in the development of therapeutic proteins. *Clin Pharmacokinet 44*, 4 (Dec 2005), 331–47.

[91] Masui, H., Castro, L., and Mendelsohn, J. Consumption of EGF by A431 cells: evidence for receptor recycling. *J Cell Biol 120*, 1 (Jan 1993), 85–93.

[92] Materi, W., and Wishart, D. S. Computational systems biology in drug discovery and development: methods and applications. *Drug Discov Today 12*, 7-8 (Apr 2007), 295–303.

[93] Meibohm, B. Pharmacokinetics and pharmacodynamics of biotech drugs. *Wiley-VCH Verlag GmbH & Co KGaA, Weinheim* (Jan 2006).

[94] Meibohm, B. The role of pharmacokinetics and pharmacodynamics in the development of biotech drugs. *Pharmacokinetics and Pharmacodynamics of Biotech Drugs: ...* (Jan 2007).

[95] Mendelsohn, J. Targeting the epidermal growth factor receptor for cancer therapy. *J Clin Oncol 20*, 18 Suppl (Sep 2002), 1S–13S.

[96] Mendelsohn, J., and Baselga, J. Status of epidermal growth factor receptor antagonists in the biology and treatment of cancer. *J Clin Oncol* (Jan 2003).

[97] Merlino, G., Xu, Y., Ishii, S., Clark, A., Semba, K., Toyoshima, K., Yamamoto, T., and Pastan, I. Amplification and enhanced expression of the epidermal growth factor receptor gene in A431 human carcinoma cells. *Science 224*, 4647 (Apr 1984), 417.

[98] Miqueli, A. D., Blanco, R., Garcia, B., Badia, T., Batista, A. E., Alonso, R., and Montero, E. Biological activity in vitro of anti-epidermal growth factor receptor monoclonal antibodies with different affinities. *Hybridoma (Larchmt) 26*, 6 (Dec 2007), 423–32.

[99] Morell, A., Terry, W., and Waldmann, T. Metabolic properties of IgG subclasses in man. *J Clin Invest 49*, 4 (1970), 673–680.

[100] Motzer, R. J., and Bukowski, R. M. Targeted therapy for metastatic renal cell carcinoma. *J Clin Oncol 24*, 35 (Dec 2006), 5601–8.

[101] Mould, D. R., Davis, C. B., Minthorn, E. A., Kwok, D. C., Elliott, M. J., Luggen, M. E., and Totoritis, M. C. A population pharmacokinetic-pharmacodynamic analysis of single doses of clenoliximab in patients with rheumatoid arthritis. *Clin Pharmacol Ther 66*, 3 (Aug 1999), 246–57.

[102] Mould, D. R., and Sweeney, K. R. D. The pharmacokinetics and pharmacodynamics of monoclonal antibodies–mechanistic modeling applied to drug development. *Curr Opin Drug Discov Devel 10*, 1 (Dec 2007), 84–96.

[103] Murdoch, D., and Sager, J. Will targeted therapy hold its promise? an evidence-based review. *Curr Opin Oncol 20*, 1 (Jan 2008), 104–11.

[104] Nowell, P. C. The clonal evolution of tumor cell populations. *Science 194*, 4260 (Oct 1976), 23–8.

[105] Ogiso, Y., Oikawa, T., Kondo, N., Kuzumaki, N., Sugihara, T., and Ohura, T. Expression of proto-oncogenes in normal and tumor tissues of human skin. *J Invest Dermatol 90*, 6 (Jun 1988), 841–4.

[106] Ozanne, B., Richards, C. S., Hendler, F., Burns, D., and Gusterson, B. Over-expression of the EGF receptor is a hallmark of squamous cell carcinomas. *J Pathol 149*, 1 (May 1986), 9–14.

[107] Peipp, M., Dechant, M., and Valerius, T. Effector mechanisms of therapeutic antibodies against ErbB receptors. *Curr Opin Immunol 20*, 4 (Aug 2008), 436–43.

[108] Peréz-Soler, R., and Saltz, L. Cutaneous adverse effects with HER1/EGFR-targeted agents: is there a silver lining? *J Clin Oncol 23*, 22 (Aug 2005), 5235–46.

[109] PLOEGER, B., GRAAF, P., and Danhof, M. Incorporating receptor theory in mechanism-based pharmacokinetic-pharmacodynamic (PK-PD) modeling. *Drug Metab Pharmacokinet 24*, 1 (2009), 3–15.

[110] Puglisi, F., and Piccart, M. Trastuzumab and breast cancer. Are we just beyond the prologue of a fascinating story? *Onkologie 28*, 11 (2005), 547–549.

[111] Rao, B. M., Lauffenburger, D. A., and Wittrup, K. D. Integrating cell-level kinetic modeling into the design of engineered protein therapeutics. *Nat Biotechnol 23*, 2 (Feb 2005), 191–4.

[112] Raymond, E., Faivre, S., and Armand, J. P. Epidermal growth factor receptor tyrosine kinase as a target for anticancer therapy. *Drugs 60 Suppl 1* (Dec 2000), 15–23; discussion 41–2.

[113] Reddy, C. C., Wells, A., and Lauffenburger, D. A. Proliferative response of fibroblasts expressing internalization-deficient epidermal growth factor (EGF) receptors is altered via differential EGF depletion effect. *Biotechnol Prog 10*, 4 (Jan 1994), 377–84.

[114] Reilly, R. M., Sandhu, J., Alvarez-Diez, T. M., Gallinger, S., Kirsh, J., and Stern, H. Problems of delivery of monoclonal antibodies. pharmaceutical and pharmacokinetic solutions. *Clin Pharmacokinet 28*, 2 (Jan 1995), 126–42.

[115] Resat, H., Ewald, J. A., Dixon, D. A., and Wiley, H. S. An integrated model of epidermal growth factor receptor trafficking and signal transduction. *Biophys J 85*, 2 (Jul 2003), 730–43.

[116] RezÂÕová, D., Kotásek, A., Suk, V., and Bfeaták, M. A new consistent chromosomal abnormality in chronic myelogenous leukaemia identified by quinacrine fluorescence and giemsa staining. *Nature*, 243 (Jan 1973), 290 – 3.

[117] Rippe, B., and Haraldsson, B. Transport of macromolecules across microvascular walls: the two-pore theory. *Physiol Rev 74*, 1 (Jan 1994), 163–219.

[118] Roepstorff, K., Grøvdal, L., Grandal, M., Lerdrup, M., and van Deurs, B. Endocytic downregulation of ErbB receptors: mechanisms and relevance in cancer. *Histochem Cell Biol 129*, 5 (May 2008), 563–78.

[119] Roopenian, D. C., and Akilesh, S. FcRn: the neonatal Fc receptor comes of age. *Nat Rev Immunol 7*, 9 (Sep 2007), 715–25.

[120] Ross, J. S., Schenkein, D. P., Pietrusko, R., Rolfe, M., Linette, G. P., Stec, J., Stagliano, N. E., Ginsburg, G. S., Symmans, W. F., Pusztai, L., and Hortobagyi, G. N. Targeted therapies for cancer 2004. *Am J Clin Pathol 122*, 4 (Oct 2004), 598–609.

[121] Russell-Jones, G. J. The potential use of receptor-mediated endocytosis for oral drug delivery. *Adv Drug Deliv Rev 46*, 1-3 (Feb 2001), 59–73.

[122] Sakai, K., Mori, S., Kawamoto, T., Taniguchi, S., Kobori, O., Morioka, Y., Kuroki, T., and Kano, K. Expression of epidermal growth factor receptors on normal human gastric epithelia and gastric carcinomas. *J Natl Cancer Inst 77*, 5 (Nov 1986), 1047–52.

[123] Saltz, L. B., Meropol, N. J., Loehrer, P. J., Needle, M. N., Kopit, J., and Mayer, R. J. Phase II trial of cetuximab in patients with refractory colorectal cancer that expresses the epidermal growth factor receptor. *J Clin Oncol 22*, 7 (Mar 2004), 1201–8.

[124] Sargent, E. R., Gomella, L. G., Belldegrun, A., Linehan, W. M., and Kasid, A. Epidermal growth factor receptor gene expression in normal human kidney and renal cell carcinoma. *J Urol 142*, 5 (Nov 1989), 1364–8.

[125] Sarkar, C. A., and Lauffenburger, D. A. Cell-level pharmacokinetic model of granulocyte colony-stimulating factor: implications for ligand lifetime and potency in vivo. *Mol Pharmacol 63*, 1 (Dec 2003), 147–58.

[126] Schadt, E. E., Friend, S. H., and Shaywitz, D. A. A network view of disease and compound screening. *Nat Rev Drug Discov 8*, 4 (Apr 2009), 286–95.

[127] Schechter, A. L., Stern, D. F., Vaidyanathan, L., Decker, S. J., Drebin, J. A., Greene, M. I., and Weinberg, R. A. The neu oncogene: an erb-B-related gene encoding a 185,000-Mr tumour antigen. *Nature 312*, 5994 (Jan 1984), 513–6.

[128] Schlomm, T., Kirstein, P., Iwers, L., Daniel, B., Steuber, T., Walz, J., Chun, F. H. K., Haese, A., Kollermann, J., Graefen, M., Huland, H., Sauter, G., Simon, R., and Erbersdobler, A. Clinical significance of epidermal growth factor receptor protein overexpression and gene copy number gains in prostate cancer. *Clin Cancer Res 13*, 22 Pt 1 (Nov 2007), 6579–84.

[129] Schoeberl, B., Eichler-Jonsson, C., Gilles, E. D., and Mueller, G. Computational modeling of the dynamics of the MAP kinase cascade activated by surface and internalized EGF receptors. *Nat Biotechnol 20*, 4 (Apr 2002), 370–5.

[130] Schoeberl, B., Pace, E. A., Fitzgerald, J. B., Harms, B. D., Xu, L., Nie, L., Linggi, B., Kalra, A., Paragas, V., Bukhalid, R., Grantcharova, V., Kohli, N., West, K. A., Leszczyniecka, M., Feldhaus, M. J., Kudla, A. J., and Nielsen, U. B. Therapeutically targeting ErbB3: a key node in ligand-induced activation of the ErbB receptor-PI3K axis. *Sci Signal 2*, 77 (Dec 2009), ra31.

[131] Semba, K., Kamata, N., Toyoshima, K., and Yamamoto, T. A v-ErbB-related protooncogene, c-ErbB-2, is distinct from the c-ErbB-1/epidermal growth factor-

receptor gene and is amplified in a human salivary gland adenocarcinoma. *PNAS 82*, 19 (Oct 1985), 6497–501.

[132] Seron, M., Braslavsky, J., and Goodwin, G. C. Fundamental limitations in filtering and control. *Springer Verlag, London* (Jan 1997).

[133] Shankaran, H., Resat, H., and Wiley, H. S. Cell surface receptors for signal transduction and ligand transport: A design principles study. *PLoS Comput Biol 3*, 6 (May 2007), e101.

[134] Shankaran, H., Wiley, H. S., and Resat, H. Receptor downregulation and desensitization enhance the information processing ability of signalling receptors. *BMC Syst Biol 1*, 1 (Nov 2007), 48.

[135] Sheiner, B. L., and Beal, S. L. Evaluation of methods for estimating population pharmacokinetic parameters. ii. biexponential model and experimental pharmacokinetic data. *J Pharmacokinet Biopharm 9*, 5 (Oct 1981), 635–51.

[136] Sheiner, L. B., and Beal, S. L. Evaluation of methods for estimating population pharmacokinetics parameters. i. michaelis-menten model: routine clinical pharmacokinetic data. *J Pharmacokinet Biopharm 8*, 6 (Dec 1980), 553–71.

[137] Sheiner, L. B., and Beal, S. L. Evaluation of methods for estimating population pharmacokinetic parameters. iii. monoexponential model: routine clinical pharmacokinetic data. *J Pharmacokinet Biopharm 11*, 3 (Jun 1983), 303–19.

[138] Sorkin, A., and Goh, L. Endocytosis and intracellular trafficking of ErbBs. *Exp Cell Res*, 314 (Aug 2008), 3093–3106.

[139] Sorkin, A., and Zastrow, M. V. Signal transduction and endocytosis: close encounters of many kinds. *Nat Rev Mol Cell Biol 3*, 8 (Jul 2002), 600–14.

[140] Starbuck, C., and Lauffenburger, D. A. Mathematical model for the effects of epidermal growth factor receptor trafficking dynamics on fibroblast proliferation responses. *Biotechnol Prog 8*, 2 (Jan 1992), 132–43.

[141] Tang, L., Persky, A., Hochhaus, G., and Meibohm, B. Pharmacokinetic aspects of biotechnology products. *J Pharm Sci* (Jan 2004).

[142] Terada, T., Ohta, T., and Nakanuma, Y. Expression of transforming growth factor-alpha and its receptor during human liver development and maturation. *Virchows Arch 424*, 6 (Jan 1994), 669–75.

[143] Thurber, G., Schmidt, M., and Wittrup, K. D. Factors determining antibody distribution in tumors. *Trends Pharmacol Sci 29*, 2 (Jan 2008), 57–61.

[144] Timms, J. F., White, S. L., O'Hare, M. J., and Waterfield, M. D. Effects of ErbB-2 overexpression on mitogenic signalling and cell cycle progression in human breast luminal epithelial cells. *Oncogene 21*, 43 (Sep 2002), 6573–86.

[145] Ullrich, A., Ullrich, A., Coussens, L., Coussens, L., Hayflick, J. S., Hayflick, J. S., Dull, T. J., Dull, T. J., Gray, A., Gray, A., Tam, A. W., Tam, A. W., Lee, J., Lee, J., Yarden, Y., Yarden, Y., Libermann, T. A., Libermann, T. A., Schlessinger, J., Schlessinger, J., Downward, J., Downward, J., Mayes, E. L. V., Mayes, E. L. V., Whittle, N., Whittle, N., Waterfield, M. D., Waterfield, M. D., Seeburg, P. H., and Seeburg, P. H. Human epidermal growth factor receptor cDNA sequence and aberrant expression of the amplified gene in A431 epidermoid carcinoma cells. *Nature 309*, 5967 (May 1984), 418–25.

[146] Urva, S., Yang, V., and Balthasar, J. Physiologically based pharmacokinetic model for T84.66: A monoclonal anti-CEA antibody. *J Pharm Sci* (Sep 2009), 1–19.

[147] van Bueren, J. J. L., Bleeker, W. K., Bøgh, H. O., Houtkamp, M., Schuurman, J., van de Winkel, J. G. J., and Parren, P. W. H. I. Effect of target dynamics on pharmacokinetics of a novel therapeutic antibody against the epidermal growth factor receptor: implications for the mechanisms of action. *Cancer Res 66*, 15 (Jul 2006), 7630–8.

[148] van der Greef, J., and McBurney, R. N. Innovation: Rescuing drug discovery: in vivo systems pathology and systems pharmacology. *Nat Rev Drug Discov 4*, 12 (Dec 2005), 961–7.

[149] van der Laan, B. F., Freeman, J. L., and Asa, S. L. Expression of growth factors and growth factor receptors in normal and tumorous human thyroid tissues. *Thyroid 5*, 1 (Feb 1995), 67–73.

[150] van Dijk, M. A., and van de Winkel, J. G. Human antibodies as next generation therapeutics. *Curr Opin Chem Biol 5*, 4 (Aug 2001), 368–74.

[151] Vaupel, P. Tumor microenvironmental physiology and its implications for radiation oncology. *Semin Radiat Oncol 14*, 3 (Jul 2004), 198–206.

[152] Watanabe, T., Shintani, A., Nakata, M., Shing, Y., Folkman, J., Igarashi, K., and Sasada, R. Recombinant human betacellulin. molecular structure, biological activities, and receptor interaction. *J Biol Chem 269*, 13 (Mar 1994), 9966–73.

[153] Wells, A. EGF receptor. *Int J Biochem Cell Biol 31*, 6 (May 1999), 637–43.

[154] Wells, A., Welsh, J. B., Lazar, C. S., Wiley, H. S., Gill, G. N., and Rosenfeld, M. G. Ligand-induced transformation by a noninternalizing epidermal growth factor receptor. *Science 247*, 4945 (Feb 1990), 962–4.

[155] Wiczling, P., Lowe, P., Pigeolet, E., Lüdicke, F., Balser, S., and Krzyzanski, W. Population pharmacokinetic modelling of filgrastim in healthy adults following intravenous and subcutaneous administrations. *Clin Pharmacokinet 48*, 12 (Dec 2009), 817–26.

[156] Wiley, H. S. Anomalous binding of epidermal growth factor to A431 cells is due to the effect of high receptor densities and a saturable endocytic system. *J Cell Biol 107*, 2 (Aug 1988), 801–10.

[157] Wiley, H. S. Trafficking of the ErbB receptors and its influence on signaling. *Exp Cell Res 284*, 1 (Mar 2003), 78–88.

[158] Wiley, H. S., and Cunningham, D. D. A steady state model for analyzing the cellular binding, internalization and degradation of polypeptide ligands. *Cell 25*, 2 (Aug 1981), 433–40.

[159] Wiley, H. S., and Cunningham, D. D. The endocytotic rate constant. A cellular parameter for quantitating receptor-mediated endocytosis. *J Biol Chem 257*, 8 (Apr 1982), 4222–9.

[160] Wiley, H. S., Herbst, J. J., Walsh, B. J., Lauffenburger, D. A., Rosenfeld, M. G., and Gill, G. N. The role of tyrosine kinase activity in endocytosis, compartmentation, and down-regulation of the epidermal growth factor receptor. *J Biol Chem 266*, 17 (Jun 1991), 11083–94.

[161] Wiley, H. S., Shvartsman, S. Y., and Lauffenburger, D. A. Computational modeling of the EGF-receptor system: a paradigm for systems biology. *Trends Cell Biol 13*, 1 (Jan 2003), 43–50.

[162] Wist, A., Berger, S., and Iyengar, R. Systems pharmacology and genome medicine: a future perspective. *Genome Med 1* (2009), 11.

[163] Yang, X., Jia, X., Corvalan, J., Wang, P., and Davis, C. Development of ABX-EGF, a fully human anti-EGF receptor monoclonal antibody, for cancer therapy. *Crit Rev Oncol Hematol 38*, 1 (2001), 17–23.

[164] Zhu, H., Baxter, L. T., and Jain, R. K. Potential and limitations of radioimmunodetection and radioimmunotherapy with monoclonal antibodies. *J Nucl Med 38*, 5 (May 1997), 731–41.

[165] Zhu, H., Melder, R. J., Baxter, L. T., and Jain, R. K. Physiologically based kinetic model of effector cell biodistribution in mammals: implications for adoptive immunotherapy. *Cancer Res 56*, 16 (Aug 1996), 3771–81.